Fall Poster Session 2025

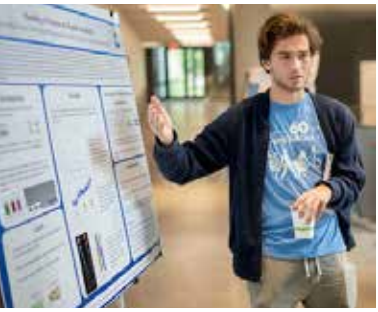

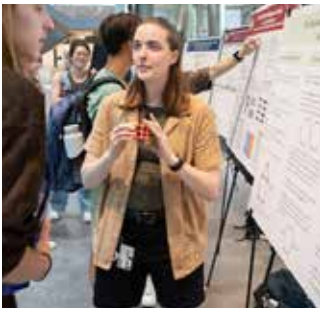

Thursday 9/25/25 • 3 PM – 5 PM
Friday 9/26/25 • 11 AM – 1:30 PM

SIGMA XI
THE SCIENTIFIC RESEARCH HONOR SOCIETY

SWARTHMORE

Sigma Xi Officers for Fiscal Year 2025/26

President:	Dawn Carone, Biology
Vice President:	Hillary Smith, Physics
Treasurer:	Joseph Nakao, Mathematics
Secretary:	Kathleen Howard, Chemistry
Administrative Coordinator:	Betsy Durning, Psychology edurnin1@swarthmore.edu

Sigma Xi Mission Statement

Sigma Xi, The Scientific Research Honor Society is the international honor society of science and engineering. One of the oldest and largest scientific organizations in the world, Sigma Xi has a distinguished history of service to science and society for more than one hundred and twenty five years. Scientists and engineers, whose research spans the disciplines of science and technology, comprise the membership of the Society. Sigma Xi chapters can be found at colleges and universities, government laboratories, and industry research centers around the world. More than 200 Nobel Prize winners have been members.

Today, Sigma Xi has nearly 60,000 members in over 500 chapters in the U.S., Canada and other countries, including Switzerland, Thailand, Lebanon, New Zealand and Australia. Sigma Xi chapters are found wherever scientific research is undertaken in universities, colleges, industrial research facilities and government laboratories. Recent presidents of Sigma Xi have included Nobel laureate Frederick Robbins, National Medal of Science winner Kumar Patel, presidential science advisor Neal Lane, and National Science Foundation Director Rita Colwell.

For more information, visit www.sigmaxi.org.

SIGMA XI
THE SCIENTIFIC RESEARCH HONOR SOCIETY

SPOT	NAME	GRAD YEAR	ADDITIONAL AUTHORS	TOPIC
1	Ben Aaron	2026	Dr. Ivan C. Christov, Ziyu Wang, Mike Xiao	Failure Modes of Thin Film Peeling
2	Furqan Ahsan	2026	Sara H. Sohail	Investigating the Role of pH in Lysozyme Amyloid Fibril Polymorphism Using Fluorescence Lifetime Imaging
3	Lucas Alland	2026	Andrei Fridman, Thomas M. Keller	Realizing Gruenberg-Kegel graphs of T-solvable groups with structurally-simple extensions of T
4	Joost Almekinders	2027		A Python Library for High-Order Low-Rank Implicit Methods to Solve Advection-Diffusion Equations
5	Veronica Amoako	2028		Understanding the adsorption of HSA to AgNPs through UV-Vis Spectroscopy and Dynamic Light Scattering
6	Joe Austrian	2026		Centimeter Level GNSS Accuracy at Swarthmore
7	Elisha (Seoyoon) Bae	2026		Talking Tech: Exploring Parent-Child Conversations About Technology Use and Screen Time
8	Yuxuan Bai	2028	Carolyn Raithel	Principal Component Analysis of Neutron Star Equations of State
9	Ryan Baldwin	2028	Pat Devlin	aba-Sets & Semi-Quotients
10	Tehya Banach	2026	Denis Tokmashev, Jonathan Washington	An ultrasound study of Russian palatalized and velarized consonants
11	Iris Barone	2026	Christopher Chung	Using capillary electrophoresis to quantify competitive adsorption of eco-corona constituents to silver nanoparticles
12	Lane Barron	2026	Karen Chan	Spatial and temporal variations of larval crabs in Puget Sound
13	Adil Beken	2028	-	Representation Theory of Sn and the LIS Function
14	Aatrey Bidkar	2026	Eoin Quinn	Aperiodic and periodic components of EEG power spectra vary by time of day
15	Kimaru Boruett	2026	Yoshiaki Kanematsu (Cornell '27)	Characterization of a Synthetic Diversity Mixer-First RF Receiver
16	Paolo Bosques-Paulet	2027		Constructing a low-rank implicit method for solving high-dimensional equations in the hierarchical Tucker tensor format
17	Jasmine Branda	2028		Implantable Probes for Long-Term Neuronal Recording
18	Nathan Brewer	2028	John Carty	Robotic Barnacle Nauplii Model
19	Nana Brobbey	2026		Staircases in the Sea: Glider-Based Insights into Ocean Mixing in the Sea
20	Alexander Buendia	2027	Prof. Sara Sohail	Automating Phasor Analysis of Fluorescence Lifetime Imaging Data

SPOT	NAME	GRAD YEAR	ADDITIONAL AUTHORS	TOPIC
21	Aiperi Bush	2028		Deferred Concolic Execution Interpreter
22	Emily Chen	2026		Symplectic Integration of Vortex Contour Dynamics
23	Julian Chen	2028		Fluorescence Lifetime Imaging Reveals Concentration Dependent Polymorphism in CsgA R5 Fibrils
24	Yu-Jing (Laine) Chen	2028	Natalia Lashley	Tenure Segregation & LIHTC Placement : How Affordable Housing Placement Reproduces Existing Inequity
25	Evan Chin	2028	Jacob Baillie, Nicolas Nguyen, Rémi Beaulac, Daniel Gamelin	Synthesis and Characterization of Novel Magnetic 2D Materials via Elemental Tuning of Alloyed Chromium Thiophosphates
26	Ava Choi	2028	Ava Choi, Alejandro Sanchez, Oliver Clackson, Kaja Arusha, Ava Craig, Tate Garcia, Annalise Di Cicco, Carolyn Bauer	Repeatability of the endocrine stress response: a 5-year longitudinal study in an *Octodon degus* cohort
27	Thanisha Chowdhury	2028	Bradley Davidson, Christian Cota	FGF Receptor Trafficking During Cell Division in Human Cells
28	Isaac Chu	2027		Exploring fundamental-mode universal relations for neutron stars
29	Deedra Closser	2028	Kaiya Spencer	Investigating Sex-Specific Anxiety Responses to High-Fat Diet in Mice
30	Genine Collins	2027		Inducing HSATII Expression in HeLa and Primary Fibroblast Cells
31	Julian Courtney-Bacher	2027	Bella Thoen, Tanvir Islam, Eve Elrod, Ahmad Stovall, and Tanvir Islam	Magnetic Field Detection via Interferometry
32	Ava Craig	2027	Yuta Sato, Ava Choi, Annalise Di Cicco, Tate Garcia	GnRH-induced testosterone levels are repeatable in male *Octodon degus*
33	Julianne Cruz	2027		Analysis of T Cell Receptors in Ewing sarcoma
34	Amba Darst-Campbell	2027	Yuyang Liu	Investigating DELE1-mediated mitochondrial stress pathways using a modified CRISPR-Cas9 genetic screen
35	Zhen Ning Deng	2026	Mia Cox, Jasmine Flowers, Chris Ngo	Transfer, Motivation, and Three-Dimensional Science Learning of Middle School Students
36	Annalise Di Cicco	2027	Sarah Heissenberger, Carolyn M. Bauer	Basal metabolic rate and glucocorticoid levels are not correlated in the rodent *Octodon degus*
37	Joseph Eyiolowope	2026	Sushaant Chawla, Jonatan Ottino-González, Michael Goran, and Shana Adise	Head Fat as a Proxy for Adiposity in Neuroimaging Studies
38	Abigail Fagersten Cavanaugh	2027		Instrumental Coping Predicts Perseverance and Optimism in High School Students, While Coping Shows Limited Links to College Students Well-Being

SPOT	NAME	GRAD YEAR	ADDITIONAL AUTHORS	TOPIC
39	Icie Favata	2028	Christopher R. Graves	Purification of the B(TriNOx^{3-}) Metal Complex
40	Leilani Fleming	2028	Nox Tan	Effects of Surface Obtrusions on Granular Creep
41	Jasmine Flowers	2028		LENS (Laboratories in Environmental Science)
42	Joseph Gamez	2028	Linda Zheng, Isabelle Malouf	Effect of MK2's Kinase and Non-Kinase Activity on Caspase-3
43	Ming Gao	2026	Professor Emad Masroor	Computational Investigations of Vortex Ring Dynamics and Helical Vortex Stability
44	Tate Garcia	2026	Josephine Low, Yuta Sato, Annalise Di Cicco, Ava Craig, Ava Choi, Alejandro Sanchez, Carolyn M. Bauer	Glucose tolerance worsens with age in a social rodent species *(Octodon degus)*
45	Arina Garifullina	2027	Kayla Hellikson	Toward Anisotropic Macroporous Channels in Hydrogels via In Situ Gas Templating
46	Jonathan Garrity	2027	Michela Zaffagni	Evolutionary conservation of circular RNAs
47	Lauren Ghil	2026		Antibody Binding to Influenza A Protein
48	Devin Gibson	2028		Metabolic Stability Across the Lifespan of the Forked Fungus Beetle *(Bolitotherus cornutus)*
49	Sho Glashausser	2026	Carlos Garcia	Distance Laplacian Cospectrality in Digraphs
50	Alex Guo	2027		Synthesis of Porous Organic Cages via Dynamic Imine Chemistry
51	Lena Habtu	2026		Assessing the Efficacy of Facial Age Assurance Technologies in Adversarial Settings
52	Nina Haddou Aguilar	2027	Kaiya Spencer, Deedra Closser, Steven Jungers	Binge Eating Disorder and Consumption Rate
53	Andrew Hendrickson	2027	Eric Xing	Bulges in left-handed G-quadruplexes formed from novel $(GT)_n$ repeats
54	Owen Hoffman	2026	Kangze Peng, Sajid Kamal, Zehua You	TargetPractice: Simulating Conversations with LLMs can Protect Against Online Scams
55	Ingrid Hsu	2028	Mariela Perez-Cabarcas, Armand Destin, Cydney Harris, Inshil Addison, Kireeti Josyula, R. Allen Lee, Jewel Padilla, and Utku Yakar	COVERT-AI: Real-time, Multimodal, and Adaptive Cognitive Support for Operational Decision Making
56	Sai Nyi Htut	2028	Daniel Adeleke	Investigating the Shear Behavior of Bentonite Polymer Composites in Varying Chemical Conditions

SPOT	NAME	GRAD YEAR	ADDITIONAL AUTHORS	TOPIC
57	Isabel Hunt	2027	Chris Graves	Reactivity of ($TriNOx^{3-}$)M group 13 metal complexes with N-H and C-H bonds
58	Jean Michel Irankunda	2028		Solar Microgreen Hub for Urban and Rural Nutrition
[illegible]	Jay Iyer	2028	Bohou Zhang	Developing Interactive Content for Dive into Systems
60	Ara-Oluwa Jacob	2027	Pat Devlin	Playing to Win: Strategies in Two Player Games
61	Dylan Jacobs	2027		Characterization of Thermoelectric Materials
62	Tobias Jaramillo	2026	Stephen Kwas	Progress Towards Pyridine Containing Macrocycles Through SNAr
63	J'ovanny Jno-Pierre	2027	Junior Lugo, Savannah Wilcox	Little sprouts: How children learn and reason about nature
64	Oliver Kim	2027	Bradley Davidson	Investigating the role of NRG/ERBB signaling in proportional heart growth
65	Samuel Kim	2027	Monzy Thomas, Eric Salazar, Cheyna Butler, Meenhard Herlyn	Optimizing Lentiviral Delivery of Transcription Factors for iPSC-to-Hematopoietic Differentiation
66	Catherine King	2027		Exploring Hydroxy-Based Nucleophile Reactivity with Pyridinal Electrophiles in Nucleophilic Aromatic Substitution Reactions
67	Jacey Koh	2028	Owen Lord	Shoulder sEMG Live Biofeedback Sensor
68	Molly LaPerle	2027	Nick Kaplinsky	Identifying Natural Variation in Heat Shock Tolerance in *Arabidopsis thaliana*
69	Kaitlyn Lee	2026	Andrea Piserchio, Ranajeet Ghose	Site-Specific 19F-NMR Elucidates Functional Roles of Trp85 and Trp99 in eEF2K Activation
70	William Lee	2026		Choroidal Abnormalities in Neurofibromatosis Type 1
71	Michelle Leonard	2028	Elizabeth Bugayev, Vahan Tadevosyan	Measuring Starlink quality of experience in rural regions
72	Andrea Lie	2028		Glioblastoma Mathematical Modelling
73	Gina Lin	2028	Dan Wang, Ami Patel	243-4 and LC-10 DMAbs produce antibodies in vivo and in vitro; and can neutralize alpha toxins in vitro.
74	Grace Liu	2027	Dr. Ki A. Goosens	Metabolic and Behavioral Effects of LEAP2 on Stress Resilience
75	Josephine Low	2027	Andrew Ratz	Climbing Trees: Ecological Mechanisms of a Novel Fruiting Morphology in *Thelephora spp.*
76	Gongfu Lyu	2027	Charlotte Debras, Dominik Jud	Oxytocin–Cortisol Interactions and Social Support in Small-Scale Societies

SPOT	NAME	GRAD YEAR	ADDITIONAL AUTHORS	TOPIC
77	Kiran Mahurkar	2027	Lynn Rothschild, Rolando Perez, Jessica Snyder	Characterizing Fungal Biomaterials for Aerospace Applications
78	Téa Malone-Bonacci	2027	Stephen Kwas, Catherine King, Anna Yang	Probing Regioselectivity in Dynamic Nucleophilic Aromatic Substitution
79	Julia Mammen	2026		AI Refusal
80	Cohen Manges	2027	Tal Scully, Dr Allon Klein, Dr Bradley Davidson	Detecting Gene Modules Associated with Trait Acquisition in the Blood Cells of an Invertebrate Chordate
81	Jenna Martinez	2027		AR Aviary
82	Margalit Mauricio	2028	Ashley Lynch, Dr. Lisa Brown	Variation in the individual immune response of female cat fleas *(Ctenocephalides felis)* against a systemic bacterial infection
83	Morgan McErlean	2026	Cella Sum, Ph.D. (CMU HCII), Asya Tarabar (Yale University)	Workplace Surveillance Incident Tracker: Supporting Workers in an Age of Workplace Monitoring Proliferation
84	Michael Melnikov	2026	Taylore Keesler, Allen Zhou, Sophia Xiao	Bayesian Wind Farm Layout Optimization
85	Lisa Messier	2026	Benjamin Lipchin, Christina Rabeler, Dawn Carone	RNA-Seq Analysis of HSATII Knockdown in Cancer Cells Reveals Downregulation of Genes Implicated in Oncogenic Pathways
86	Olivia Montini	2026	Justin Quinn (Penn State University)	Additively Manufactured Quick-Acting Watertight Door Dog Analysis
87	Allison Morales	2026	Beatriz Cabello MPH, David W. Johnson, Ph.D.	Who's Logging On? School Staff Engagement With Online Mental Health & Equity Courses
88	Emiliano Morales-Lopez	2027	Nyvisalsnuk Rith, Nsoki Mavinga, Tendai Mugwagwa	Modeling the Transmission Dynamics of the Monkeypox Virus Infection with Intervention Measures
89	John Nicholson	2026	Georgios Kementzidis, Erin Wong, Ruichen Xu, Yuefan Deng	Multistep Generative Backmapping of Coarse-Grained Structures
90	Lucas Oberdiek	2026		Exploration of Peptoid Nanosheets as a Novel Water Filtration Membrane Material
91	Mojisoluwa Oludare	2026	Kathryn Riley	Investigating the complex mechanisms modulating the dissolution of silver nanoparticles: pH, size & the presence of biomolecules
92	Elle Pedaci	2027		Multivariate classification of visual image categories from scalp EEG data
93	Natalie Pham	2026	Tessa Palafu (mentor), Kelsie H. Okamura, Ph.D. (mentor)	Implementation of a culturally-grounded ENDS intervention program for Hawai'i's youth
94	Hannah Poon	2027	Liesel Blau	Backward Scrunching: Planarian Escape from Predation
95	Katleo Pule	2027	Erin Coyle, Andrew Hendrickson, Eric Xing, and Liliya A. Yatsunyk	Biophysical Characterization of Intramolecular Left-Handed G-Quadruplexes

SPOT	NAME	GRAD YEAR	ADDITIONAL AUTHORS	TOPIC
96	Jai Rapaka	2026		Fluorescence lifetime imaging to assess amyloid polymorphism
97	Nyvisalsnuk Rith	2028	Nsoki Mavinga	Stability and Bifurcation Analysis on Fishery Models with Strong Allee Effect and Holling's Type III Functional Response
98	Gabriela Rodriguez	2027	Tall Scully, Hannah Gruner, Bradley Davidson, and Allon Klein	Exploring the evolution of chordate innate immunity through the study of tunicate blood cells.
99	Brenda Romero	2027		Investigating the Role of Intron Retention in the Heat Shock Response in Arabidopsis
100	Jesus Saucedo Bucio	2026	Sintana E. Vergara	From food waste to worm food: Quantifying greenhouse gas emissions from vermicomposting
101	Grady Savage	2026	Hillary Smith	Diffraction Analysis of Chalcogenide Glass Structure
102	Charlie Schuetz	2027		Electrical Energy Harvesting From Vortex Induced Vibrations Abstract
103	Akiva Sherin	2027		Exploring the Independent Sets of Trees
104	Hanqi (Sunny) Shi	2026	Kaito Hikino '27	"Nowcasting" Flu Hospitalizations using Google Search Data
105	Matthew Shiley	2026	Nora Jiang	Development of a Lightweight Hydrogen Fuel Cell Vehicle
106	Sakura Shimozono	2027	Dora Cai	Investigating the Relationship between Lpp Activity and Trauma Exposure in Undergraduate Students
107	Yara Shobut	2027		B+ Index Tree for Swarthmore Database (SwatDB)
108	Presley Simelus	2028	Jibin Sadasivan, Lindsay Case	Exploring How Proteins Regulate Cell Signaling
109	Zoe Sperduto	2026	Kenneth Relovsky '27	Multi-Scale Testing of Novel Cross-Laminated Timber (CLT) Buildings for Century-Scale Carbon Sequestration
110	Sophia Springer	2026		Traits of immediate male social partners do not alter female behavior in a social beetle *(Bolitotherus cornutus)*
111	Nichole Suero Gonzalez	2027	Frank Durgin	Looking at Density and Number in Depth
112	Emily Sun	2027	Liliya Yatsunyk	Biophysical Characterization of BRAF-Derived DNA Sequences that Hold the Potential to Form Five-Tetrad G-Quadruplex Structures
113	Kyler Sy	2027		Modifying R-group electron-modifying substitutions on the TriNOx ligand system
114	Zoe Tang	2027	James Flagg, Paris Lewis, Dr. Mason Manning, Dr. John Nagy	Distinguishing Stochastic Fluctuations from Deterministic Population Dynamics

SPOT	NAME	GRAD YEAR	ADDITIONAL AUTHORS	TOPIC
115	Isabella Thoen	2027		Modeling Interferometric Pressure Sensors Using COMSOL
116	Elizabeth Ting	2026	Christopher R. Graves	On the reactivity of ($TriNOx^{3-}$) metal complexes with CH_2X_2(X = Cl, Br, I)
117	Jaron Tinsley	2026	Julian Krauze	Privatizing Queries over a Large Corpus of Real-World Network Data
118	Angelo Phillipe Valencia	2027	Abigail Reed	Gravitational Delensing Analysis of a Dusty-Star Forming Galaxy
119	Luciana Valencia	2027		Swimming behaviors of veliger in response to vorticity
120	Lily von Behren	2028		Identifying heterogeneity at the neural plate border in *Xenopus laevis*
121	Alina Vykliuk	2026		Developing a Digital Dictionary for Endangered Languages
122	Howard Wang	2026	Howard Wang	A Spatiotemporal Model of T-Cell Population Dynamics in the Lymph Node
123	Jeffrey Wang	2027	Qinghai Wang	Lump Sum Investing vs. Dollar Cost Averaging: Evidence from Historical Data and Bootstrapped Simulations
124	Aviva Weiser	2026		Behavioral data for different levels of prediction error in event boundaries
125	Lester Wessels	2028	Christina Rabeler, Dawn Carone	GapmeR Mediated Knockdown of HSATII Accumulations
126	Ania Wong	2028	Karina Vong, Christopher Ma, Gary Bañuelos	Saline Irrigation Effect on Total Phenolic Content in Pistachio Seed Coats
127	Katie Wu	2027		Exploring factors associated with Pediatric Post-Heart Transplant Pulmonary Vein Stenosis: A single-center retrospective chart review
128	Eric Xing	2026	Paul Seth, Erin Coyle, Andrew Hendrickson, Katleo Pule, Liliya Yatsunyk	Interaction of a Hybrid LH/RH G-Quadruplex with a G4 Ligand
129	Yuki Yamada	2027	Michael Caprise, Mary Garcia-Barrios, Kathryn R. Riley	Advancing Quantitative Analysis Tools to Evaluate the Environmental Reactivity of Nanoplastics
130	Bohou Zhang	2027	Jay Iyer	Developing Interactive Exercises for Dive Into Systems
131	Hannah Zhang	2027	Andy Xin, Anna Hansson, Grace Chen, Ryleigh Vallejo, Gerry Huang	The Relationship Between PFAS Exposure in Artificial Turf and Cancer
132	Winston Zhang	2027		Preparation of Membrane Mimics for Structural Characterization of Influenza A M2 Protein
133	Wuqian Zhang	2026	Hillary Smith	Ab initio Molecular Dynamics study of Ab Initio Molecular Dynamics Simulation of $Pt_{60}Cu_{20}P_{20}$ Bulk Metallic Glass

SPOT	NAME	GRAD YEAR	ADDITIONAL AUTHORS	TOPIC
134	Xiuming Zhang	2026	Milan Tenn, Gaocheng Liu, Finnegan McKibbon	Covering Radius of Translation Surfaces
135	Jennifer Zhao	2028	Jason Hu, Joseph Eyiolowope, Eric Xing, Liliya A. Yatsunyk	DNA Sequences With Potential to Form Five-Tetrad G-quadruplexes
136	Anzel Zhen	2028	Qianjin Guo	Generation of SDHA and SDHD Knockout Cell Lines to Investigate Metabolic Consequences of Rare pheochromocytomas and paragangliomas (PPGLs) Mutations
137	Nicholas Zuk	2026	Josepheen De Asis-Cruz M.D., Ph.D.	Brainstem and Central Autonomic Connectivity Alterations in Neonates with Congenital Heart Disease

SIGMA XI
THE SCIENTIFIC RESEARCH HONOR SOCIETY

Fall Poster Session 2025

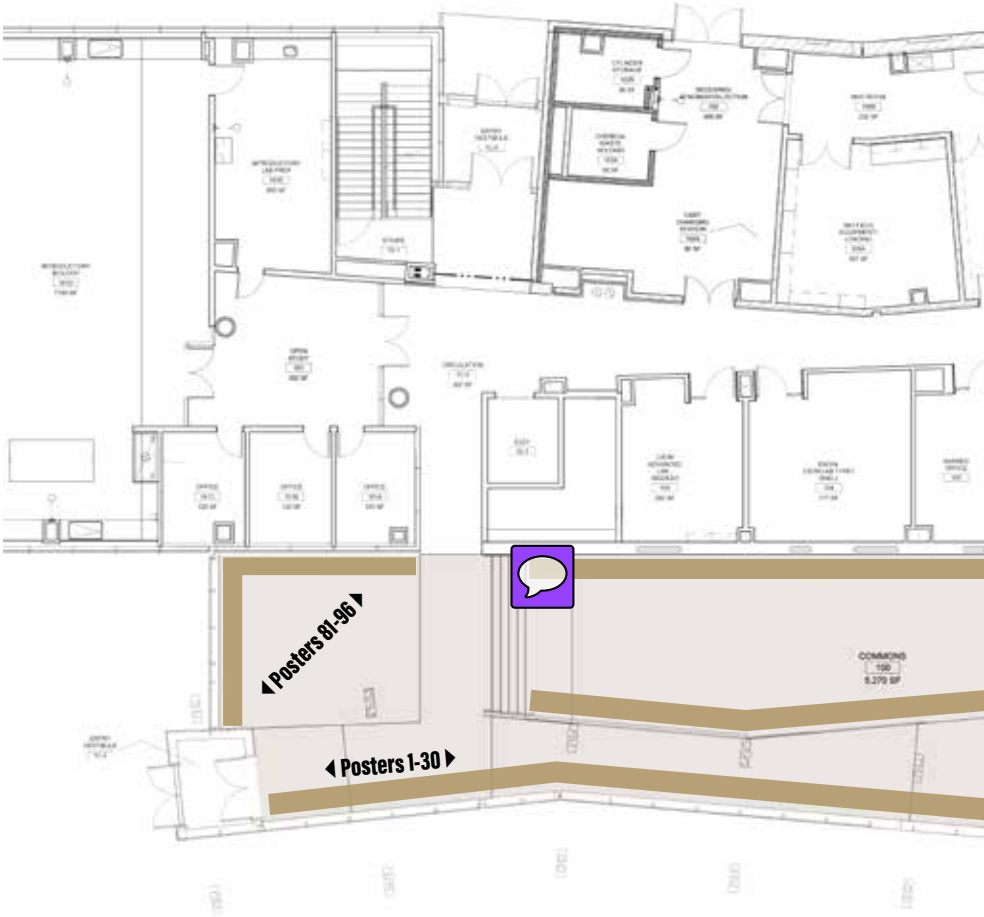

Singer Hall (West)

Indicates poster display areas

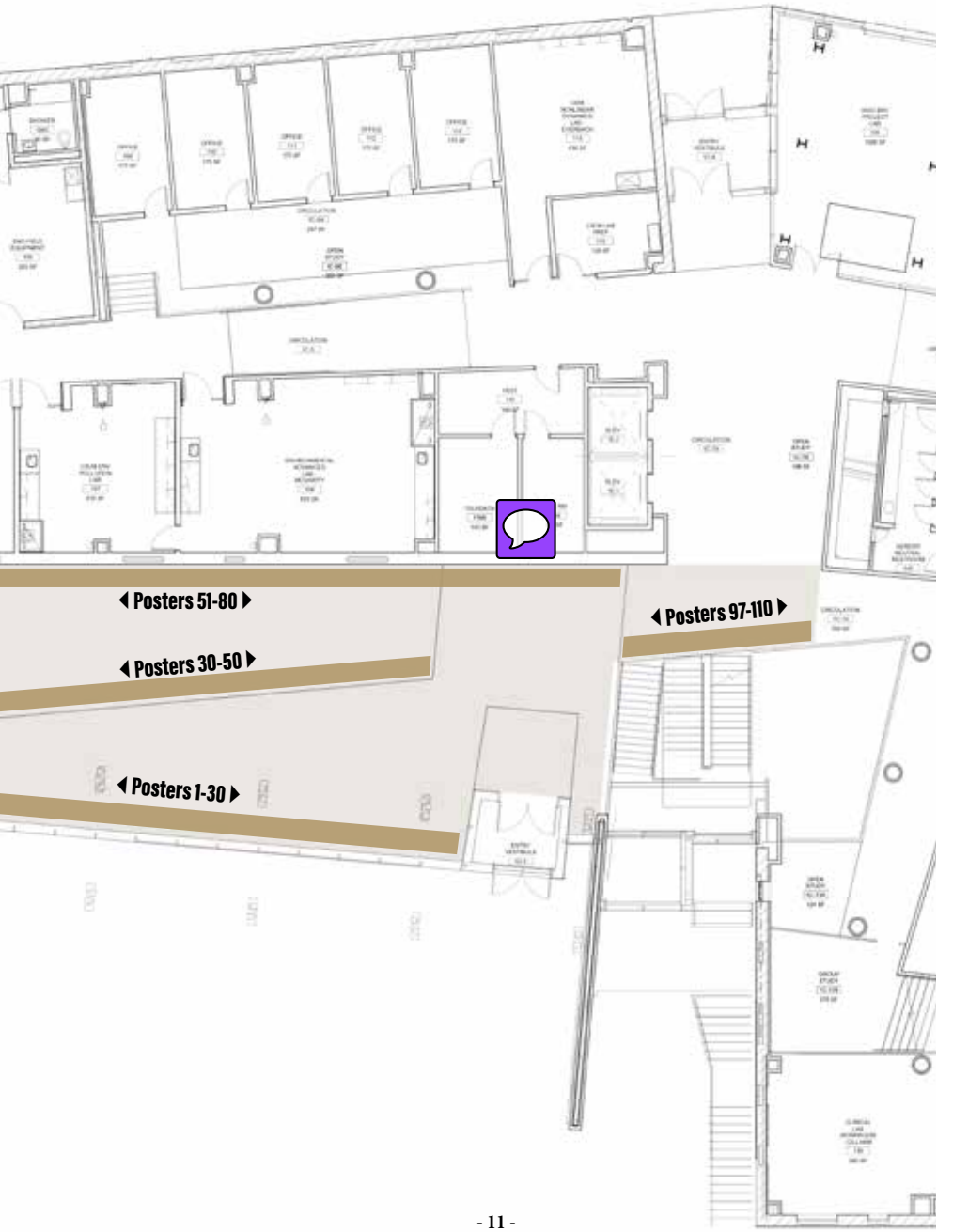
Posters 51-80
Posters 30-50
Posters 1-30
Posters 97-110

1 Failure Modes of Thin Film Peeling

Ben Aaron, Mike Xiao, Ziyu Wang, Dr. Ivan C. Christov • Purdue University
baaron1@swarthmore.edu

Peridynamics, a framework for non-local continuum mechanics, and the cohesive zone model (CZM), which characterizes fracture along a cohesive layer, have acted as important tools in mechanical engineering for modeling fracture mechanics of crack propagation. However, film peeling, a mechanics problem with appropriate constraints for a peridynamics and cohesive zone model, has been understudied despite relevance to a range of physical applications, including the everyday adhesive tapes or the laminates of structural materials. We aim to identify the conditions and failure modes under which a tear occurs when a thin film adhered to a rigid substrate undergoes bending while being peeled. This work also identifies parameters for which the film is peeled off cleanly without leaving residue. Using the PDMATLAB2D coding framework for peridynamics in 2D planes, we simulate peeling under plane strain and quasi-static loading conditions, allowing for the model to reach a steady state as loading is incremented to minimize inertial effects. Relevant tested variable parameters include the thickness of the adhesive film, the angle of loading, and the rigidity of the film. This study compares our results across levels of fineness in our simulations and in reference to the limited existing models to validate and verify our findings. Three modes of peeling are recognized in the parameter space: clean peeling, failure at a connection point, and failure after film lifting. Instances of the failure modes correspond with high adhesive strength in cases of connection failure, and low film strength in cases of failure after lifting. This research addresses the film peeling problem with recommendations for parameters of interest in future modeling. Further testing of the findings could be achieved with experimentation with adhesives of known material properties, especially the adhesives used in tapes, stickers, and other products for which a clean peel is desired.

2 Investigating the Role of pH in Lysozyme Amyloid Fibril Polymorphism Using Fluorescence Lifetime Imaging

Furqan Ahsan, Sara H. Sohail • Dept. of Chemistry and Biochemistry, Swarthmore College, PA 19081
fahsan1@swarthmore.edu

Amyloid fibrils are highly ordered protein aggregates characterized by cross-β sheet structures that form through self-assembly. While frequently linked to neurodegenerative amyloidosis such as Alzheimer's and Parkinson's, they also serve functional roles in biological systems, including hormone storage and structural scaffolding in bacterial biofilms. Their formation follows a nucleation-dependent polymerization pathway that is highly sensitive to the surrounding chemical environment, and pH has a significant role in modulating protein aggregation behavior by altering protonation states and charge distributions. Hen egg white lysozyme (HEWL), a small globular protein prone to fibrillization under acidic conditions, was used as a model system to examine the effects of pH on fibril formation and polymorphism. Samples were incubated for 24 h at 40 °C under four buffered conditions (pH 2.0, 3.0, 5.0, 7.4) and analyzed using fluorescence lifetime imaging microscopy (FLIM) with Thioflavin T (ThT). Phasor analysis was used to quantify ThT lifetime distributions, while confocal imaging provided morphological information. Circular dichroism (CD) spectroscopy was used to probe secondary structure of HEWL before and after incubation. Aggregates readily formed under all conditions but displayed striking pH-dependent differences: at pH 2.0, fibrils assembled into crowded, short-to-moderate length filaments with broadened phasor distributions shifted toward shorter lifetimes (~1.0 ns), consistent with greater heterogeneity and multiple aggregation pathways, while pH 3.0 fibrils were evenly distributed with the tightest phasor clustering near ~2.0 ns, and pH 5.0 produced rope-like fibrils with a homogeneous lifetime population. At pH 7.4, fibrils contained thick, fragmented bundles with compact clustering but minor heterogeneity. These results highlight pH as a critical determinant of amyloid fibril morphology and polymorphism, with extreme acidity destabilizing the native state and enabling multiple aggregation routes, while near-neutral conditions favor the assembly of more uniform aggregates. Overall, this work underscores the sensitivity of fibril assembly to solvent environment and demonstrates the utility of FLIM-phasor analysis for resolving structural diversity in amyloids formed at different conditions.

3 Realizing Gruenberg-Kegel graphs of *T*-solvable groups with structurally-simple extensions of *T*

Lucas Alland, Andrei Fridman, Thomas M. Keller • Swarthmore College

lalland1@swarthmore.edu

Given a finite group *G*, its (Gruenberg-Kegel) prime graph is a graph whose vertices are the prime divisors of $|G|$ and where edges $\{p,q\}$ exist whenever *G* contains an element of order *pq*. We continue the study of prime graphs for *T*-solvable groups; that is, groups whose composition factors are either abelian or isomorphic to some fixed simple group *T*. For a large class of such groups, we prove that their prime graph complements are always realizable by a solvable group and a quasi simple or almost simple *T*-solvable group acting by automorphisms on a direct product of elementary abelian groups. We additionally provide some examples of interesting classes of groups matching the assumptions of our main theorem.

4 A Python Library for High-Order Low-Rank Implicit Methods to Solve Advection-Diffusion Equations

Joost Almekinders, Dr. Joseph Nakao • Swarthmore College

Jalmeki1@swarthmore.edu

I worked with Professor Joseph Nakao on developing a Python library for his high-order low-rank implicit numerical method, the Reduced Augmentation Implicit Low-Rank (RAIL) integrator, designed for solving advection-diffusion equations and related models. The RAIL method combines features of dynamical low-rank (DLR) methods and step-and-truncation (SAT) tensor methods to maximize efficiency, accuracy, and stability.

While RAIL is an excellent algorithm, much of the existing code base was hard-coded for specific cases, which limited its usability for broader research applications. The goal of my project was therefore to construct a flexible, user-friendly Python library that implements the RAIL method in a way that can be easily adapted to different problems and extended in future work.

I began by implementing basic cases of first- and second-order schemes, ensuring correctness against known solutions. From there, I progressively generalized the implementation so that the library could accommodate any diagonally implicit Runge-Kutta (DIRK) or implicit-explicit Runge-Kutta (IMEX) method through a general Butcher tableau input. This shift from hard-coded schemes to a fully general framework was the key design choice that made the library broadly useful to other researchers. The completed library can run RAIL simulations with any DIRK or IMEX scheme, performing both the accuracy and rank tests across methods.

By the end of the summer, the project successfully delivered a Python library for the RAIL method. This library will support Professor Nakao and his collaborators in testing further extensions of RAIL, applying it to other PDE models, and comparing its efficiency and accuracy against other low-rank integrators. Overall, it provides a foundation for future research into implicit low-rank methods.

5 Understanding the adsorption of HSA to AgNPs through UV-Vis Spectroscopy and Dynamic Light Scattering

Veronica Amoako

Silver nanoparticles (AgNPs) are everywhere. They're used in water filtration, makeup products, textiles, and many more household items. Despite this, there is limited research on the impact of these nanoparticles once they are released into the environment. In the Riley Lab, we ventured to use UV-Vis Spectroscopy and Dynamic Light Scattering (DLS) to better characterize the behavior of these AgNPs when in solution with Human Serum Albumin (HSA). We used UV-Vis techniques to measure wavelengths absorbed by AgNPs after HSA has adsorbed onto the surface of the particle. Using this data, we applied the Langmuir Isotherm model to quantify the shift in λ_{max} as HSA concentration increased to determine the equilibrium constant for the process. It was found that as NaCl concentration increased, absorbance decreased due to increased aggregation between the nanoparticles, likely the result of the salt eroding the citrate cap separating the particles from

each other. Through temperature-based analysis, we also found that increasing the temperature corresponded with an increase in the Ka value, indicating that the adsorption of HSA to AgNPs is an endothermic process. We also used DLS to determine the presence and extent of aggregation between the nanoparticles when in solutions of increasing NaCl concentrations. Similarly to the UV-Vis, we found that as NaCl concentration increased, aggregation between nanoparticles increased as well.

6 Centimeter Level GNSS Accuracy at Swarthmore

Joseph Austrian, J. Douglas Willen • Swarthmore College

Jaustri1@swarthmore.edu

The purpose of this research was to establish an on-campus base station for Real-time Kinematic positioning correction data. GNSS-RTK allows for geolocation to one centimeter of precision, which if implemented on Swarthmore's campus will greatly increase the accuracy of maps of underground and surface utilities, flowers and plants in the arboretum, and location services for student projects. Research included which hardware to purchase for the antenna and base station, how to establish and upload initial data to a correction server, and how to make that server accessible 24/7 to Swarthmore staff and students. At this point, the station has been constructed, and the antenna needs to be re-oriented for a 24-hour data collection period to start. Once this data is uploaded to the online service, anyone within ten kilometers of the antenna using a GNSS rover will be able to record positional data supplemented by the RTCM (Radio Technical Commission for Maritime Services) correction data.

7 Talking Tech: Exploring Parent-Child Conversations About Technology Use and Screen Time

Elisha (Seoyoon)Bae

As digital devices become increasingly integrated into children's daily lives, families are grappling with how to manage screen time and ensure safe, responsible technology use. While much research has examined adolescents' attitudes and behaviors, less is known about younger children and how families talk about these issues together. This study looks at the conversations between parents and children about technology use, screen time rules, and internet safety.

Building on a prior parent-only survey (Study 1) that found family conflict over screen time predicted higher child behavioral difficulties, and that "stick" style rule justifications were associated with greater child screen use, this follow-up study (Study 2) examines how these themes emerge in naturalistic dialogue. Using the Children Helping Science online data collection platform, we recruited parent–child dyads who engaged in a semi-structured discussion about technology rules from home asynchronously.

Conversations were transcribed using Trint and coded for content across multiple domains. For example, conversations were coded for different kinds of rules (e.g., time limits, restrictions on device usage), explanations for these rules (e.g., health issues, authority, convenience), and concerns about internet safety (e.g., privacy, deception, harmful content).

Preliminary findings support two key hypotheses: (1) parents who discuss more potential harms of technology have children who echo these concerns, and (2) both parents and children believe other families are more lenient with screen time, suggesting a social comparison bias. Additional patterns include children frequently asking "why" when rules were explained, emotional dynamics such as parental guilt (when they use devices as 'babysitters'), and defensiveness from the child (when their problematic behavior is brought up with regard to using technology), as well as interesting conversations about whose job it is to keep the internet safe. Notably, families rarely discussed pressing issues like deceptive design, algorithmic manipulation, or cyberbullying.

This research contributes to developmental psychology by highlighting how children's attitudes toward technology are co-constructed through family dialogue. Findings have the potential to inform educational tools and interventions that promote healthier, more collaborative conversations about technology usage.

8 Principal Component Analysis of Neutron Star Equations of State

Yuxuan Bai, Carolyn Raithel • Physics and Astronomy, Swarthmore College

ybai1@swarthmore.edu

Neutron stars (NS) are a type of collapsed star formed from a supernova that are ~10 km in radius and weigh ~1-2 solar masses. They are governed by a theoretical, functional, pressure-density equation of state (EOS). The EOS can be numerically integrated to produce a corresponding mass-radius (MR) curve that represents the range of possible NS observables. A change in the EOS represents a different theory of the internal physics of neutron stars and this effects a complex change in the shape of the observable MR curve. A deeper understanding of this complex relationship will allow researchers to most effectively constrain the theoretical EOS using current and future NS observations.

We try to simplify this relationship using principal component analysis (PCA), a linear dimensionality-reduction technique. For a given set of input data of E samples with n *feature* data points (features), PCA calculates a new orthogonal basis set of n *feature*-dimensional vectors, called principal components (PC), such that each PC maximizes the variance explained in the input. Importantly, a linear combination of an arbitrary number n *comp* of PC vectors can be used to estimate the original data set in a n *comp*-dimensional space, effectively "compressing" the data. In addition, these PC vectors can themselves be interpreted as the major "patterns of variation" in the original data.

We apply PCA to a large data set of highly-varied EOS functions and demonstrate that a small number of PC vectors consistently and accurately recreates the original data. We demonstrate that we can consistently and accurately reconstruct the MR curves using a small number of PC vectors, and using more PC vectors increases the accuracy of the MR recreations. Crucially, this suggests that PCA can be successful in extracting the major modes of variation among EOS functions that result in major variations in MR curves. This allows us to potentially find simple, general relationships between EOS curves and MR curves, compare the two spaces, and analyze any given set of theoretical EOS models.

9 aba-Sets & Semi-Quotients

Ryan Baldwin, Pat Devlin • Swarthmore College

rbaldwi2@swarthmore.edu, pdevlin2@swarthmore.edu

Throughout this summer, my faculty advisor Pat Devlin and I conducted a thorough investigation on the structure of finite-sets under a particular operation (rule) on the set: for every element a, b in the set, aba was also an element of the set.

These sets, paired with the aba-operation, formed a larger set with a special property referred to as "aba-closure," a set generated under the operation is aba-closed with itself entirely. We later found examples of this kind of aba-closed set in two discrete subgroups of isometries of the plane— the dihedral group Dn, and the cyclic group Cn. Due to the complexities of these algebraic objects, we also studied the algebraic structure of crystallographic groups and how they behave in both the plane R^2 and 3-dimensional space R^3.

Although we were working with groups explicitly, we later then realized that aba-closed sets had similarities to the structure of an ideal, an algebraic object found in rings. However, ideals can maintain closure when operated with other elements in the ring, whereas aba-closed sets do not always have this property a priori. We searched for a firm example of a "semi-coset," which would have this property similar to that of an ideal. Once we found such a set, we would later develop a theory analogous to quotient groups. These algebraic structures are used to view the behavior of the group through "regrouping" well-divided chunks of the group in order to construct isomorphisms between groups (i.e. we can prove two seemingly different groups are really the same up to relabeling).

Using a specific semi-coset L⊆D3, we tested our developed theory on what we called semi-quotient groups. We constructed a semi-quotient group by (1) computing the set {dihedral group D3 modulo L} and (2) imposing an aba-operation on the set. Not only was the resulting semi-quotient a group under the operation of D3, but it was an existing aba-set within D3— we found the set to be isomorphic to the cyclic group C3. However, we realized that the divisor was related to a normal subgroup in D3.

As mathematicians, we continued to search for a firm example to support our hypotheses and spent the remaining weeks working in the nonabelian group of order 75. We believe that there may exist a semi-coset we could use to further test our theory on the relationship between semi-cosets and properties between semi-quotient isomorphisms.

10 An ultrasound study of Russian palatalized and velarized consonants

Tehya Banach, Jonathan Washington • Swarthmore College

Tbanach1@swarthmore.edu

This pilot study addresses the following questions: (1) Are previous claims of a pharyngeal difference between the Russian palatalised (Cʲ) and "velarised" (Cˠ) series supported? (2) Are Russian velar Cs distinct from other Cs in their implementation of the Cʲ~Cˠ contrast? (3) Is the mid high vowel in Russian an allophonic realisation of the front high vowel occurring after Cˠs, or can it be considered a distinct phoneme of the language? and (4) What is the impact of adjacent V backness on Cʲ and Cˠ articulation?

Recordings were made with the Articulate Instruments Micro system using AAA software and the Articulate Instruments ultrasound stabilisation headset in a single session in December of 2020 by author 2, who recorded himself. Author 2 is a middle-aged L1 speaker of Russian who has lived in Russia his whole life and uses Russian on a daily basis. He is a linguist and an English teacher, and has working knowledge of Mandarin and several South Siberian Turkic languages. Stimuli were embedded in the carrier sentence Слово X отличное, "The word X is splendid." Each sentence was repeated 3 times. The 2nd repetition was used for study. Using Praat, segments were delineated and annotated for adjacency to front Vs (i, e), back Vs (a, o, u), and [ɨ]. Segments adjacent to a mix of these or another consonant in the same word were excluded. Ultrasound frames closest to segment midpoint were manually traced using UltraTrace and plotted using ultrapolaRplot to depict mean lines and standard deviation bands in a polar coordinate system.

(1) For Cʲ, TB is raised towards the palate and TR is advanced in the pharynx, while for Cˠ, TB is low and TR is retracted, supporting previous accounts. Cʲ is similar to both /i/and /j/, although TB is lower. For averaged Cʲ and Cˠ, respectively; /Kʲ/~/Kˠ/ and /nʲ/~/nˠ/stand out as distinct from other categories, with a raised TB for Cʲ and a raised tongue dorsum for Cˠ. Hence /nʲ/ and /nˠ/ may more appropriately be true palatal /ɲ/ and plain/n/, respectively, for this speaker. /Kˠ/ appears to be velar with TR retraction. (2) The velars do exhibit a robust Cʲ~Cˠ distinction, but implement it differently than other Cs: Kʲ maintains front-velar contact and TR position is not exceedingly distinct from Kˠ. Additionally, TB is raised into the palate for Cʲ and TB retracted into the pharynx for Cˠ.(3) The distinction between Cˠi and Cˠɨ does not appear robust, but the data is too sparse to draw strong conclusions. (4) Adjacent vowel backness has mostly negligible impact on tongue position.

11 Using capillary electrophoresis to quantify competitive adsorption of eco-corona constituents to silver nanoparticles

Iris Barone, Kathryn R. Riley • Swarthmore College

ibarone1@swarthmore.edu

Silver nanoparticles (AgNPs) and the formation of eco-coronas have applications in the environmental and medical industries. Eco-coronas form when molecules adsorb to the AgNP surface, altering the particle's fate and toxicity. Understanding surface interactions of AgNPs with different molecules in a complex matrix is crucial to tuning AgNPs for desired applications. Citrate coated nanoparticles of three different sizes were studied: 10, 20, and 40nm AgNPs. Bovine serum albumin (BSA) and Suwannee River humic acid (SRHA) were used as model protein and organic matter, respectively. Several binding conditions were studied, including independent, competitive, and sequential adsorption of BSA and SRHA with each AgNP. Previous corona characterization included dynamic light scattering (DLS) and UV-vis spectroscopy Langmuir isotherms. The secondary structure of BSA was previously quantified using circular dichroism (CD) spectroscopy. The current work focuses on capillary electrophoresis (CE) and the pull-down assay to quantify the amount of BSA and SRHA adsorbed in each corona condition. First, the incubation time for this assay was optimized to minimize non-specific adsorption of BSA and SRHA. The initial findings of this assay show the

binding of a BSA-SRHA complex to the AgNP and confirm SRHA displacement of surface BSA according to the Vroman effect. Nonequilibrium capillary electrophoresis of equilibrium mixtures (NECEEM) will be used to quantify the binding and rate constants of the different adsorbate conditions. Data from qualitative and quantitative analyses, as well as preliminary results from the pull-down assay will be presented.

12 Spatial and temporal variations of larval crabs in Puget Sound

Lane Barron, Dr. Karen Chan • University of Washington

Dbarron1@swarthmore.edu

Most marine invertebrates have complex life histories, including crabs that metamorphose from planktonic larvae (zoea and megalopae) to benthic adults. Despite their commercial, ecological, and cultural importance in the Pacific Northwest, larval crab transport are not well characterized. Puget Sound is a dynamic fjord in Washington that encompasses multiple sub-basins. Using field plankton survey, we explored how physical conditions shape abundance, distribution and taxonomic composition of larval crabs. Oblique tow samples were collected from the Strait of Juan de Fuca, Hood Canal, and Main Basin in spring, summer, and fall. Zoea and megalopae were identified to the family level through microscopy. Zoea were present across all seasons, and as expected, were more abundant than megalopae, which were not observed in spring. Surprisingly, Hood Canal, a shallow site with sluggish flow, had the highest zoea abundance, although individuals were smaller in size, suggesting potential local retention. The Strait had the most megalopae, suggesting potential outer coast supplementation. Pinnotheridae zoea dominated the Strait, while Cancridae zoea were most prevalent in Hood Canal; both families were present in the Main Basin throughout all seasons. Correlating abundance data with physical conditions, e.g., temperature, chlorophyll concentration, and pH, help us understand the environmental drivers underlying crab population supply in Puget Sound. These insights are critical for informing management strategies in the face of changing ocean conditions.

13 Representation Theory of Sn and the LIS Function

Adil Beken, Pat Devlin • Swarthmore College

abeken1@swarthmore.edu

In this project, we explored the representation theory of the symmetric group and how it can be applied to answer questions about the longest increasing subsequence (LIS) function. The longest increasing subsequence function is a map from Sn to the natural numbers that assigns to each permutation the length of its longest increasing subsequence, i.e., the longest subsequence whose entries appear in increasing order. This function has many applications in computer science and combinatorics and has been extensively studied. For example, its average over the whole group Sn is known to be approximately $2\sqrt{n}$. However, less is known about the average of this function over subgroups of Sn. Our main goal for this project was to find such averages for subgroups of Sn. To achieve this, we used the Plancherel formula for the Fourier transform on locally compact groups. The formula connects the sum over a group of the product of two functions and the irreducible representations of this group. In this case, the two functions were the indicator function of a subgroup and the LIS function, which, when multiplied and summed over the group, give the sum of the LIS function over the desired subgroup. This approach allowed us to express the average of the LIS function over a given subgroup in terms of irreducible representations, matrices, and trace values. After that, we examined these formulas and attempted simplifying them or calculating the result for different subgroups using properties of irreducible representations and characters.

14 Aperiodic and periodic components of EEG power spectra vary by time of day

Aatrey Bidkar, Eoin Quinn, Brian Metzger • Swarthmore College

abidkar1@swarthmore.edu

A central pursuit of clinical neuroscience has been the identification of biomarkers for neuropsychological disorders. Following an influential paper by Donoghue and colleagues (2020), the field has seen renewed interest in using aperiodic and periodic spectral features of EEG to better

understand the neural underpinnings of behavior and cognition. More recently, researchers have used aperiodic spectral features (1/F slope and intercept) to identify novel biomarkers, especially for treatment-resistant forms of depression (e.g., Hacker et al. 2024; Xiao et al. 2023). 1/F slope is thought to reflect the balance of neural excitation and inhibition (EIB), with shallower slopes indicating greater excitation and neural activation (Gao et al. 2017). Lendner and colleagues (2020) showed that 1/F slope varies as a function of arousal, potentially confounding observed associations between 1/F slope, behavior, cognition, and mood. The present study assesses time of day as a potential confound. Preliminary analyses of frontal resting state EEG data in 47 participants suggest that aperiodic slope, but not aperiodic offset or alpha power, is correlated with time of day. These findings suggest that time of day may be a potential mediator of 1/F behavioral associations, including mood. To further explore these relationships, we intend to run mediator and moderator analyses to better understand the nature of the association between 1/F and mood. By analyzing data from 64 electrodes (standard 10-10 system), we intend to construct a more global picture of the relationship between periodic and aperiodic spectral features, time of day, and mood.

15 Characterization of a Synthetic Diversity Mixer-First RF Receiver

Kimaru Boruett, Prof. Alyosha Molnar • Cornell University

eboruet1@swarthmore.edu

This research focused on the characterization of a novel wideband, mixer-first synthetic diversity receiver operating from 2–6 GHz. Modern wireless systems face significant challenges from spectrum congestion, where strong out-of-band interferers can generate in-band artifacts through mechanisms like reciprocal mixing and intermodulation. To address this, the receiver under test departs from previous LNA-based designs by omitting the low-noise amplifier, with the goal of improving system linearity. The architecture employs a four-channel passive front-end with synthetic diversity to maximize the signal-to-noise ratio and enhance overall data rate.

My primary contribution was the development and enhancement of a semi-automated testbed using MATLAB, VISA, and SCPI commands. This framework automated the control of instruments like signal generators and power supplies, enabling efficient and repeatable sweeps across the receiver's operational frequency range and at various power levels.

Key performance metrics were characterized by evaluating the receiver's sensitivity and linearity. These included the Noise Figure (NF), which quantifies noise added by the system as the ratio of input to output SNR. Linearity was assessed using the Blocker 1-dB Compression Point (B1dB), found by increasing blocker power until the desired signal drops 1 dB, and the Third-Order Intercept Point (IIP3), measured using a two-tone test. Exploratory tests were also conducted to investigate harmonic down-conversion and spur-induced artifacts using single-tone stimuli.

The data analysis pipeline involved capturing raw I/Q data across the four receiver channels. This data was then pre-processed through synchronization and DC-offset removal before undergoing FFT analysis in the frequency domain. To ensure measurement accuracy, particularly for sensitive IIP3 tests, channel-by-channel debugging was performed. Overall, this work successfully produced a comprehensive dataset characterizing the 2-6 GHz mixer-first receiver, enabling a direct performance comparison with prior LNA-based designs.

16 Constructing a low-rank implicit algorithm for solving high-dimensional equations in the hierarchical Tucker tensor format

Paolo Bosques-Paulet, Joseph Nakao • Swarthmore College

pbosque1@swarthmore.edu

Partial Differential equations can be found across physics, biology, and finance. Efficient computation of PDE solutions open the gateways to high performance and high accuracy models in all of these contexts. Standard integrators for PDE solutions quickly exhaust the storage capacity of most computers. To combat this problem, tensors that store the PDE solutions at each time step are decomposed (via the Tucker decomposition) into a storage friendly product of Matrices and a smaller

tensor. However, for high dimensional problems, even operations with the Tucker decomposed PDE solutions are too costly. In this project, the aim is to develop a completely novel algorithm using the Hierarchical Tensor Decomposition to efficiently compute the solutions to diffusion equations. A working algorithm using Hierarchical tensor decompositions is developed for 3D diffusion equations with 1D laplacian. This laid the foundation for a working algorithm for 4D diffusion equations with 2D laplacian. First order accuracy is developed for both algorithms.

The present algorithm can be extended in dimension and to advection diffusion problems. PDEs of this type model problems in plasma physics, fluid dynamics, price of stock options, and many more important fields.

17 Implantable Probes for Long-Term Neuronal Recording

Jasmine Branda, Nicole Collette, Lucas Carstensen • Lawrence Livermore National Laboratory

jbranda1@swarthmore.edu

Investigation of neural circuit function during behavior requires stable, real-time recording of neuronal activities. Engineers at Lawrence Livermore National Laboratory (LLNL) have developed a multi-shank, multi-electrode probe that allows for recording from up to 128 neurons simultaneously. A defining feature of the probe is its exceedingly delicate, thin-film design, which makes it extremely flexible. This high degree of flexibility reduces the risk of tissue damage and immune responses, which are significant problems associated with conventional rigid probes. However, implantation of such a highly flexible probe is a major challenge. We report development of a new surgical protocol that ensures precise and reproducible implantation of the LLNL probe in the rat brain. Our proof-of-concept studies focused on inserting the probe into the CA1 hippocampal region, which plays a critical role in memory processing and learning, and is particularly vulnerable to age-related damage. Recording neuronal activities in CA1 should provide important insights into neurodegenerative disorders. We demonstrated successful implantation by coating the probe with tracer dye, inserting it into CA1, retracting the probe, collecting the brain, generating live tissue slices using a vibrating microtome (Compresstome), and then verifying proper probe placement via fluorescence microscopy and tissue health via histological staining and light microscopy. This work establishes a new capability for safe and effective implantation of the LLNL probe, which offers opportunity for long-term, high-density neuronal recording during behavior. In the future, the probe design may include additional features that enable neural stimulation, chemical sensing, and optogenetics, thereby expanding the scope and resolution of neural circuit analyses.

18 Robotic Barnacle Nauplii Model

Nathan Brewer, John Carty, Dr. Carr Everbach • Swarthmore College

nbrewer1@swarthmore.edu, jcarty1@swarthmore.edu

All barnacle species progress through a developmental period known as the nauplius stage. Characterized by a three-part segmented body contained within a carapace structure, nauplii swim with a unique stroke pattern. Three pairs of appendages move in patterned sequences to propel the nauplii at very low Reynolds numbers. Though largely sessile in maturity, barnacle larvae in this stage are highly mobile with varied morphology across species. Understanding the impact of the carapace morphology on the hydrodynamics of nauplii motion is key to understanding constraints on ecological functions and dispersal of marine invertebrates. These questions guide our collaborators' research in the Quantitative Plankton Ecology Lab (QPEL) at the University of Washington, Seattle. The microscopic scale of the nauplii makes accurate hydrodynamic force data nearly impossible to gather, necessitating the construction of a robotic model at scale. The equations dictating Reynolds number allow us to maintain the low Reynolds environment at a higher scale by utilizing a more viscous solution of Karo syrup and water.

We set out to construct a modular clockwork mechanism to accurately replicate the angular sweep and phase of the nauplii appendages. Utilizing a single motor with a vertical driveshaft, we successfully replicated lab-gathered angular sweep data to within 5-degree accuracy. The appendages were

designed with an internal hollow slider to maintain a constant appendage length through the sweep and minimize any piston effects of the viscous fluid. Each appendage set was made modular, as to allow us to change the vertical position of each appendage, helping us to gather further data about the out of plane motion effects. The motor for these appendages is controlled by a light-activation circuit of our design. In order to aid setup for testing, the nauplius robot is designed with an adjustable-threshold, adjustable-output light activation mechanism. This allows the robot to be set up in the dark and activated without reaching into the tank and potentially disturbing the force data equipment. All of these internals are integrated beneath a biologically accurate *polyascus plana* carapace, enabling our collaborators at UW to gather accurate force data.

Though this project was initially undertaken for the researchers at the QPEL, our robot has potential in other industry sectors. Viscous environments require specialized locomotion to run efficiently, which our robot was designed for. Extraterrestrial environments, such as the ice slush boundary on the subsurface oceans of Europa, are difficult for more conventional robots to explore, making biomimetic robotics a valuable research area in rapidly expanding sector of space exploration.

19 Staircases in the Sea: Glider-Based Insights into Ocean Mixing in the Sea

Nana Brobbey and Joe Gradone

Thermohaline staircases are step-like layers in the ocean which are formed when warmer, saltier waters sit on top of colder, fresher water. These layers are formed from double-diffusive mixing due to heat and salt diffusing at different rates. Studying ocean mixing helps us characterize how water masses interact and influence the broader physical and biogeochemical processes in the ocean. Oceanic mixing in the form of thermohaline staircases is an important process in the Caribbean Sea as alters the water masses in the upper-limb of the Atlantic Meridional Overturning Circulation (AMOC) system. However, ocean mixing is poorly understood in the Caribbean due to the historical lack of in situ observations. In 2024, an autonomous underwater glider conducted two 600 km transects in the Central Caribbean and provided high-resolution sampling of thermohaline staircases. This study uses an automated classifier algorithm developed for understanding glider data to reveal spatial and temporal variability of thermohaline staircases. We find that staircases are present in the central latitudes of the Caribbean, and their presence is confined to certain ranges: a range of 1.5-1.75 for density ratio, a temperature gradient less than 0.04, and a salinity gradient less than 0.005. Calculated values for Turner angle suggest that diffusive mixing decreases with depth where it is strongest at 300-400 meters to its weakest at near 800 meters. Over the course of the 2 months sampled, the pattern and characteristics of thermohaline staircases are nearly consistent. This suggests that there are hotspots of diffusive mixing in the Caribbean, but further investigation needs to be done. Future work will explore how varying the vertical resolution of the data input to the classification algorithm affects staircase detection, machine learning approaches for staircase detection, and the role of background currents on staircase variability.

20 Automating Phasor Analysis of Fluorescence Lifetime Imaging Data

Alexander (Aleco) Buendia and Prof. Sara Sohail • Swarthmore College

abuendi2@swarthmore.edu

Fluorescence Lifetime Imaging Microscopy (FLIM) is a powerful technique for quantifying the local molecular environment of a fluorophore by analyzing its fluorescence decay dynamics. FLIM has numerous applications, including analysis of cellular environments, protein-protein interactions, and microplastic identification. Our lab uses FLIM to characterize the complex self-assembly of amyloid fibrils in vitro. Amyloid protein aggregates are associated with numerous neurodegenerative diseases, including Alzheimer's and Huntington's disease, and are also being explored as novel biomaterials due to their unique functional properties. Amyloid kinetics are characterized by the assembly of soluble, disordered monomers into insoluble fibrils. Structural differences in fibril morphology, known as polymorphism, are strongly influenced by environmental factors like pH, temperature, and ionic strength. Polymorphism is an interesting physical phenomenon of amyloid assembly, which we seek to understand better.

To characterize amyloid polymorphism, our lab utilizes phasor plots applying a Fourier transform to

the time domain data and then visualizing in a two-dimensional phasor space. Phasor analysis is fit-free and creates an effectively higher resolution FLIM image. However, the conventional workflow of phasor analysis relies on time-consuming manual data processing followed by manual segmentation of the phasor plot, a step that is inherently subjective and creates a bottleneck for high-throughput analysis. To address this issue, we developed an automated processing and analysis system using an unsupervised machine learning algorithm, specifically a Gaussian Mixture Model (GMM) for automated clustering of phasor plot data. GMM is particularly well-suited for FLIM applications due to the Gaussian distribution of decay populations in phasor space. We aimed to provide a user-friendly tool with a graphical user interface that automates the processing and clustering of FLIM-phasor data, allowing a quantitative and high-throughput analysis for any researcher using FLIM imaging.

21 Deferred Concolic Execution Interpreter

Aiperi Bush, Zachary Palmer • Swarthmore College

abush1@swarthmore.edu

One of the biggest challenges in debugging computer programs is managing the sheer number of different possible execution pathways. Programs that need to be debugged often have very complicated branching, and can take a very long time to debug since each of these paths must be explored to determine if there's an error. An efficient debugger needs to carefully choose inputs so it can hit as many paths as possible without repeating any pathways. An existing debugging tool developed at Johns Hopkins University approaches this problem via concolic execution: a technique that combines the use of concrete values as test inputs with the use of symbolic values to keep track of the program's branching. The debugger generally works very effectively, usually finding bugs in less than a second. However, some tests take around 8 minutes to finish running, which is impractical for use in an active development environment.

This project seeks to develop a new debugger that improves the performance of the existing project. Our debugger uses a deferred system, where certain portions of code are set aside for future evaluation while the debugger focuses on later sections of the program. This technique allows our tool to target areas of the code which are more likely to have errors, speeding up the process of debugging.

We formalized the specific steps that our debugger would use to evaluate the test program. These specifications were similar to the operational semantics that defined execution for functional languages such as OCaml, but they had to keep track of unusual information, such as the sections of code that had been deferred for future evaluation. Additionally, we needed to ensure that the deferred system would give us the same result as the eager interpreter despite running things out of order. If a particular set of inputs yielded an error within our existing concolic system, the deferred system also needed to identify it.

Preliminary progress shows that our code is a little faster on some programs and a little slower on others. We think we can make some basic optimizations to improve performance, which could significantly improve the time it takes to identify certain kinds of errors. Additionally, the median amount of time spent debugging is more consistent under the new deferred system, which is significant because a program that consistently evaluates moderately fast is far more reliable than a program that only sometimes runs fast.

22 Symplectic Integration of Vortex Contour Dynamics

Emily Chen, Emad Masroor • Swarthmore College

Echen6@swarthmore.edu

This project focused on replicating and validating early research in contour dynamics initiated by Zabusky, whose pioneering work established contour dynamics as a powerful tool for studying two-dimensional, incompressible, inviscid flows. Contour dynamics studies the evolution of these flows as it describes entirely by the motion of vortex boundaries, rather than solving the full vorticity field on a grid. This reduction transforms the problem into a Hamiltonian system, where the boundary is advected according to the Biot–Savart law. This Hamiltonian formulation offers a segway for highly efficient numerical simulation. The main objective of this project was to reproduce Zabusky's results

using a modern algorithmic framework and, in particular, to implement a symplectic time-stepping scheme. Symplectic integrators are well suited for Hamiltonian systems since they preserve the underlying symplectic structure of phase space, preventing growth of numerical error in conserved quantities such as area. The simulations successfully reproduced features of contour dynamics, including the roll-up of vortex sheets, the preservation of area enclosed by the contour, and the generation of fine-scale filamentary structures. The consistency between my results and the original work provides a robust validation of both the symplectic approach and the underlying theoretical framework. Furthermore, the numerical experiments confirmed that the symplectic scheme significantly improves stability over long time horizons compared to traditional explicit integrators. This work allows for future extensions of contour dynamics to more complex domains, higher-order symplectic methods, and three-dimensional spaces. This project highlights the importance of contour dynamics within the Hamiltonian framework, showcases the benefits of symplectic integration, and provides a validated computational foundation for advancing theoretical and numerical studies of vortex-dominated flows.

23 Fluorescence Lifetime Imaging Reveals Concentration Dependent Polymorphism in CsgA R5 Fibrils

Julian Y.J. Chen and Sara H. Sohail • Swarthmore College Department of Chemistry and Biochemistry
jchen16@swarthmore.edu

Amyloid fibrils are highly ordered, β-sheet-rich protein assemblies found across all domains of life. While historically associated with neurodegenerative diseases, functional amyloids—such as *E. coli* curli fibrils—demonstrate that amyloid formation can serve physiological roles. The R5 repeat of the curli subunit protein CsgA provides a reductionist system for investigating the biophysical properties of functional amyloid assemblies. We are specifically interested in the polymorphism of R5 amyloids, or the diversity of structures they can form. We use time-correlated single photon counting (TCSPC)-based fluorescence lifetime imaging microscopy (FLIM) to assess how R5 concentration modulates fibril structure.Using the amyloid-binding fluorescent dye Thioflavin T (ThT), we observe a shift in ThT fluorescence lifetime at different concentrations of R5. Aggregates formed at 10 μM R5 exhibit significantly longer lifetimes than those formed at 100 μM R5. This effect is not attributable to dye incubation. Dilution experiments confirm that ThT lifetimes remain stable post-aggregation, indicating that there are concentration-dependent polymorphs that represent metastable folding states. Previous studies suggest that longer ThT lifetimes could possibly correspond to tighter dye binding to the fibril. Steady-state fluorescence anisotropy measurements indicate that ThT is, in fact, more rigidly bound to 100 μM R5 fibrils than to 10 μM R5 fibrils, ostensibly contradicting shorter ThT lifetimes observed at 100 μM. These complementary experiments further highlight the structural complexity of each polymorph. Confocal FLIM and transmission electron microscopy (TEM) images further reveal a distinct population of thin, protofibrillar structures unique to 10 μM samples, with 100 μM samples exhibit dense, globular aggregates consistent with established literature. In addition, Nile Red fibril-bound lifetimes remain constant across concentrations, suggesting that differences in β-sheet architecture, rather than hydrophobic exposure, underlie the observed concentration-dependent lifetime behavior. These findings support a model of concentration-dependent structural selection in R5 fibrillization, with implications for the rational control of amyloid-based nanomaterials.

24 Tenure Segregation & LIHTC Placement: How Affordable Housing Placement Reproduces Existing Inequity

Yu-Jing (Laine) Chen, Natalia Lashley, Peter Hepburn • Eviction Lab
ychen10@swarthmore.edu, nlashle1@swarthmore.edu

The Low-Income Housing Tax Credit (LIHTC) program is the largest US housing subsidy program, intended to expand the amount of accessible and affordable rental options. Past research has evaluated LIHTC's relation to racial and income segregation; however, patterns of segregation by housing tenure—namely renters and homeowners—remain underexplored. This study addresses that gap by analyzing tract-level census and housing data across the 100 largest metropolitan areas (MSAs) from

1980 to 2019, supplemented by case studies of New York, Philadelphia, Chicago, and Houston MSAs. We aim to answer two questions:1) Is LIHTC placement disproportionately concentrated in renter-heavy tracts? 2) Does LIHTC exacerbate or mitigate tenure segregation over time?

Descriptive analysis and regression analysis indicate that neighborhoods with high renter concentration have consistently been more likely to receive LIHTC units, which reinforces tenure divides rather than promoting mixed-tenure housing. The recipient neighborhoods also tend to be racially minoritized and low-income, underscoring the intersection of tenure, racial, and income segregation. To pinpoint the second question, LIHTC-treated tracts have become more renter-concentrated than untreated tracts over the full period of the program's implementation. Aimed at advancing the practice of equitable housing, this study highlights the importance of critically examining the placement strategies and suggests that future policy reforms should be designed to prevent over-clustering of rental units.

25 Synthesis and Characterization of Novel Magnetic 2D Materials via Elemental Tuning of Alloyed Chromium Thiophosphates

Evan Chin[1], Jacob Baillie[2], Nicolas Nguyen[2], Rémi Beaulac[1], Daniel Gamelin[2]
[1]Swarthmore College, [2]The University of Washington
echin2@swarthmore.edu

Layered 2D van der Waals (vdW) materials exhibit unique tunable magnetic and optical properties, holding great potential for their application as semiconductors, catalysts, and in computer memory. In particular, chromium-based vdW materials, such as the chromium trihalides (CrX_3, X = Cl, Br, I), chromium sulfur bromide (CrSBr), and chromium thiophosphate ($CrPS_4$), have recently received a lot of attention due to their magnetic properties that persist even down to few/monolayer samples. Altering the elemental composition of these materials has the potential to alter their properties, expanding the range of possible applications relying on these materials. In this study, we synthesized a set of alloyed chromium thiophosphates ($Cr_{1-x}M_xPS_4$, M = V, Mn, Fe, Cu, Ga, Y) where $0<x<1$. To accomplish this, a modified chemical vapor transport (CVT) synthesis methodology was developed to enable higher throughput. The resulting crystals were characterized by X-ray diffraction (XRD), scanning electron microscopy (SEM), and energy-dispersive X-ray spectroscopy (EDX). The optical and electronic properties of selected promising samples were investigated further using near-infrared luminescence spectroscopy. Analyzing the elemental compositions and structures of the synthesized crystals, we identified vanadium as a successful candidate for alloying. From the photoluminescence spectra of the vanadium alloy, highly efficient quenching of the chromium spectra is observed. These results demonstrate the ability to synthesize certain $Cr_{1-x}M_xPS_4$ alloys through CVT and the potential to manipulate structural and optical properties through alloying.

26 Repeatability of the endocrine stress response: a 5-year longitudinal study in an *Octodon degus* cohort

Ava Choi, Carolyn Bauer • Swarthmore College
achoi4@swarthmore.edu

Glucocorticoids, such as cortisol, are the major mediators of the endocrine stress response in vertebrates, also known as the hypothalamic-pituitary-adrenal axis. At baseline levels, cortisol supports basic metabolic functions. Once a stressor is introduced, cortisol levels significantly increase. This mediates physiological functions that help animals cope with these stressors and return to homeostasis. Exposure to high levels of cortisol, however, increases chances of chronic stress-related pathologies such as diabetes, infertility, and hypertension. Thus, negative feedback, or the ability to decrease cortisol levels after stress inducement, is another critical component of the stress response, as weak negative feedback leaves individuals exposed to great integrated amounts of cortisol. Cortisol levels have been assumed to be repeatable in individual animals, yet this assumption has only been tested over short periods of time and never over the entire lifespan of most species. In this study, we used a social rodent species, the common degu *(Octodon degus)*, under controlled laboratory conditions to test the hypothesis that the endocrine stress response

will change with age but remain repeatable within a cohort of males and females over their lifetime. To test this, we took blood samples to assess baseline cortisol levels, stress-induced cortisol levels, and cortisol negative feedback strength from the same cohort of degus at ten different timepoints between 1-58 months of age. We found that baseline cortisol levels are low early in life and steadily increase until about 10 months of age. Stress-induced cortisol levels followed similar trends but showed an additional increase at 58 months of age. Negative feedback strength weakened with age and was weaker in females compared to males. In terms of repeatability, we found that negative feedback strength, but not baseline and stress-induced cortisol levels, was significantly repeatable over time within our degu cohort. Our results suggest that degus experience greater total cortisol exposure as they age, which may increase their risk for developing pathologies related to chronic stress. These results help contextualize the relationship between age and the endocrine stress response. We also found that cortisol negative feedback strength is the most repeatable component of the degu's stress profile. Additionally, these results suggest that an individual's baseline and stress-induced cortisol at one time point are not representative of a future time point, opposing the assumption that the endocrine stress response is repeatable over an animal's lifetime.

27 FGF Receptor Trafficking During Cell Division in Human Cells

Thanisha Chowdhury, Bradley Davidson • Swarthmore College

tchowdh1@swarthmore.edu

Growth factor receptors regulate cellular growth and differentiation. Mutant growth factor receptors have been linked to cancer and are targets for cancer treatment. During mitotic entry, the plasma membrane with internalized receptors is internalized into endosomes to facilitate cell rounding while during mitotic exit, the membrane is recycled back to the surface along with receptors to promote division. In our lab we study the trafficking of Fibroblast Growth Factor Receptors (FGFR) in the invertebrate *Ciona robusta* and our published work indicates that FGF receptors are internalized along with the associated membrane during mitotic entry, and then stored through inhibition of endosome degradation and recycling pathways. We are investigating whether this model of receptor internalization and storage applies to human cells by examining the localization of FGFR-GFP fusion proteins in HeLa cancer cell lines. Transfected FGFR-GFP HeLa cells were synchronized in interphase using CDK-1 inhibitors, and then released for 30 minutes to allow them to enter into mitosis prior to fixation and staining. Our initial analysis indicates that the intensity of FGFR-GFP staining along the plasma membrane decreased during mitotic entry, supporting hypothesized receptor internalization during this period. We also observed that vesicle size decreased during mitotic entry, which does not support the hypothesized storage of receptors via inhibition of the degradation pathways during this period. Future studies will focus on imaging FGFR-GFP cells during the remaining stages of mitosis in order to fully characterize receptor trafficking and inhibiting CDK-1 during mitotic entry to further test the viability of the proposed model .

28 Exploring fundamental-mode universal relations for neutron stars

Isaac Chu, Carolyn Raithel • Swarthmore College

ichu1@swarthmore.edu

A neutron star is the collapsed core of a massive star, which is left behind after a supernova. Due to this, neutron stars house the densest matter that exists in the universe, making them a great subject of study for understanding how matter interacts under exceptionally extreme conditions. Gravitational waves from binary neutron star systems offer a powerful way of probing the equation of state (EOS) of dense matter, which describes the pressure associated with a particular density of matter. Although the dominant EOS effects enter through the tidal deformability, at high frequencies, dynamical tides can become important. Previous works have shown that dynamical tides associated with the f-modes of neutron stars can significantly affect the gravitational waveform, and that neglecting these f-modes can lead to large systematic biases in the inferred tidal deformability already by the fifth (O5) LIGO-Virgo observing run. To account for this, some waveform models employ universal, EOS-insensitive relations to estimate the f-mode frequency based on other parameters like the tidal deformability. To assess the universality of such relations, we examine the f-mode frequencies for a diverse sample of

EOSs by solving the linearized fluid perturbation equations for the f-mode frequency and damping time in full general relativity. We calculate the f-mode frequencies for ~30,000 randomly-generated parametric EOSs, including several pairs of tidal deformability "doppelgangers." These doppelgangers have identical mass vs. tidal deformability relations, but different mass vs. radius curves. Using the parametric EOS sample as a baseline, we analyze previously-proposed universal relations and explore trends in the residuals, to search for possible systematic breakdowns in these universal relations. We also pursue multi-parameter extensions of these existing relations, continuing to explore residual trends and measures of universality.

29 Investigating Sex-Specific Anxiety Responses to High-Fat Diet in Mice

Deedra A. Closser and Kaiya R. Spencer, Dr. Wambura C. Fobbs • Swarthmore College, Department of Psychology

Preceding studies have only considered the effect of sex or high-calorie diets on anxiety-like behavior in isolation; however, our lab intends to explore the interaction between these two variables. Previously, our lab used an Open Field Test (OFT) to assess anxiety-like behavior of male and female mice following 6 weeks on either a high-fat or standard chow diet. When compared to chow-fed mice, we observed increased anxiety-like behavior in HFD-fed females but reduced anxiety-like behavior in HFD-fed males. To expand our assessment, we tested new cohorts of male and female mice at the 6-week time point with four anxiety-testing behavioral assays: the OFT, the Light-Dark Box Test, Elevated Zero Maze, and Novelty Suppressed Feeding (NSF) Test. We were interested in determining if the differential impact of HFD on anxiety between the sexes was consistent across all four measures of anxiety-like behavior. The mice were introduced to either the HFD or standard chow diet before testing began, and the male cohort was started 2 weeks ahead of the female cohort (n=10 for each diet group within each sex cohort). Thus far, we have only analyzed the OFT and NSF Test data. In the OFT, there was a trend towards the HFD-fed males spending less time in the center of the arena than the chow-fed males, indicating greater anxiety-like behavior. In the NSF Test, HFD-fed males also exhibited behavior consistent with higher anxiety-like behavior than chow-fed mice: increased latency to eat and reduced food intake. In females, no significant differences were observed between diet groups in the OFT. In the NSF, however, HFD-fed females exhibited significantly longer latency to eat than chow-fed females, suggesting elevated anxiety-like behavior in this measure. The impact of HFD on anxiety-like behavior varied across measures, with stronger effects observed in the NSF than in the OFT. Overall, our current results contrast with earlier cohorts where female mice showed greater anxiety-like behavior than males across measures; in this cohort, differences were primarily observed in HFD males, who displayed trends of heightened anxiety-like behavior in both OFT and NSF tests, while female effects were limited to the NSF test.

30 Inducing HSATII Expression in HeLa and Primary Fibroblast Cells

Genine Collins, Dawn Carone, Ph.D., and Christina Rabeler • Swarthmore College, Carone Lab
gcollin1@swarthmore.edu

Human Satellite II (HSATII) is a noncoding sequence of satellite DNA that is composed of 26 base pair tandem repeats and is located near the centromere of many chromosomes. In cancer cells, heterochromatin decondensation enables transcription of HSATII DNA (Hall et al. 2017), resulting in nuclear RNA accumulations and cellular malformation. In order to study the development of these cancerous phenotypes and their effect on healthy cells, we must first determine if HSATII transcription is more dependent on chromosomal location or DNA sequence.

We previously conducted sequence analysis on several heterogeneous locations of HSATII in the genome, which ensures that any expression-related correlation between individual sequences is due to its location in the genome. To prepare all nine sequences for study, we followed a previously developed procedure for cloning HSATII DNA into the AAVSI-TRE3G TALEN plasmid, which allows for inducible expression of the HSATII insert once it successfully integrates at the AAVS1 safe harbor locus on chromosome 19.

To study HSATII expression, we transfect the plasmid into HeLa and primary fibroblast cell lines, both of which do not endogenously express HSATII. Previous attempts to do so, via a lipid-mediated

delivery system, had limited transfection efficiencies and were ineffective in establishing stable lines. By optimizing an electroporation procedure for each cell line, we achieved a higher transfection efficiency and established a stable line in HeLa cells.

By transfecting each prepared plasmid in both a cancer cell line (HeLa) and primary fibroblast cell line, we can compare the relative rate of cell division in the cancer cell to the development of such a phenotype in the primary fibroblast cells. We can then isolate the HSATII sequence(s) that yield(s) the most expression and fastest progression of cancerous phenotypes in the primary fibroblasts.

31 Magnetic Field Detection via Interferometry

Julian Courtney-Bacher, Eve Elrod, Tanvir Islam, Ahmad Stovall, Bella Thoen, Dr. Lynne Molter
Singer Hall Optic and Photonics Research Laboratory
jcourtn1@swarthmore.edu

Interferometry allows for very sensitive detection of changes to a system from outside stimuli. Interferometry involves splitting light into two paths, affecting one to create a path length difference, and then recombining the two to create a resultant interference pattern. In this research endeavor, it was explored to see if interferometry could be used to detect the presence of an external magnetic field. Ferrofluid, a water-based solution containing magnetic nanoparticles, was infused into the optical fiber in one of the two paths of the interferometer setup. As an external magnetic field is introduced to the interferometer system the effective path length, this refers to the change in path length caused by the refractive index in the medium through which the light travels, of the ferrofluid arm will increase. Thus, changes in the resultant interference pattern could be observed to relate the phase shift to the strength of an external magnetic field. Optimizations of the interferometer configuration were completed to minimize power loss by limiting the amount of optical fiber entries via the introduction of free space transmission. Additionally further work was completed to effectively fill the length of an optical fiber with ferrofluid via the capillary effect. In the future, further work will be done to resolve issues involving poor power transmission through the water-based ferrofluid currently being used in the system. Additionally, a possible fully connectorized setup for the interferometer is being considered to reduce the labor and time-consuming nature of continual alignment and reduce the variation of results.

32 GnRH-induced testosterone levels are repeatable in male *Octodon degus*

Ava Craig, Yuta Sato, Ava Choi, Annalise Di Cicco, Tate Garcia, Carolyn M. Bauer • Swarthmore College
acraig3@swarthmore.edu

Circulating testosterone levels are regulated by the hypothalamic-pituitary-gonadal (HPG) axis; in males, gonadotropin-releasing hormone (GnRH) is released from the hypothalamus, ultimately resulting in the production and secretion of testosterone (T) from the testes. Injection of exogenous GnRH (a GnRH challenge) is often used to produce a standardized response from an organism's HPG-axis by inducing maximal testosterone production. Because T plays an important role in multiple reproductive traits, many studies are interested in using an animals' baseline or GnRH-induced T levels as proxies of various reproductive variables, such as aggression, mating strategy, or reproductive success. However, these correlations rely on the assumption that T levels are repeatable, where the T level of an individual at one timepoint is predictive of their T levels at other timepoints. For this study, we chose to examine the repeatability of T levels in male *Octodon degus,* a diurnal rodent species native to central Chile. *O. degus* exhibit their highest endogenous T levels at 6:00 am during their inactive period and low T levels during their active period. Once every 2 weeks for a total of 8 weeks, we collected blood samples from 4-year-old male *Octodon degus* at both 6:00 am and 2 hours following a GnRH challenge. We found that while GnRH-induced T levels are significantly repeatable, baseline T levels were not significantly repeatable over an 8-week time period. These results suggest that GnRH-induced testosterone may be a more stable and reliable trait in field studies, although future studies should determine whether GnRH-induced T is biologically relevant when correlating with different reproductive traits.

33 Analysis of T Cell Receptors in Ewing sarcoma

Julianne Cruz, Dr. Ulrike Gerdemann • Boston, MA

jcruz2@swarthmore.edu

Ewing sarcoma is a rare pediatric malignancy of bone and soft tissues. Though immune cells, including T lymphocytes, have been observed within the Ewing sarcoma tumor microenvironment, the repertoire of T cell receptors (TCRs) in patient-derived samples has not yet been comprehensively characterized. Because TCR repertoires encode the history of antigen recognition and clonal expansion, profiling their composition may provide insight into how the immune system engages with Ewing sarcoma tumors.

In this project, we analyzed TCR sequencing data obtained from T cells isolated from Ewing sarcoma patient samples. Using pipelines made in R and Python, we performed quality control, data preprocessing, and repertoire profiling. Analyses included clonotype frequency distributions, diversity metrics, and V-J segment usage quantification. We were particularly interested in the paring of variable (V) and joining (J) segments, which together define the antigen-recognition region of the TCR, using scirpy workflows to visualize and reveal potential trends in segment recombination or selection. The goal was to determine whether consistent patterns emerged among patients, which could provide insight into how T cell receptors involved in recognizing Ewing sarcoma are structured. Preliminary findings revealed some recurring V–J associations, suggesting that shared immunological features may underlie the T cell response to this cancer. While the functional consequences of these patterns remain to be investigated, such findings underscore the utility of computational immunogenomics approaches for characterizing immune repertoires in rare cancers.

Overall, this work demonstrates how computational methods can be applied to high-throughput sequencing data to uncover characteristics of the TCR repertoire in Ewing sarcoma. The hope is that the analytical framework developed here, which includes diversity profiling, gene segment quantification, and network-style visualization, can offer a scalable approach for studying immune responses in rare cancers. In the long term, such analyses may contribute to the development of immunotherapeutic strategies by revealing the repertoire features most relevant to recognizing and targeting Ewing sarcoma tumors.

34 Investigating DELE1-mediated mitochondrial stress pathways using a modified CRISPR-Cas9 genetic screen

Amba Darst-Campbell, Kivanc Birsoy • The Rockefeller University

Adarstc1@swarthmore.edu

The mitochondria is a highly evolved organelle that serves as the hub for energy production and metabolic regulation. To coordinate energy distribution and production, mitochondria must communicate with the cell by sensing outside stress and relaying mitochondrial stress. Mutations in mitochondrial stress and repair pathways are hallmarks in multiple human diseases such as breast cancer, leukemia, Parkinson's, and Alzheimer's. Recent studies have uncovered heme-regulated eIF2α kinase's (HRI) critical role in relaying mitochondrial stress signals to the cytosol via an upstream pathway involving the mitochondrial protease OMA1 and its poorly characterized substrate DELE1. By understanding the stress conditions that lead to DELE1 accumulation, we can uncover how mitochondria relay precise stressors to the cytosol. Here we use a modified forward CRISPR-Cas9 lentivirus knockout screen to identify genes involved in DELE1 accumulation. Our modified Cas9 system takes advantage of the MS2 RNA loop-MS2 coat protein (MCP) interaction to preserve the linkage between the cellular genome and proteome.

35 Transfer, Motivation, and Three-Dimensional Science Learning of Middle School Students

Zhen Ning Deng, Mia Cox, Jasmine Flowers, Chris Ngo, K. Ann Renninger, and Kathryn R. Riley
Swarthmore College

zdeng2@swarthmore.edu

In order to address instructors' questions about learning in the Science for Kids workshops, this study explored students' ability to transfer, their motivation (belonging, interest, and self-efficacy), and their understanding of science, assessed based on three dimensions (cross-cutting concepts, disciplinary knowledge, and science and engineering practices). For science, it is necessary for students to develop working knowledge about the processes, procedures, theories, and concepts and to be able to transfer this understanding of one science activity to the next. Prior research on motivation and learning in the Science For Kids Workshops suggest that explicit instruction can provide an important foundation for inquiry learning, and has the potential to inform the instructional support needed for students to meaningfully engage science, positioning them to transfer. We used mixed methods (running observations of the workshop, task-based interviews, artifact analysis, and knowledge tests) to study 15 (8 boys, 7 girls) workshop participants. The students worked together as lab partners throughout five weeks of the workshop. Based on prior findings, lab partnerships were assigned based on the students' relative levels of motivation at the beginning of the workshop. Study findings suggest that the context of instruction serves to facilitate the depth of science transfer.

All lab partnerships demonstrated increases in knowledge of the workshop content. Results also indicated that student partners who had low relative motivation at the beginning of the workshop showed gains in motivation and transfer over time, whereas those with high relative motivation, either maintained or showed increases in both motivation and transfer. It appears that transfer not only can be observed, tracked, and prompted; our data suggest that whether and how students' transfer is a function of context: opportunities to explore, guided discussion, support on an individual level such as instructor interactions with individual lab partner pairs, culturally-relevant content (e.g., studying Chester water treatment, connecting energy content to their music performance).

36 Basal metabolic rate and glucocorticoid levels are not correlated in the rodent *Octodon degus*

Annalise Di Cicco, Sarah Heissenberger, and Carolyn M. Bauer • Swarthmore College

adicicc1@swarthmore.edu

Animals are constantly faced with environmental challenges such as fluctuating abiotic conditions, threats of predation, and conspecific competition. In order to cope with these changing conditions, multiple physiological systems coordinate to help animals maintain homeostasis. One such system is the endocrine stress response, which is ultimately mediated by glucocorticoids. Glucocorticoids regulate the allocation and utilization of carbohydrates, and under stressful conditions, glucocorticoids will rapidly increase to facilitate increased energy demands required for successfully coping with stressors. Metabolism, which is regulated via multiple physiological systems, is another important process that is necessary for responding to environmental challenges. Metabolism is generally measured via metabolic rate, or the pace at which glucose is converted into usable energy through cellular respiration. Therefore, when encountering a stressor, an animal's glucocorticoid levels and metabolic rate both substantially increase. While several studies have found positive correlations between metabolic rate and glucocorticoid levels within various species, these studies generally include both pre- and post-stressor timepoints in their analysis. This leaves a knowledge gap about metabolic rate and glucocorticoid levels in the absence of a stressor. We hypothesized that a positive correlation between metabolic rate and glucocorticoid levels is also present under non-stressed, baseline conditions. Using 34 adult *Octodon degus,* a non-traditional rodent model, we conducted flow-through respirometry to assess basal metabolic rate and took blood samples to measure baseline cortisol levels, stress-induced cortisol levels, and cortisol negative feedback efficacy. Degus oxygen consumption was measured using a small mammal respirometer. From these data we calculated the minimum amount of oxygen that each animal required during their inactive period (VO_2 min)

as a proxy for basal metabolic rate. Cortisol concentrations were assessed using a cortisol enzyme immunoassay kit. Contrary to our hypothesis, we did not find a significant correlation between basal metabolic rate and cortisol measures. These results suggest that an animal's basal metabolic rate is not predictive of its endocrine stress profile and that during stressors, glucocorticoids and metabolic rate may increase independent of one another.

37 Head Fat as a Proxy for Adiposity in Neuroimaging Studies

Joseph Eyiolowope, Sushaant Chawla, Jonatan Ottino-González, Michael Goran, and Shana Adise

Obesity affects brain structure and function, yet many neuroimaging studies do not account for adiposity. Head fat from brain MRI has been used to estimate Subcutaneous fat in adults but has not been done in children. Since most neuroimaging includes head fat, it may serve as a proxy when direct adiposity measures are unavailable. We compared head fat to BMI percentile, Subcutaneous, Visceral, Liver, and Pancreas fat to assess its potential as a proxy across fat depots with varying biological sensitivity. Data were drawn from *El Sendero,* a longitudinal birth cohort with assessments through age six; this analysis used data from the six-year visit. The sample included 67 children (58% female; 100% Latino/a/x/Hispanic). Head fat was derived from T1-weighted MRI using the Boney toolbox and expressed as a ratio to intracranial volume. Abdominal fat (Subcutaneous, Visceral, Liver, Pancreas) was obtained using Dixon abdominal MRI. BMI was calculated from height and weight and converted to percentiles using WHO growth charts. BMI percentile, Subcutaneous fat, and Visceral fat were strongly correlated with each other (Spearman $\rho = 0.90–0.83$), while Liver and Pancreas fat were weakly associated ($\rho = 0.54–0.40$). Head fat ratio strongly predicted, Subcutaneous fat ($R^2 = 0.54$), and Visceral fat ($R^2 = 0.47$), and moderately predicted BMI percentile ($R^2 = 0.30$). When covariates (age and sex) were removed from the models, R^2 values remained consistent, suggesting that head fat ratio independently captures variance in these adiposity measures. Liver and pancreas fat showed weaker associations ($R^2 = 0.12$ and 0.06, respectively). Head fat derived from brain MRI strongly predicted Subcutaneous and Visceral fat, and showed a moderate association with BMI percentile in children. These findings suggest that head fat may serve as a proxy for adiposity in neuroimaging studies where direct fat measures are unavailable. In contrast, liver and pancreas fat were not well predicted by head fat, likely due to factors such as genetics or dietary patterns.

38 Instrumental Coping Predicts Perseverance and Optimism in High School Students, While Coping Shows Limited Links to College Students' Well-Being

Abigail Fagersten Cavanaugh, Jane Gillham and Barbara Thelamour • Swarthmore College
afagers1@swarthmore.edu

Adolescence and early adulthood are crucial periods of psychological development, during which effective coping strategies play a protective role in promoting well-being and resilience. Social support coping strategies, such as seeking empathy or advice, may serve as protective factors against stress. This study examined how emotional and instrumental (e.g., seeking advice) forms of support coping relate to psychological well-being, particularly during key developmental periods. Cross-sectional data were collected from adolescents at an urban, predominantly immigrant high school in Philadelphia. A longitudinal study was conducted on college students from a small liberal arts college in the Mid-Atlantic, from which data were collected twice. Emotional and instrumental coping were assessed with the instrumental and emotional support coping subscales of the Coping Orientation to Problems Experienced Inventory (COPE), in both populations. Students' well-being in the high school population was measured using the Perseverance and Optimism subscales of the Engagement, Perseverance, Optimism, Connectedness, and Happiness measure of adolescent well-being (EPOCH). Students in the College Wellness Study (CWS) completed the Satisfaction with Life Scale (SWLS) and the Subjective Happiness Scale (SHS). In the high school sample, instrumental coping was positively associated with perseverance and optimism, whereas emotional coping was not. In the college sample, meditation analyses provided limited evidence that coping predicted well-being through loneliness. These findings suggest that instrumental coping may be especially beneficial for high schoolers' well-being, while direct problem-solving strategies may play a stronger role during the college years.

39 Purification of the B(TriNOx^{3-}) Metal Complex

Icie Favata, Professor Graves • Swarthmore College

ifavata1@swarthmore.edu

Developing metal coordination complexes capable of metal-ligand cooperative (MLC) activation of small molecules is a compelling area of research. We are currently investigating the coordination chemistry of group 13 metal complexes supported by non-innocent ligand frameworks, with a focus on the tripodal, tris(nitroxide) ligand system, TriNOx^{3-} complex. To this end, we focused our investigation on the synthesis and purification of the B(TriNOx^{3-}) complex. Our goal was to purify B(TriNOx^{3-} complex in order to explore the reactivity of (TriNOx^{3-})M (M=B) with CH_2X_2 in the future. Solubility tests were conducted to determine what solvents would be applicable for layered and slow evaporation reactions. After determining what solvents our complex would dissolve in, we began different variations of layered reactions using bulk and non-bulk starting reagents. To this end, we also set up different variations of slow evaporation reactions. We tested these reactions at room temperature and in the freezer to see if crystallization would occur. In the end, we found that most of our reactions stayed in their layered arrangements with a few crashing out into our starting material. This has led us to conclude that we should continue this investigation by trying new methods of synthesizing the B(TriNOx^{3-}) complex utilizing different starting materials and reagents. We also plan to investigate the B(TriNOx^{3-}) complex solubility with chlorinated solvents to see if different purification strategies can be used.

40 Effects of Surface Obtrusions on Granular Creep

Leilani Fleming, Nox Tan, Professor Cacey Bester • Swarthmore College

lflemin1@swarthmore.edu, atan1@swarthmore.edu

Granular media, characterized by a conglomeration of macroscopic grains, is unique in that the grains can exhibit properties of both solids and liquids, depending on the conditions. The movement of this media—anything from soil to rocks to icebergs—is not easy to model. The high impact that small variations in energy, grain arrangements, humidity, and temperature have on the large number of grains involved make it difficult to mathematically predict how even a pile of grains will flow when disturbed.

We tested the effect of surface obtrusions on the flow of a pile of grains. The setup involved pouring photoelastic grains—which, with the help of polarizing filters, show the forces among individual grains in the pile—into a two-dimensional frame, and tapping the pile. We analyzed images from each trial to determine pile changes including the movement, or creep, of grains and the shifts in forces.

A non-flat base reduced the creeping movement deep within the pile, particularly of a base of diagonal obtrusions, and no difference in flow was observed in the top layers of the pile. This could aid geological research by potentially being applied to predict soil movement or understand underlying bedrock based on topographic movement, and could aid industry by being used to optimize the flow or the stability of granular media.

Further research would include testing out different ways to disturb the system. The implementation of an "active grain", which sits in the pile of grains and vibrates, would show the effects of an internal disturbance. While the tapping arm may represent an earthquake shifting soil and rocks, an active grain would show the effect of something like an animal on an unstable hillslope. The role of disturbances combined with the varying base shapes would lead to a better understanding of what factors affect creep and failure of piles of granular media.

41 Laboratories in Environmental Science

Jasmine Flowers, Dr. Kathryn Riley • Swarthmore College

Jflower1@swarthmore.edu

LENS (Laboratories in Environmental Science) Program centers around its three core principles of fostering an environment built upon interest, motivation, and belonging. LENS is a program designed to not only expose but foster emerging individual interest in chemistry for rising middle school

students from CCSA (Chesters Charter Scholars Academy), via 15 hands-on experiments. In 2024, the Pennsylvania Keystone Exams showed that less than 16% of CCSA students met or exceeded the proficiency requirements in science. Our ultimate goal is to partner with CCSA to implement an 8th Grade environmental science school year curriculum. This curriculum would not only increase students' proficiency in science but also to foster well-developed individual interest in some students. This could result in students being prepared for the intellectual rigor they will face as they continue on to higher education STEM courses. This interest can produce a more diverse STEM field, as currently less than 5% of STEM doctoral degrees are received by underrepresented minorities. To scale the LENS Program for implementation in a school year curriculum, this summer, we created video recordings of the experiments as a resource for classroom experiment integration, added transfer tasks to the curriculum, conducted student interviews to collect data on the LENS' impact, and invited community partners to observe the program.

42 Effect of MK2's Kinase and Non-Kinase Functions on Caspase-3

Joseph Gamez; Sarah Kamal, M.D.; Mahendra Damarla, M.D. • Johns Hopkins School of Medicine
jgamez1@swarthmore.edu

Introduction: Acute Respiratory Distress Syndrome (ARDS) is a life-threatening condition that causes over 74,000 deaths annually in the United States. A well-established cause of ARDS is endothelial barrier dysfunction, which occurs due to endothelial cell (EC) apoptosis, a highly regulated process of programmed cell death. Our lab aimed to investigate the molecular mechanisms of apoptosis. Previous studies have suggested a disconnect between caspase-3, an executioner caspase, and a cell fully undergoing apoptosis. Our lab investigated caspase-3's ability to translocate into the nucleus and found that mitogen-activated protein kinase-activated protein kinase 2 (MAPKAPK-2), a serine/threonine kinase, seems to promote nuclear translocation of caspase-3. In this study, we aimed to determine if MK2 directly binds to caspase-3 and whether phosphorylation influences caspase-3 activity. I hypothesized that caspase-3 and MK2 directly bind to one another and that phosphorylation increases caspase-3 activity.

Methods: Human lung microvascular endothelial cells (HLMVEC) from caspase-3 knockout (KO) cells were used to test caspase-3 activity of various mutant constructs. ECs were first analyzed using a Caspase Glo Assay, followed by western blot analysis. His-nickel pulldowns were performed to test potential binding between a histidine-tagged caspase-3 and glutathione s-transferase (GST) MK2 which was followed by western blot analysis to confirm the presence of proteins. Inactive, active, and binding domain mutants of caspase-3 were used to investigate differences in binding capacity.

Results: MK2's different constructs were one of the following: (1) Wild-Type (WT), (2) Active Mimic (AM), a constitutively active mutant, or (3) Dominant-Negative (DN), which inhibits MK2-dependent phosphorylation and suppresses endogenous MK2 activity. The Caspase-3 Glo Assay showed that some MK2 constructs, like the WT and AM, exhibit similar caspase-3 activity. However, the Dominant-Negative MK2 construct resulted in significantly lower caspase-3 activity than Wild-Type. Following the His-Nickel pulldown, Western blot analysis showed that only inactive caspase-3 and MK2 have reciprocal binding, meaning caspase-3 directly binds to MK2 and vice versa. The mutated caspase-3 binding domain (BD) had weak MK2 binding with caspase-3.

Conclusion: Although the constitutively active MK2 construct does not increase caspase-3 activity, the dominant negative had significantly less activity than the WT. This suggests that MK2-dependent phosphorylation may not influence caspase activity. MK2's effect on caspase-3 may be different than just caspase-3 phosphorylation. In the pulldowns with inactive and active caspase-3, data show that MK2 only binds to the inactive form of caspase, meaning that there could be potential differences in binding depending on the activation state of caspase-3. MK2 also seems to have difficulty binding to caspase-3 when its binding domain is mutated, further supporting direct binding. Ultimately, MK2 and caspase-3 directly bind to each other; thus, this interaction may be important in nuclear translocation of caspase-3 and resultant apoptosis.

43 Computational Investigations of Vortex Ring Dynamics and Helical Vortex Stability

Ming Gao, Professor Emad Masroor • Swarthmore College

mgao1@swarthmore.edu

This research examines vortex ring interactions through computational and theoretical approaches, focusing on both infinite periodic arrays and helical vortex configurations. Building on classical studies of two-ring interactions—characterized by pass-through and leapfrogging behaviors—the project extended analysis to coaxial arrays of vortex rings. Using direct numerical simulation of the 3D Biot–Savart law and periodic extension of the Green's function, we aimed to model the self-induced motion of vortex rings while incorporating the effect of finite core thickness. We applied canonical transformation to Hamiltonian mechanics to produce phase portraits of 3D vortex rings in a 2D plane of Hamiltonian coordinates. Currently, we have made phase portraits in certain sets of parameters in Hamiltonian coordinates, and we aim to investigate, and characterize, the behaviors of interactions of two infinite coaxial arrays of vortex rings, under a variety of parameters related to the relative thickness, distance, size, and circulation of the rings.

In addition to the array analysis, this research investigates the stability of a thin vortex ring embedded in a helical vortex—a configuration relevant to propeller and wing-tip vortices. Unlike ring vortices, modeling the self-induced velocity of a helical vortex is more complex, as it requires considering the geometry of the vortex rather than treating it as a point vortex. We performed a direct integration of the Biot–Savart law to model the self-induced velocity of a helical vortex and successfully reproduced results from various studies that derive the self-induced velocity while taking into account the vortex thickness. With sufficient knowledge of the induced velocity field from the helical vortex, we are now investigating its impact on the stability of a thin vortex ring positioned within the helical vortex.

44 Glucose tolerance worsens with age in a social rodent species *(Octodon degus)*

Tate Garcia, Carolyn Bauer • Swarthmore College Biology Dept.

tgarcia1@swarthmore.edu

Diabetes is characterized by chronic hyperglycemia, or elevated blood glucose levels. Hyperglycemia in diabetics is caused by insulin dysfunction, as insulin is a hormone that helps body cells take up glucose from the bloodstream. In humans, the prevalence of diabetes increases with age, especially diabetes caused by increased resistance to insulin's actions (Type II diabetes). Diabetes and obesity are related, as increased body fat can lead to insulin resistance. Degus (*Octodon degus,* Chilean rodents related to guinea pigs) have divergent insulin and glucagon structures compared to other mammals. Degus can spontaneously develop diabetes and are susceptible to cataracts and obesity, which are comorbidities with diabetes. This led us to examine the relationship between age, sex, and glucose tolerance in captive degus ranging from 3-months to 5-years of age. We hypothesized that glucose tolerance decreases with age and that females have poorer glucose tolerance than males, as the female degus in our colony tend to have higher body fat ratios than the males. To assess glucose tolerance, we employed glucose challenges. We fasted animals overnight and then took baseline blood glucose readings with a glucometer. Then we injected each animal with a large amount of glucose and took blood glucose readings at 15, 30, and 60 minutes post-injection. Degus with higher integrated blood glucose levels (calculated as the area under the curve [AUC]) are considered to have worse glucose tolerance and are therefore more "diabetic." Our prediction regarding glucose tolerance was met, as 4- and 5-year-old degus had significantly higher glucose AUCs compared to 3-month-old, 10-month-old, and 3-year-old degus, and this trend was stronger in females than in males. However, we found that baseline fasting glucose levels did not significantly vary between age groups. Since we measured a cohort of degus at both 3 and 10 months as well as a separate cohort at both 4 and 5 years of age, we therefore assessed repeatability of AUC measurements. However, we found that glucose tolerance is not significantly repeatable between these respective time points. In all, these findings suggest that glucose regulation in degus becomes more impaired as they age, and that older degus may be more susceptible to diabetes. Future studies will look into relationships between glucose regulation and cognitive ability in degus.

45 Toward Anisotropic Macroporous Channels in Hydrogels via In Situ Gas Templating

Arina Garifullina, Kayla Hellikson, Vivian Feig • Stanford University School of Engineering, Mechanical Engineering Department

agarifu1@swarthmore.edu

Macroporous hydrogels consist of crosslinked polymer networks and are characterized by high water content and resemblance to the extracellular matrix. Such hydrogels display larger pores that can act as scaffolds for cell infiltration, making them a great candidate for tissue regeneration applications. To gain further control over macroporous pore features, anisotropy can be introduced to biomimic the natural architecture of tissue. Anisotropy introduces directionality to the pore orientation, which is beneficial to vascularization processes that increase rates of tissue regeneration. Additionally, for these systems to be easily translated to patients, it is desirable that they can be administered as injections and form in situ. However, combining this level of control with injectability is a challenge. Previously, pores in injectable gels were developed by gas-generating reactions. However, such methods resulted in poorly controlled pore structures. We hypothesized that manipulating the dynamic properties of the gel and the kinematics of bubble formation could help fabricate well-controlled porous structures, such as anisotropic channels. To study these properties, we used two gel systems: a gelatin-based system that can form permanent covalent or physical crosslinks in a time-dependent manner, and a granular gel system that has shear-thinning and self-healing properties. For both systems, magnesium was used as a gas-forming agent, with simethicone included as a surfactant to destabilize bubble walls and promote controlled coalescence. In the gelatin-based gel system, magnesium was either mixed in pre-gelation or injected into set gels through a needle under different surfactant conditions. In contrast, the granular gel system was prepared in a custom setup between two glass slides to allow easy imaging, where magnesium solution was injected, and surfactant was mixed in. Then, bubble formation, coalescence, and channel alignment were then observed over time. Overall, gelatin-based gels showed limited bubble movement and did not yield significant anisotropic structures, while granular gels displayed robust bubble coalescence and the formation of aligned pore channels when magnesium concentration was high and bubbles were in close proximity. Taking these observations into consideration can be used to inform the creation of a new technique to formulate highly controlled anisotropic macroporous architectures within gel systems.

46 Evolutionary conservation of circular RNAs

Jonathan Garrity, Dr. Michela Zaffagni, Prof. Sebastian Kadener • Department of Biology, Brandeis University, Waltham, MA 02454

jgarrit1@swarthmore.edu

Circular RNAs (circRNAs) constitute a class of stable RNAs whose functions are largely unknown. circRNAs are produced by backsplicing, a process in which the splice donor site of an exon is spliced to the splice acceptor site of an upstream exon rather a downstream exon. circRNAs are present in archaea, plants, fungi and metazoans and have been proposed to perform many different biological functions, from helping to regulate production of full length linear RNAs to serving as sponges for other small regulatory RNAs such as microRNAs. However, the functions of most circRNAs remain unexplored. In addition, little is known about what features of circRNAs exhibit evolutionary conservation. To examine circRNA function and evolution, we performed a comparative analysis using RNA sequencing data from 8 Drosophila species with divergence times of up to 30 million years. To date, we have examined circRNA conservation at multiple levels, including the host gene, exon(s) of origin, and magnitude of expression. We also have examined whether the features known to contribute to the formation of a circRNA sites can be used to predict the extent of evolutionary conservation of a circRNA. These features include reverse complementary matches

(RCMs) between flanking introns, RNA Binding Protein (RBP) binding sites, and the putative strength of canonical splice junctions. Our preliminary results suggest that while RCMs are important for the generation of less well-conserved circRNAs, the generation of highly conserved

circRNAs likely relies on other features, such as the presence of RBP binding sites. These findings suggest that the generation of evolutionarily conserved circRNAs may proceed by molecular mechanisms that are distinct from those involved in producing less-conserved circRNAs.

47 Antibody Binding to Influenza A Protein

Lauren Ghil, Professor Kathleen P. Howard • Swarthmore College, Swarthmore, Pennsylvania 19081

lghil1@swarthmore.edu

Matrix protein 2 (M2) is a tetrameric membrane protein found in the viral coat of the influenza A virus and on the surface of infected cells. M2 plays an integral role in the lifecycle of influenza, and it is known for its high sequence conservation across many different strains. Current vaccines are not fully effective against all the circulating strains each year, and they might not provide any protection against a potential pandemic strain. The high sequence conservation of M2 across a wide range of strains makes this protein a desirable target for a potential universal vaccine. Understanding the structure and antibody binding properties of the M2 protein would contribute to the development of more effective vaccines. There are a number of monoclonal antibodies currently being researched as possible candidates for a universal antiviral. Antibody 14C2 is the first ever monoclonal antibody discovered for M2. Due to its known tight binding, this antibody is often used as a standard for M2-antibody studies. Unlike many previous studies in the literature which used truncated M2 in non-native environments, we are working with the full-length M2 tetramer embedded in a lipid bilayer membrane. After creating viable, stable samples of our M2-nanodiscs, we introduced 14C2 antibody to observe the complex's binding abilities using biolayer interferometry (BLI). We observed 14C2 antibodies to M2 monomers in solution as well as the M2 tetramer in nanodiscs. We are also pursuing electron microscopy to visualize the complex of M2 nanodiscs bound to the antibody.

48 Metabolic Stability Across the Lifespan of the Forked Fungus Beetle *(Bolitotherus cornutus)*

Devin Gibson, Vince Formica • Mountain Lake Biological Station

dgibson1@swarthmore.edu

Standard metabolic rate (SMR) is a key trait in understanding an organism's life history, yet baseline rates for insect systems are scarce. Additionally, insects comprise a large portion of animal diversity, yet most insect metabolic studies emphasize short lived species, or the first weeks post eclosion. This leaves a gap in our understanding of long lived insects and their energy use patterns. Long lived species, such as the forked fungus beetle *(Bolitotherus cornutus)* offer the ability to test whether metabolic rates show age and sex related changes over a multi-year timescale. As it has previously been established that behavioral phenotypes change as they age (Mitchen et al. 2020), we are asking whether baseline physiology likewise shifts across lifespan. Individuals were collected from captive populations with marked ages of 1-6 years. Using flow through respirometry, we measured oxygen consumption (VO_2) and carbon dioxide production (VCO_2). Generalized linear mixed models (GLMMs) tested for effects of age, sex, and body mass. As expected, SMR scaled positively with body mass, indicating larger beetles had higher oxygen consumption rates. Despite sexual dimorphism in morphology (notably male horn size) and different behaviors (aggression in males), we found no evidence of consistent sex differences in metabolic rate. After adjusting for mass, age was also not a predictor of SMR. These results suggest this long lived insect can maintain stable metabolic maintenance over multiple years. Further work quantifying excess post-exercise oxygen consumption (EPOC) will be critical to link species physiology to behavior and ultimately, to its impact on fitness in this system.

49 Distance Laplacian Cospectrality in Digraphs

Sho Glashausser, Carlos Garcia, Carolyn Reinhart • Swarthmore, PA

sglasha1@swarthmore.edu

Digraphs consist of vertices and edges, where edges represent directed connections between vertices. They can be used to represent various types of information, such as social networks or the spread of gossip. Visual representations of digraphs are helpful in these contexts, but we can understand

them better by converting their information into a numerical array known as a matrix. Using the eigenvalues of the matrices, a fundamental algebraic property, we can explore mathematical properties of the digraphs that are not immediately evident. In particular, we focus on the Distance Laplacian matrix, which captures the distances between vertices and also the total distance from a vertex to all other vertices. Ideally, a matrix's set of eigenvalues should be different for distinct digraphs. However, multiple digraphs sometimes produce the same eigenvalues, making them cospectral. We accomplished two main objectives: identifying digraphs that have a unique set of eigenvalues and constructing families of cospectral digraphs. In both cases, we prove their existence on an arbitrary number of vertices, yielding infinitely many instances. For unique eigenvalues, we focused on digraphs with exceptionally high or low numbers of edges. We developed two major methods of constructing cospectral digraphs. One uses twin vertices, two vertices within a digraph that behave similarly. The other uses the existence of a particular subgraph called the transitive tournament.

50 Synthesis of Porous Organic Cages via Dynamic Imine Chemistry

Alex Guo, Anna Yang • Swarthmore College

aguo1@swarthmore.edu

Porous Organic Cages (POCs) are an emerging category of organic compounds with favorable structural components such as well-defined porosity, high surface area, and low density. Cages have applications in many fields, such as pharmaceuticals, energy storage, and reaction catalysis through host-guest interactions, a trait of their well-defined porosity. To begin synthesizing these cages, we utilize Dynamic Covalent Chemistry (DCvC), a synthetic system utilizing reversible bond formation to produce a thermodynamic product via its 'error-correcting' nature. To selectively favor a single compound, we are navigating the energy landscape of the dynamic system by altering thermodynamic and kinetic controls to change the thermodynamic equilibrium. Here, we use imine condensation via a tri-topic aldehyde precursor with an alternating 'up-down' substitution pattern or 'bowl' conformation to geometrically guide the system towards a [4+6] tetrahedral imine cage via phenylene diamine building blocks. Further development of this system allows for exploration of the thermodynamics and kinetics that define the DCvC landscape.

51 Assessing the Efficacy of Facial Age Assurance Technologies in Adversarial Settings

Lena Habtu, Dr. Shaanan Cohney • University of Melbourne

lhabtu1@swarthmore.edu

Countries around the world are implementing increasingly strict age restrictions, particularly for social media users below certain age thresholds. While these regulations hold social media platforms accountable rather than penalizing individual users, it is likely that young users will attempt to bypass these restrictions by manipulating how old they appear. This project investigates how age-verification technologies perform in real-world adversarial settings, providing insight into their vulnerabilities and limitations. We identified circumvention methods that would be easily accessible to young users – such as disguises, facial modifications, and altered expressions – and tested them against three leading age-assurance providers. In doing so, we assessed the extent to which these methods impact the accuracy of age-estimation applications, aiming to identify weaknesses in existing systems and explore ways to strengthen them. By simulating real-life use circumstances, our study revealed that while certain methods are effective in aging-up users, the outcomes are variable, which raises serious concerns about the reliability of facial age estimation as an age-assurance method.

52 Binge Eating Disorder and Consumption Rate

Nina Haddou Aguilar, Wambura Fobbs, Ph.D. • Swarthmore College

nhaddou1@swarthmore.edu

Binge eating disorder is defined by recurrent episodes of binge eating—discrete moments in which patients eat an amount of food that is considerably larger than what most people would eat in the same time period— and can involve "eating much more rapidly than normal" (DSM-5). We used an intermittent limited access model in which mice were given access to a high-fat/ high-sugar diet

during 1-hour binge sessions to determine whether such exposure was sufficient to produce an elevated rate and amount of food consumption.

During the binge sessions, mice were presented with the opportunity to poke for either Western Diet (a high-fat/high sugar diet) or Standard Chow from an operant device for one hour on Mondays, Wednesdays, and Fridays for 6 weeks. At all other times, mice had standard chow and water freely available in their home cages. In order to determine whether there was an increase in eating rate and food consumption in comparison to the first sessions, but also compared to the control (chow) group, we measured the food consumption throughout 18 binge sessions. I later wrote a Python algorithm that computed the cumulative food consumption rate at sessions 2, 8, and 18. The slope of the cumulative consumption curve reveals the food consumption rate. Although there was some individual variability, the mice that had access to WD during the binge sessions did consume more food and calories than the control group and ate at a faster rate, especially at the beginning of all sessions we assessed. This effect was even more visible during the last binge session. We can conclude that intermittent, limited access to WD is sufficient to produce these core components of binge eating disorder.

53 Bulges in left-handed G-quadruplexes formed from novel $(GT)_n$ repeats

Andrew Hendrickson

G-quadruplexes (GQs) are DNA structures composed of 4 interacting strands (compared to 2 in B-DNA) in guanine-rich regions. Guanine bases interact via Hoogsteen bonds in lateral fashion, forming a planar tetrad that is further supported by π-π orbital stacking and interactions with monovalent cations integrated in an ion channel. Different topologies of strand 5'-3' end orientation, loops, and handedness are possible depending on the glycosidic conformation of guanines, solvent, co-solute, etc. Sequences with the potential to form GQs are commonly found in telomeric and promoter - especially proto-oncogene - regions, and GQs that form in these regions have been found to inhibit the extension of telomeres by blocking the access of telomerase to the DNA strand. GQs are also able to be targeted by small-molecule ligands, potentially acting as therapeutic targets for cancer and other diseases.

Left-handed G-quadruplexes (LHGQs) are a subdivision of GQs with unique helicity and strict sequence dependence, forming only with specific sequences of G and T repeats. Studies have determined that certain promoter regions known to cause diseases have the potential to form LHGQs, formed by motifs of (GGT)n repeats. Computational tools can be used for finding sites of interest for predicting GQ formation from genomic sequences; the Viglasky lab has utilized G-Qinder, which has predicted that sequences of (GT)n also have the potential to form LHGQs. In this project, we were interested in further exploring the stability of LHGQs with small insertions – called "bulges" – created by the inclusion of these (GT)n repeats in known LHGQ-forming sequences. From the sequences predicted by G-Qinder to form LHGQs, we will be utilizing biophysical characterization (CD and UV spectroscopy) and x-ray crystallography to characterize the structures in solution and obtain 3-dimensional models of the GQs. We will also examine the 2 unusually high-quality x-ray crystallographic LHGQ structures obtained. With the confirmation of two similar LHGQ structures, future studies may be able to widen the parameters used to search for LHGQs and the genomic target sites they provide.

54 TargetPractice: Simulating Conversations with LLMs Can Protect Against Online Scams

Owen Hoffmann

Fraud continues to proliferate online, from phishing and ransomware to imposter and pig butchering scams. Every year, it causes billions of dollars in losses to the US economy — leaving behind a heavy financial and psychological toll on victims. Yet automated approaches adapt slowly and may not reliably protect users from falling prey to new types of fraud. These limitations highlight the need for user-centered, active training that builds resilience against evolving scams.

We developed TargetPractice, a conversational interface that inoculates users against scams through

simulation, dynamic interaction, and real-time feedback. TargetPractice simulates scams with two large language model (LLM)-powered agents: a scammer and a target. Users, positioned as an advisor, must help the target defend against the scammer by providing real-time advice. This design balances psychological safety and realism by exposing users to staged, phase-structured scam conversations (Trust Building, Manipulation, Extraction) while providing immediate, phase-specific expert feedback.

We evaluated TargetPractice through a between-subjects study (N=167) comprising three experimental and one control condition. The quantitative outcomes of our mixed-methods analysis showed that pairing advice-giving with multiple-choice questions significantly increased scam recognition (+8%). Users' change in self-efficacy and response-efficacy were also 19% and 9% higher, respectively. Qualitatively, we find that users more frequently provide action-oriented advice over urging caution or providing emotional support. TargetPractice highlights the potential for inter-agent conversational UIs to augment learning. These findings demonstrate how dynamic, inter-agent LLM simulations can create effective, scalable, and psychologically safe scam training experiences. Overall, TargetPractice offers a pathway toward more engaging, configurable, and general-audience scam resistance training.

55 COVERT-AI: Real-time, Multimodal, and Adaptive Cognitive Support for Operational Decision Making

Ingrid Hsu, Mariela Perez-Cabarcas • U.S. Army DEVCOM Army Research Laboratory; Aberdeen Proving Ground, MD

ihsu1@swarthmore.edu

With the explosion of information in today's world–whether in classrooms, workplaces, or on the battlefield–humans are increasingly overwhelmed by vast, often unstructured streams of multimodal data. In complex, fast-paced environments, human cognition struggles to keep up. This cognitive overload impairs our ability to understand, communicate, and act effectively in real time; in mission-critical settings, even such minor lapses in attention or comprehension can lead to failure or loss of life. Intelligent systems present the opportunity to offload these cognitive burdens onto machines.

To address this challenge, we introduce **COVERT-AI** *(Cognitive Optimization via Embedded Real-time Artificial Intelligence)*, a multi-modal, user-centered system that integrates human factors, artificial intelligence (AI), and interface design to enhance situational awareness and provide personalized cognitive support based on specific user needs and evolving operational context. Developed by a multi-disciplinary team, COVERT-AI progressed from proof-of-concept research to the development of a functional, agent-based experimental platform through iterative pilot testing and system evaluation, with the goal of informing the design of future user studies and wearable system interfaces. Our work, within the AI system subteam, focused on system integration, incorporation of emotional context, and prompt engineering to optimize language model outputs.

In addition to leveraging multi-modal foundation models and retrieval-augmented generation (RAG), COVERT-AI employs advanced prompt engineering strategies–including in-context learning, sequential reasoning, and aggregation techniques–as well as a Prompt Strategy Selector that dynamically tailors prompting techniques based on task complexity and user state. The system also incorporates emotional context, detected in real time through voice and language via Hume AI, to proactively identify confusion and adjust responses accordingly. This work lays the foundation for using lightweight, real-time prompt engineering, particularly when combined with emotional awareness, to improve AI reliability, depth, and contextual alignment without the added complexity of fine-tuning.

Overall, COVERT-AI advances the Army's vision for human-AI teaming by streamlining mental model formation and communication for situational understanding and mission readiness in cognitively demanding, real-world scenarios.

56 Investigating the Shear Behavior of Bentonite Polymer Composites in Varying Chemical Conditions

Sai Nyi Bhone Htut, Advisor Name: Daniel Adeleke • Engineering Department, Swarthmore College
shtut1@swarthmore.edu

Bentonite Polymer Composites (BPC) are emerging as promising materials for hydraulic barrier systems, particularly in environments with high salinity such as landfills, which is due to their ability to maintain low hydraulic conductivity under harsh chemical conditions. However, an effective clay barrier must also possess sufficient mechanical strength, particularly in complex geometry, an area of BPCs that are currently under-explored due to their recent development. Therefore, the purpose of this study is to investigate the fundamental shear parameters of BPC such as cohesion and soil friction angle in different leachate conditions. The materials tested in this study consist of sodium bentonites amended with two types of polymers at targeted loading of 4% and 8%. Direct shear tests were conducted in accordance with ASTM D3080 standard at two different chemical environments: dilute concentration (10mM) and aggressive concentration (200mM) of CaCl2 solution. The results suggest that increasing the ionic concentration leads to a decrease in soil's cohesion while simultaneously increasing the soil's friction angle. Additionally, as polymer loading increases from 4% to 8% in dilute concentration, both BPC1 and BPC2 exhibit shear strength reduction. Contrarily, in aggressive environments, BPC1 exhibits shear strength reduction while BPC2 exhibits both decrease and increase in shear strength, as polymer loading increases. A significant application of this study is the resourcefulness in selecting barrier materials for future landfill projects and the long-term mechanical performance prediction in varying environmental conditions.

57 Reactivity of ($TriNOx^{3-}$)M group 13 metal complexes with N-H and C-H bonds

Isabel Hunt

Developing metal coordination complexes capable of metal-ligand cooperative (MLC) activation of small molecules is a compelling area of research. We are currently investigating the coordination chemistry of group 13 metal complexes supported by non-innocent ligand frameworks, with a focus on the tripodal, tris(nitroxide) ligand system, $TriNOx^{3-}$. Our group has previously demonstrated the activating ability of ($TriNOx^{3-}$)M (M = Al, Ga) complexes with O-H bonds. In this contribution, we present initial investigations into the reactivity of these complexes with C-H and N-H bonds. Several substrates with pKa values ranging from 15-30 were reacted i n various ratios with the TriNOx complexes, with NMR evidence of varying degrees of activation.

58 Solar Microgreen Hub for Urban and Rural Nutrition

Jean Michel Irankunda

This project focused on designing and building a solar-powered microgreen cultivation hub tailored for underserved communities. The primary goal was to create a low-cost, modular system capable of sustainably producing nutrient-dense food in off-grid or low-resource settings. By integrating solar panels and an automated aeroponic irrigation system, the hub can operate independently of traditional power and water infrastructure, making it viable in areas where these resources are scarce or unreliable.

The system was constructed using locally available and affordable materials to ensure accessibility and ease of replication. The modular design enables scalability and adaptability, allowing users to expand or modify the system according to specific community needs or environmental conditions. During the research and development phase, emphasis was placed on testing the feasibility of solar-powered automation for nutrient delivery, water cycling, and environmental monitoring within the microgreen growth chamber.

The final prototype demonstrated efficient energy use, consistent plant growth, and minimal water consumption compared to traditional soil-based cultivation. The automated features also significantly reduced labor requirements, making the system approachable even for users without prior agricultural experience.

This project directly supports the United Nations Sustainable Development Goals (SDGs) 2 and 7

by addressing food insecurity through localized, sustainable farming practices and by promoting access to clean, renewable energy for agricultural use. The work lays a foundation for future iterations and community-driven adaptations of the system, with the long-term vision of empowering food sovereignty and sustainable development in under-resourced areas.

59 Developing Interactive Content for Dive into Systems

Jay Iyer and Bohou Zhang; supervised by Tia Newhall and Kevin Webb • Martin Hall, Swarthmore College

[illegible]r1@swarthmore.edu and bzhang2@swarthmore.edu

We developed new exercises for Dive Into Systems, creating interactive exercise components covering topics like binary, assembly, computer architecture, and multithreading. Our components procedurally generate "good" practice problems that test the students on edge-cases and important details. We also worked on data collection tools to gather anonymous usage data from students and measure how the exercises are being used.

60 Playing to Win: Strategies in Two Player Games

Ara-Oluwa Jacob, Pat Devlin

This project explores strategy in two-player games through both mathematical analysis and algorithmic implementation. I studied games like Chomp, the Subtraction Game, Mancala, and Red-Blue Hackenbush. For Hackenbush, I used surreal numbers to evaluate game positions. For the Subtraction Game and Mancala, I built Python programs and AI models to enhance winning strategies. My Subtraction Game tool classifies positions in real time, while the Mancala bot consistently beats an online opponent. The project highlights how game theory, graphs, and computation together reveal the structure behind strategic play.

61 Characterization of Thermoelectric Materials

Mr. Dylan Jacobs, Dr. Benjamin L. Greenberg • US Naval Research Laboratory, Washington, DC

djacobs2@swarthmore.edu

Thermoelectric materials constitute an important frontier in renewable energy research due to their ability to convert waste heat into usable electricity. Thermoelectrics comprise semiconductors, such as silicon and germanium, that generate electric current when subjected to temperature gradients, due to thermal diffusion of mobile charge carriers. The ratio between output voltage and unit temperature gradient–termed Seebeck coefficient–can be optimized by increasing the thermoelectric material's electrical conductivity and decreasing thermal conductivity to efficiently facilitate electron flow while slowing heat transfer to maintain the driving thermal gradient across the material. While n/p-doped silicon-germanium (SiGe) semiconductors have relatively high electrical conductivity, they also have prohibitively high thermal conductivity. To circumvent this problem, researchers at the US Naval Research Laboratory utilize atomic layer deposition (ALD) to coat SiGe nanoparticles with nanolayers of thermally insulating oxide, such as SiO2. Sintering these nanopowders into thermoelectric compacts creates electrically conductive channels through a thermally insulating thermoelectric, ideally increasing its Seebeck coefficient.

Sintered compacts must be characterized to determine their electrical and thermal properties. Measuring electrical conductivity is straightforward; however, thermal conductivity measurements require advanced techniques, such as laser flash analysis (LFA), which involves rapidly heating a thermoelectric sample through a laser pulse and measuring its corresponding temperature-time graph. To maintain high signal/noise ratios and achieve accurate readings, the LFA instrument's temperature sensor must be cooled to the temperature of liquid nitrogen (LN2), which is depleted rapidly due to evaporation. To solve this problem, I developed an automated liquid nitrogen dispensing system, data-logging system, and graphical user interface to communicate between and monitor the LFA, LN2 dispenser, and laboratory computer. I then used the LN2-dispenser-equipped LFA system to measure the thermal conductivity of thermoelectric SiGe samples, ultimately showing a 10x reduction in thermal conductivity compared to previous samples.

62 Progress Towards Pyridine Containing Macrocycles Through SNAr

Tobias Jaramillo, Anna Yang • Swarthmore College

tjarami1@swarthmore.edu

Nanotubes are a highly valued area of study because of their high degree of applicability in numerous fields. Some examples of applications include in medicine as supplementary ion channels in human cells or in materials, for example in batteries. Scalable and cost-effective production of nanotubes, however, is a complex feat using traditional synthetic methods. Furthermore, prompting nanotube formation (or disassociation), preferably through a simple chemical stimulus, would offer a degree of valuable control.

Thus, we seek to elaborate upon work exploring pyridine containing macrocycles. These pyridine containing macrocycles have been shown by the Dichtel group and others to be responsive to pH changes in prompting nanotube formation. Specifically, in acidic conditions the nitrogen in the pyridine is protonated and then anions act as ion bridges stabilizing macrocycle stacking and thus nanotube formation. Likewise, in neutral or basic conditions, the nitrogen is deprotonated and thus nanotube assembly is disincentivized.

Incorporating pyridine into the macrocycles also enables a secondary advantage when looking at macrocyclization, or the process of synthesizing the macrocycles themselves. Macrocyclization under the traditional methodology of step-wise synthesis is complicated, limiting, and victim to kinetic traps. Therefore, we are interested in using dynamic covalent methods to approach macrocyclization. Dynamic covalent chemistry utilizes conditions under which traditionally static covalent bonds are formed reversibly, thus allowing the thermodynamic final product to predominate.

The dynamic reaction we use is nucleophilic aromatic substitution (SnAr). SnAr was chosen because the covalent bonds which are formed are more persistent than other dynamic covalent bonds such as imine-based connections or boronate ester based connections. The bonds formed in SnAr are resistant to hydrolysis unlike imines or boronate esters. Furthermore, the incorporation of pyridine within the macrocycle, considered initially because of the advantages for stimulating nanotube formation, adds an ideal electrophilic moiety to act in partnership with a nucleophilic moiety for macrocycle formation via SNAr.

We have made advances specifically in creating computational models to better understand the properties of potential products and the nature of the reactive species themselves. I created a focused model for structures of the type of current interest to the research group, allowing the prediction of hydrogen chemical shift in HNMR with an average error of 0.09 ppm and a root mean squared difference of 0.17 ppm. Furthermore, I was able to create a library of predicted CNMR spectra and IR spectra for a set of related compounds to assist in identifying species in reactions with multiple possible products and in which two or more species would be difficult to differentiate simply by qualitative analysis of the spectra. I modelled nucleophilic attack on fluoropyridine precursors by oxygen-based nucleophiles to better understand the transition states and intermediate molecules. As part of this effort, I modelled the reactivity of different fluorinated positions on the electrophile to better understand the interactions between activating R groups and the pyridinal ring itself.

63 Little sprouts: How children learn and reason about nature

J'ovanny Jno-Pierre, Junior Lugo, Savannah Wilcox, Dr. Emily Foster-Hanson • Singer 132

kidlab@swarthmore.edu

In the current project, we are examining how different experiences with nature relate to different mechanisms of conceptual change in children. For the past year, we have been collecting data using anonymous "plants and animals guessing game" worksheets that children can complete in-person at community events and passive research stations at local public libraries. Using anonymous worksheets that kids complete on their own–sometimes without a researcher even being present–has allowed us to collect a large amount of data quickly. So far, we have collected data from 901 children using these methods; 248 are part of a preregistered planned sample of 1,000 that we expect to complete in the coming months. In this work, we have built relationships with community partners serving

populations of children that systematically differ in their experiences with nature, including the Scott Arboretum and Gardens, the Delaware Center for Horticulture, Smith Memorial Playground, and Delaware County Public Libraries. This will allow us to compare concepts and processes across children with different backgrounds, using data collection site as a proxy for individual experiences to maintain anonymity.

Our goal is to examine correlations between age, ecological reasoning (Coley 2012), human inclusion in nature, nature connectedness, overt conservationism/morality, covert conservationism/morality, and self self-size (Bai et al 2017), and to examine how these vary depending on children's experiences including time spent in nature and time spent reading books or watching shows about nature. In our pilot data, we found that the more kids say they spent time in nature, the closer they said they feel to nature. Ecological reasoning was also related to how much kids said they consumed nature media.

The findings from this correlational study will help to inform our future research on how children learn about nature through their experiences and social interactions. For example, in the next phase of this project we are examining how children learn about nature through conversations with their parents on a simulated "forest walk." Families will participate asynchronously online using the Children Helping Science study platform, and we will record their conversations using the families' webcam to later transcribe and code. We will then longitudinally track these children's nature reasoning using the same platform, with measures based on those in our worksheets study.

64 Investigating the role of NRG/ERBB signaling in proportional heart growth

Oliver Kim, Bradley Davidson • Department of Biology, Swarthmore College

okim1@swarthmore.edu

During heart development, distinct regions of the organ proliferate at different rates to achieve the overall correct size and shape. In vertebrate hearts, this proportional growth is partially governed by NRG/ERBB signaling, but extensive gene and isoform diversity has made it difficult to fully characterize the contributions of this pathway. Here, we address this deficit by investigating heart growth in *Ciona robusta,* an invertebrate chordate with a compact genome and simple heart structure. Where vertebrates possess four NRGs with many isoforms, we identified just two candidate NRG orthologs in *C. robusta.* Further, scRNAseq data indicates that both *Ciona* NRG orthologs and *Ciona* orthologs to the cognate ERBB receptors are expressed in the heart. Notably, one of these receptors, EGFRa, is expressed in a line of progenitors that drive heart growth. Based on these findings, we hypothesized that NRG/EGFRa signaling modulates the proliferation of these cardiac progenitors. To test this, we generated a dominant-negative form of *C. robusta EGFRa* and drove its expression in the heart lineage. We also employed pharmacological ERBB, MAPK, PI3K, and PLC inhibitors to disrupt NRG/ERBB signaling and canonical downstream pathways. These loss-of-function assays were conducted on *C. robusta* juveniles, which were then treated with DAPI (nuclear stain) and phalloidin (F-actin stain) to assess progenitor number or with DAPI and EdU (proliferation marker) to assess progenitor proliferation. Hearts were imaged using fluorescence confocal microscopy and analyzed in FIJI to quantify treatment effects. Although disruption of NRG/ERBB signaling did not significantly alter progenitor number, we did detect decreased proliferation in a specific, distal progenitor population. These preliminary results lay the groundwork for further analysis of NRG/ERBB signaling in *C. robusta* heart growth. Insights in *Ciona* may inform vertebrate and ultimately human models to better understand how the heart grows.

65 Optimizing Lentiviral Delivery of Transcription Factors for iPSC-to-Hematopoietic Differentiation

Samuel Kim, Cheyna Butler, Eric Salazar, Monty Thomas, Meenhard Herlyn
The Wistar Institute, 3601 Spruce St, Philadelphia, PA 19104

skim17@swarthmore.edu

Induced Pluripotent Stem Cells are adult cells that have been reprogrammed backinto a pluripotent state, meaning that these cells can become nearly any type of cell in the body, including blood-forming cells known as hematopoietic stem cells. Ourgroup is interested in using iPSCs to study how

the immune system interacts with cancer, because iPSCs can provide a renewable and customizable source of human cells. However, turning iPSCs into functional immune cells like HSCs is still a challenge. We don't fully understand which genes or signals are needed to guide this process. TFs are key regulatory proteins that can activate or repress entire developmental programs, acting like genetic "switches" to control cell fate. One way to help iPSCs become HSCs is to introduce specific genes using lentiviruses—a type of virus modified in the lab to safely deliver genetic material into cells. Lentiviral vectors are widely used in research due to their ability to transduce both dividing and non-dividing cells and to maintain long-term expression of the inserted genes. In this project, our goal was to produce a set of lentiviral vectors, each containing a different transcription factor (TF). To work properly, these lentiviruses need to be made at a high enough concentration (called titer) so they can efficiently infect other cells. We tested their ability to infect 293T cells, a commonly used human cell line, as a first step. The lentiviral system we have developed will enable systematic testing of various TF combinations to determine which are most effective in guiding differentiation toward HSCs.

66 Exploring Hydroxy-Based Nucleophile Reactivity with Pyridinal Electrophiles in Nucleophilic Aromatic Substitution Reactions

Catherine King, Anna Yang • Swarthmore College

cking3@swarthmore.edu

Dynamic covalent chemistry (DCC), a synthetic strategy where reversible reactions are carried out under equilibrium, enables the "self-correcting" synthesis of complex molecules by driving unstable side products to reform into thermodynamically favorable ones. DCC is highly efficient but suffers from a limited toolkit of compatible reactions, restricting the variety and scope of applications. Nucleophilic aromatic substitution (SNAr) reactions have been explored in the literature as a potential candidate for DCC, but there has been limited research on pyridine-based SNAr. Our lab is focused on establishing the viability of dynamic SNAr with pyridinal electrophiles, in hopes that pyridine's electron-withdrawing nature and biological relevance will lead to the development of high yield, self-correcting, functional macrocycles. To better understand if pyridinal SNAr is compatible with DCC, we first focused on exploring the reversibility of the reaction under different conditions. Hydroxy nucleophiles are thought to be good candidates for reversible SNAr due to their ability to be both good nucleophiles and good leaving groups. We competed catechol and phenol, which differ in nucleophilicity and effective molarity, against each other in reactions with 2,3 difluoropyridine or 2,3 difluoro-(4-trifluoromethyl) pyridine to gain more insight into what factors were most important in determining the product distribution. We found that when there are no additional electron-withdrawing substituents on the electrophile, nucleophilicity is most impactful at lower temperatures; however, at higher temperatures, the gap in activation energy becomes insignificant and both nucleophiles react at similar rates. With a CF3 electron-withdrawing group added to the electrophile, mixed results occurred based on different concentrations and temperatures. Overall, continued work needs to be done to identify patterns and explore other factors that may be affecting the reactivity of different nucleophiles with 2,3 difluoropyridine and its derivatives.

67 Shoulder sEMG Live Biofeedback Sensor

Jacey Koh, Owen Lord, Professor Joseph Towles • Swarthmore College: SH Lab 124

jkoh1@swarthmore.edu | olord1@swarthmore.edu

The research develops a low-cost wearable device with real-time biofeedback to assist physical therapy patients to engage correct muscles when practicing rehabilitation exercises. Shoulder pain often results from altered movement patterns that lead to muscle compensation. Such improper muscle activation delays recovery and risk reinjury. Therefore, proper muscle engagement is critical. Physical therapy aids patients to relearn optimized movement patterns to improve joint functions and reduce strain on their injured muscles. However, restoring a healthy movement pattern is often difficult as distinguishing correct from incorrect muscle activation is challenging. This research addressed this by designing a wearable device consisting of affordable MyoWare surface EMG (sEMG) sensors with a Python-based PyQt5 graphical user interface. The device monitors and evaluates shoulder muscle activation, providing real-time biofeedback presenting competing muscle pairs. The final product is an

integrated hardware-software system that is capable of collecting and analyzing real-time EMG sensor data to support rehabilitation.

68 Identifying Natural Variation in Heat Tolerance in *Arabidopsis thaliana*

Molly LaPerle, Nick Kaplinsky • Swarthmore College

mlaperl1@swarthmore.edu

Humans are dependent upon on the cultivation of crops for food and have utilized artificial selection and genetic modification to optimize crop resilience and yield. An understanding of how plants respond to high temperatures is crucial to adapting agriculture to rising temperatures, which increasingly pose a ubiquitous threat to crop production. The cellular response of plants to heat stress involves production of a range of Heat Shock Proteins (HSPs), which prevent the heat-induced denaturation of proteins essential for cell function. While plant cells possess some HSPs at baseline temperatures, HSP production must be induced in response to heat stress to equip the cell to withstand the stress, which results in a time delay between identifying a stressor and producing adequate amounts of HSPs. It is well documented that *Arabidopsis thaliana* seedlings subjected to a moderate heat shock are, after a short recovery period, able to withstand a higher heat shock which kills plants not exposed to the prior acclimation temperature. This mechanism is known as acquired thermotolerance. I explored natural variation in Arabidopsis heat shock responses by testing thermotolerance and acquired thermotolerance in a range of different ecotypes, which are members of the same species differentially adapted to a particular environment. I utilized two assays, one plate-based and one water-based, for phenotyping seedling responses to heat shock which I replicated with several different ecotypes. I identified that different ecotypes of Arabidopsis exhibit variation in thermotolerance and acquired thermotolerance using the widely researched ecotype Columbia as wild type. Identifying individual strains which exhibit enhanced or diminished thermotolerance or acquired thermotolerance compared to Columbia presents the opportunity to explore the genetic basis for these differences.

69 Site-Specific ^{19}F-NMR Elucidates Functional Roles of Trp85 and Trp99 in eEF2K Activation

Kaitlyn Lee, Andrea Piserchio, Ranajeet Ghose • The City College of New York

klee9@swarthmore.edu

The calmodulin (CaM) dependent eukaryotic elongation factor-2 kinase (eEF2K) downregulates protein synthesis by phosphorylating Thr56 of eEF2, which impairs ribosomal engagement. CaM binding affinity depends on a CaM-targeting motif (CTM) containing the critical Trp85, and it is further modulated by several phosphorylation sites located on the kinase N-terminal tail and on the regulatory loop. We proposed that, upon CaM binding, the formation of the active form of the enzyme is mediated by an "activation spine" (A-spine), a structural linkage coupling Trp85, the C-terminal lobe of CaM (CaMC), and the kinase domain (KD) active site through a regulatory element (RE) hosting Trp99. Mutations of either Trp85 or Trp99 disrupt catalytic efficiency; however, only Trp85 is essential for CaM binding. Several crystal structures exist for the active form of a kinase construct lacking the disordered regions (eEF2K_TR), yet the structural features of the downregulated state are currently unknown. To probe the regulatory role of these residues and shed light on the overall activation process, we employed site-specific incorporation of fluorinated tryptophan residues at positions 85 and 99 using engineered tRNA/tRNA synthetase pairs. Incorporation of ^{19}F atoms in eEF2K_TR enabled residue-selective monitoring of these critical moieties via fluorine nuclear magnetic resonance (^{19}F-NMR) spectroscopy. Fluorinated samples were prepared, and spectra were acquired for the fully active (phosphorylated, CaM-bound) and the downregulated (unphosphorylated, CaM-free) forms of eEF2K_TR. Each condition was additionally examined in H2O and D2O buffers to assess solvent exposure through monitoring of the isotope effects on the local chemical environment. Comparative ^{19}F-NMR analysis revealed that in the downregulated state, Trp99 samples multiple conformations, some of which appear to be solvent-exposed. Upon activation, Trp99 seems to rigidify and to assume a conformation distinct from the inactive state. This suggests

that Trp99 is not just a critical scaffolding residue but mediates the transmission of the allosteric signal for CaM binding. In the downregulated state, Trp85 appears to be unstructured and solvent-exposed. Hence, we disprove the hypothesis that modulation of CaM affinity may depend on Trp85 docking to the inactive KD in a manner dependent on the phosphorylation state of the kinase N-terminus or the regulatory loop. These results demonstrate that ^{19}F-labeling at strategic residues is a powerful approach for dissecting site-specific conformational changes in large, multi-domain enzymes. This work not only elucidates the structural basis of eEF2K activation but also illustrates the utility of site-specific fluorination and ^{19}F-NMR for studying dynamic regulatory elements in protein kinases.

70 Choroidal Abnormalities in Neurofibromatosis Type 1

William Insuk Lee, Dr. Yin Allison Liu M.D. Ph.D. • University of California Davis

Wlee2@swarthmore.edu

Neurofibromatosis Type 1 (NF1) is an autosomal dominant disorder characterized by the production of tumors originating from the neural crest. The tumors result from a lack of neurofibromin, a protein that modulates cell growth. As the name suggests, NF1 mainly affects the myelin sheath around nerve fibers which are a result of affected Schwann cells. The traditional manifestations and clinical criteria are based on skeletal, cutaneous, neurologic, and ocular symptoms. A clinical diagnosis of NF1 includes café au lait macules, lisch nodules, optic pathway gliomas, skeletal dysplasia, neurofibromas, and the focus of this research, the Choroidal Abnormality. Diagnosis of NF1 generally occurs in the late pediatric age group. In the Neuro-ophthalmology clinic, lisch nodules (benign hamartomas of the iris) and optic pathway gliomas are observed via slit lamp examination or MRI respectively, however, these manifestations of NF1 are absent until age 5. Choroidal abnormalities are a newer observation that may allow for an earlier diagnosis of NF1 before the appearances of lisch nodules and other NF1 manifestations. Utilizing Near-Infrared Fundoscopy, Choroidal abnormalities present as hyperreflective spots on the retina (bright white spots on a darker gray background). The Choroidal abnormalities histologically correspond to melanocyte aggregation or Schwann cell-derived clumps. While Lisch Nodules are generally present after age 5, the Choroidal abnormalities can be detected as early as 2 years of age. Earlier detection offers patients options. Medication to treat NF1 by suppressing tumor growth exists. Giving physicians the tools to detect NF1 in the earlier years may result in an improvement in patient quality of life as well as extend a patient's lifespan.

71 Measuring Starlink quality of experience in rural regions

Michelle Leonard, Elizabeth Bugayev, Vahan Tadevosyan, Vasanta Chaganti • Swarthmore College

ebugaye1@swarthmore.edu, mleonar1@swarthmore.edu, vtadevo1@swarthmore.edu, vchagan1@swarthmore.edu

Starlink is a novel satellite-based internet service provider (ISP) which began operations in 2019. By routing data packets through mega-constellations of satellites in low-Earth orbit (LEO), Starlink offers both lower latencies compared to geosynchronous satellites and greater connectivity in rural areas which lack the infrastructure to support fixed broadband or wireless Internet access. At the same time, LEO satellites have drawn concern for their rapid orbit relative to the Earth's surface that require frequent satellite hand-offs to maintain a given connection, which could cause periodic network disruptions. While Starlink continues to launch thousands of satellites annually to expand its global reach, there is a clear need for greater insight into Starlink's performance in the first few years of its lifespan, especially in key rural areas. This research additionally has the potential to inform technological policy in countries which have yet to grant Starlink legislative approval. We investigate a breadth of established Internet measurement techniques and datasets from networks literature, including crowd-sourced datasets such as the NDT and Cloudflare speedtests as well as RIPE test boxes. We then identify rural and technologically underserved regions across the globe according to the criteria of geographic isolation, population size, population density, and the presence or absence of existing Internet infrastructure, and develop a set of data-filtration criteria to isolate data from those regions. Key metrics examined were round-trip latency and packet loss. Our findings show that Starlink performance in selected regions is comparable or superior to other network providers. Our research builds on previous work by other authors to measure Starlink's quality of experience; the

resulting dataset, to our knowledge, represents the first longitudinal, global attempt to catalog Starlink performance in rural areas.

72 Glioblastoma Mathematical Modelling

Andrea Lie, Dr.Piovoso

This study presents a mathematical model that simulates interactions between glioma, neurons and glial cells, both with and without chemotherapy, to investigate more effective treatment regimens. The model consists of a system of differential equations, adapted from established frameworks, that describe the dynamics of glioma, glial, and neuronal cell populations during chemotherapy administration. Using MATLAB, we explored a range of chemotherapy protocols over a 500-day period, systematically varying drug concentration, treatment duration, and dosing cycle length. Simulation results indicate that specific combinations of chemotherapy "on" days and cycle intervals can significantly reduce glioma cell populations while preserving neuronal viability. These findings highlight the potential for optimizing chemotherapy schedules to maximize tumor suppression and minimize neural damage. While preliminary, this work provides a computational foundation for developing personalized glioma treatment strategies and underscores the value of mathematical modeling in therapeutic design.

73 243-4 and LC-10 DMAbs produce antibodies in vivo and in vitro; and can neutralize alpha toxins in vitro.

Gina Lin, Dr. Ami Patel • The Wistar Institute Vaccine and Immunotherapy Center

glin1@swarthmore.edu

MRSA (methicillin resistant staphylococcus aureus) causes bacterial infections that primarily infect the respiratory tract. Historically, antibiotics were used to treat symptoms of S. aureus and as a result developed antibiotic resistance. Most strains of MRSA produce alpha toxins.

Alpha toxins create pores on the surface of cell membranes. They do this by binding to the ADAM-10 surface protein, which then causes the formation of a heptameric ß-barrel and ultimately cell lysis. Additionally, once alpha toxin binds to ADAM-10, it breaks down the protein E-cadherin, which mediates cell-cell adhesion, contributing to damage of the epithelial tissue.

An approach to combat antibiotic resistance is by using MAbs (monoclonal antibodies) which can bind to and neutralize alpha toxins, preventing further infection. Mabs (monoclonal antibodies), are synthetic antibodies that are designed to target specific antigens. But, since MAbs have a short half-life and face delivery related complications, DMAbs offer a promising alternative.

DMAbs (DNA encoded monoclonal antibodies) are engineered to encode optimized antibody genes, potentially providing a safer, stable, and more sustainable approach to targeting antibiotic resistant infections.

In this research, two DMAbs were tested for production efficacy *in vivo* and *in vitro.* The 243-4 antibody (by Aridis) binds to the rim domain of alpha toxins, (the structure that allows for binding to the eukaryotic membrane), specifically to the R66 residue (arginine at position 66). The LC-10 antibody (by Medimmune/AstraZeneca) binds to the alpha toxin epitope centered at R200, located on an adjacent part of the rim domain (the amino acid residue at position 200). This interaction physically hinders alpha toxin interaction with ADAM- 10. Both 243-4 and LC-10 DMAbs transfected into cells produced MAbs that had the ability to neutralize alpha toxins; and DMAbs injected into mice models produced MAbs.

74 Metabolic and Behavioral Effects of LEAP2 on Stress Resilience

Grace Liu, Dr. Ki A. Goosens • Department of Psychiatry, Center for Translational Medicine and Pharmacology, Icahn School of Medicine, New York, NY 10029

gliu3@swarthmore.edu

Ghrelin is a peptide hormone produced in the stomach and released into the circulation that stimulates appetite by acting as an endogenous ligand for the growth hormone secretagogue receptor (GHSR). Although elevated ghrelin is capable of increasing hunger in rodents and humans, recent

studies have shown that ghrelin levels are also elevated after chronic stress in rodents and trauma-exposed humans. Chronic stress can induce multiple stress responses, including decreased glucose tolerance, heightened fear responses, and weight loss, effects that are likely mediated in part by elevated ghrelin. Liver-expressed antimicrobial peptide 2 (LEAP2) is an endogenous antagonist of GHSR that is produced by liver cells and released into the blood. By binding to GHSRs, LEAP2 prevents ghrelin from activating its receptor. We hypothesize that LEAP2 modulates ghrelin-sensitive stress responses. More specifically, we hypothesize that overexpression of LEAP2 in the liver of mice reduces stress-induced elevation of blood glucose levels, fear responses, and stress-induced weight gain. All mice received liver-targeted injections of either an AAV8-LEAP2 virus or phosphate-buffered saline (PBS) four weeks prior to behavioral testing. The effects of LEAP2 overexpression on chronic stress responses will be evaluated using glucose tolerance tests, fear conditioning, and longitudinal assessments of body composition. Preliminary results on body composition suggest a potential role for LEAP2 in modulating body composition in male mice and lay the groundwork for further experimentation. Future studies will include glucose tolerance tests, fear conditioning trials, continued body composition analysis, and measurement of corticosterone levels.

75 Climbing Trees: Ecological Mechanisms of a Novel Fruiting Morphology in *Thelephora spp.*

Josephine Low, Andrew Ratz, Peter Kennedy • Cedar Creek Ecosystem Science Reserve, East Bethel, MN 55005
jlow1@swarthmore.edu

Fungi of the ectomycorrhizal-associating genus *Thelephora* exhibit morphological plasticity by fruiting in both coralloid and crust forms. Fruiting bodies of *Thelephora spp.*, likely *T. terralis* or *T. americana*, have been observed to opportunistically climb on tree stems, though this has not yet been described nor mechanistically explained. This study uses the Forest and Biodiversity 2 (FAB2) experimental platform of Cedar Creek Ecosystem Science Reserve to evaluate the factors contributing to *Thelephora* climbing, namely host tree clade, physical properties of the structure being climbed on, and distance from an existing climbing sporocarp. Poplar wood and polyethylene plastic stakes were installed at distances of 5 cm, 25 cm, and 50 cm from sporocarps on tree trunks in a total of 26 10m x 10m tree plots containing either oaks, pines, both oak and pine, oaks with arbuscular mycorrhizal (AM) tree species, pines with AM species, or both lineages with AM species. A comprehensive survey of tree species, as well as organic and inorganic structures supporting Thelephora sporocarps in FAB2 is supported by community science data on iNaturalist. Furthermore, aboveground *Thelephora* presence in all 148 10m x 10m tree plots in FAB2 across phylogenetic and functional diversity axes was correlated with ITS sequencing data showing belowground fungal diversity in FAB2 soil samples taken in 2022. Tissue samples from *Thelephora sporocarps* were sequenced for species-level identification to clarify the relationship between ectomycorrhizal host specificity and the apparent non-specificity of structures supporting sporocarps. This presentation represents preliminary data from a project ongoing from Summer 2025 to Spring 2026.

76 Oxytocin–Cortisol Interactions and Social Support in Small-Scale Societies

Gongfu Lyu, Charlotte Debras, Dominik Jud, Prof. Adrian V. Jaeggi, Prof. Caleb Axelrod
Institute of Evolutionary Medicine, University of Zürich • Institute of Evolutionary Anthropology, University of Zürich • Swarthmore College

Human social behavior emerges from the dynamic interplay between neuroendocrine signaling and ecological context. Oxytocin (OT) and cortisol (CORT) are two central yet interacting hormonal systems: OT has been widely linked to affiliation and social bonding, while CORT mobilizes energy and coordinates responses to stress. However, mounting evidence suggests that their relationship is neither linear nor uniform, but highly context-dependent, varying across phases of reactivity and recovery, and shaped by social and ecological conditions. Despite these insights, our understanding of OT–CORT coordination in naturalistic, small-scale settings remains limited.

This study examines OT–CORT interactions in the Tsimané, an indigenous forager–horticulturalist population in the Bolivian Amazon. The Tsimané subsistence ecology and kin-based social organization provide a valuable contrast to industrialized populations, where most previous

research has been conducted. Morning urine samples were collected and assayed for OT and CORT concentrations, offering a window into baseline endocrine function and its variability across individuals. To capture the social dimension, we employed standardized questionnaires in which participants reported perceived availability and frequency of support from kin, friends, and community members. These self-reported social support scores allowed us to directly assess whether stronger social networks predict differences in hormone regulation.

Rigorous data integration and cleaning were performed using harmonization pipelines in R to address missing values and repeated measures. We then developed a Bayesian hierarchical modeling framework to jointly estimate OT, CORT, and their interactions while incorporating inter-individual variability and questionnaire-based social support effects. Bayesian methods are particularly well suited for these data, as they accommodate small sample sizes, allow partial pooling across individuals, and provide a principled way to model probabilistic, context-sensitive dynamics.

Preliminary results indicate that individuals embedded in stronger social support networks show higher baseline hormone intercepts but steeper negative slopes across time, a pattern consistent with social buffering. In other words, social support appears to modulate endocrine reactivity, aligning with the hypothesis that close social ties can protect against stress by shaping the coordination of OT and CORT.

By situating endocrine interactions within an ecological and cultural framework, this work contributes to a more nuanced, evolutionary grounded understanding of human stress and social adaptation. Our findings highlight the value of integrating hormonal assays with questionnaire-based social measures through Bayesian inference and underscore the importance of including small-scale societies in the study of biostatics and neuroscience.

77 Characterizing Fungal Biomaterials for Aerospace Applications

Kiran Mahurkar, Lynn Rothschild, Rolando Perez, Jessica Snyder • NASA Ames Research Center

kiran.ruthel.mahurkar@gmail.com

Since the agricultural revolution, humans have used biomaterials to make our clothes, support our houses, and interact with our environment; over the last century, our manufacturing has shifted strongly towards synthetic materials like plastics and composites. This is especially true in newer fields like the aerospace industry, where an emphasis on material performance has pushed non-engineered materials aside. Synthetic biology, however, offers a solution to the complex supply chains and high carbon footprint of these materials with the potential for equivalent performance characteristics.

One potential biomaterial source comes from saprotrophic fungi. Commonly known as "white rot fungi," these species are found all over the world and play a major role in the breakdown of woody detritus. To do this, they grow a dense network of tendrils

(mycelium) into their food source. In addition to facilitating nutrient transport, these mycelial networks bind loose substrate together into a solid mass. We can exploit this ability to create biomaterials with a wide range of compositions and properties.

Due to their novelty, these materials have not been widely characterized. Although some commercial applications exist (e.g., replacement for polystyrene packing foams), potential properties remain unexplored. Existing research suggests that, in addition to possible strength/weight attributes ranging from low-density foams to concrete, fungal biomaterials may have the capacity to self-heal and inhibit undesirable ignition.

To further explore these possibilities, we examined the effect of non-toxic chemical additives on the flammability characteristics of fungal biomaterials. In addition to confirming that these materials have an inherent flame-resistance, ongoing experiments focus on quantifying and comparing the responses of materials with varying additives.

One of the primary potential applications for fungal biomaterials in the aerospace industry is in the construction of human habitats directly on the lunar and martian surfaces. Due to the high cost/mass ratio of current launch systems, in-situ resource utilization (ISRU) has emerged as a highly desirable attribute in any habitat design.

Fortunately, silicon—one of the additives we tested—is found in abundance on the lunar surface. In addition, some saprotrophic fungi express the ability to extract it directly from silicate minerals. This enables the potential conversion of lunar regolith directly into flame-retardant additives during ISRU-based manufacturing.

78 Probing Regioselectivity in Dynamic Nucleophilic Aromatic Substitution

Téa Malone-Bonacci, Anna Yang • Swarthmore College

Tmalone1@swarthmore.edu

Dynamic covalent chemistry is a method for synthesizing large, complex molecules such as macrocycles, cages, and covalent frameworks. It utilizes reversible reactions of simple building blocks under thermodynamic control. Nucleophilic aromatic substitution (SNAr) is a well-studied reaction but is not traditionally considered reversible. This project explored SNAr reactions using pyridine electrophiles and hydroxy or thiol nucleophiles to create dynamic covalent systems and build macrocycles.

Early work this summer showed that exchange was difficult to achieve with most difluoropyridine electrophiles. While we were unable to observe exchange with phenol reactions, thiophenols successfully underwent exchange until equilibrium was reached. We tested this by starting the reaction from three different initial conditions using two different thiophenols at equal concentrations. HPLC was run at various timepoints, and in each case, the product distribution eventually stabilized. For all starting points, a similar final distribution was observed, indicating equilibrium had been reached.

These results align with our understanding of the nucleophiles' nature. Hydroxy nucleophiles form ester linkages that donate electron density, deactivating the resulting product and making it less susceptible to additional SNAr reactions, thereby making reversibility difficult. Thiols, however, are both stronger nucleophiles and better leaving groups due to their large, polarizable electron clouds. Our findings suggest that the thioether linkage may facilitate the electrophile's interaction with further nucleophilic attack.

In addition to exchange reactions, we designed a reaction scheme to probe the extent of thiol bond activation by combining monosubstituted reaction products with additional nucleophiles. The results were somewhat inconclusive but suggest avenues for further investigation.

In the original macrocycle design, two well-characterized options were considered. The ether-linked macrocycle was shown via Gaussian modeling to be shape-persistent and planar, with a smooth surface and extensive conjugation expected to enable π–π stacking and higher-order structures. Thioether linkages, in contrast, are typically kinked but can be tuned to planar forms under reducing conditions—an aspect that could be used in designing environmentally responsive materials.

Given our results indicating the difficulty of achieving dynamic exchange with phenols, we turned to exploring a mixed nucleophile: 2-mercaptophenol. We found that most electrophiles were substituted exclusively with sulfur at the more activated position when a significant difference in activation existed between sites. This suggests that a mixed nucleophile containing both hydroxy and thiol groups can be used for regioselective substitution, potentially enabling directed formation of macrocycles.

79 AI Refusal

Julia Mammen

Opposition to the development and use of Artificial Intelligence (AI) systems has expanded as the harms associated with it become more apparent. The growing resistance to AI is perceived by some as futile, technophobic, and regressive. Throughout history, people have resisted new technologies. Technologies are more than physical artifacts — they are socio-technical infrastructures which create and perpetuate certain worldviews. The refusal to accept the paradigms imposed by socio-technical infrastructures is often seen as regressive. Yet, through a lens of feminist theory, the generative aspect of these refusals becomes apparent. Refusals of AI come in many forms because different locations within the infrastructure of AI offer different opportunities to refuse and thus different strategies of refusal are employed. Furthermore, agents of refusal vary in the strategies available to them, as infrastructure exists and perpetuates power structures that asymmetrically distribute power. This research explores strategies of refusal in the context of history, infrastructure and power.

80 Detecting Gene Modules Associated with Trait Acquisition in the Blood Cells of an Invertebrate Chordate

Cohen Manges, Tal Scully, Dr Allon Klein, Dr. Bradley Davidson • Swarthmore College

cmanges1@swarthmore.edu

The evolutionary acquisition of a novel cellular trait may be driven by coding mutations that alter protein function or non-coding mutations that alter gene expression or non-coding mutations that alter transcription factor expression. In the latter case, these non-coding mutations could result in the simultaneous co-option of a downstream gene module (a group of co-expressed, functionally related genes), causing a change in that cell's protein content and thus function. I am conducting a comparative analysis of single cell RNA sequencing data from the blood cells of three tunicate species, *Ciona robusta, Ciona intestinalis*, and *Ciona savignyi,* to explore whether gene module co-option is associated with cellular trait acquisition. Previous work has identified orthologous cell states shared across these data sets that likely represent orthologous blood cell types. I developed a Pearson Correlation based algorithm to analyze gene co-expression across all blood cell states, searching for groups of genes that are highly co-expressed in all blood cell types, indicating shared regulation and possibly function. I predicted I'd find a large group of functionally related genes coexpressed in the blood cells by priming the algorithm with genes previously known to be involved in a tunicate-specific blood cell trait, vanadium sequestration. Surprisingly, the vanadium-sequestration gene set failed to exhibit conserved co-expression across orthologous cell states in these three species. I am currently attempting to apply this algorithm to a larger presumptive gene module associated with phagocytosis using less selective parameters to capture a gene module not specific to a single cell type, but rather related to a broadly applied cellular trait.

81 AR Aviary

Jenna Martinez, Keith O'Hara • Swarthmore College

jmartin7@swarthmore.edu

Typically when images are projected on large surface areas, either one large projector or multiple projectors are used to be able to encompass the entire area. These configurations are efficient in creating large scale projections, but can be expensive and excessive when projecting a small moving image around a large space and across multiple planes. In these more specific use cases, a smaller, mobile projection would be preferable. One use case for this technology is the creation of an augmented reality aviary consisting of user created birds flying around and interacting with the objects in a room by "perching" on them. This is the end goal of this project. To achieve the mobile projection required for an AR Aviary, a mirror and camera were mounted to a pan/tilt servo rig and placed in front of a stationary projector. With this setup, the mirror is able to bend the projection pointed at it and move it around the room. Furthermore, the attached camera is able to move with the mirror and send visual information to the computer for keystone correction. On its own, the rig can be controlled by an external gamepad, allowing a user to manually move whatever is projected up, down, left, or right. Within the context of the AR Aviary, the movement of the projection would not be controlled by a person, but rather by automated behavior of the birds. Here, one bird would serve as the "selected" bird and the rig would follow its flight path, revealing the bird's virtual realm as it traverses space. The end goal of this project is to set up an exhibit in the newly completed Martin Hall where students can contribute their own bird designs through a website, and view their virtual birds merging with the physical environment.

82 Variation in the individual immune response of female cat fleas *(Ctenocephalides felis) a*gainst a systemic bacterial infection

Margalit Mauricio, Dr. Lisa Brown • Georgia Southern University

mmauric1@swarthmore.edu

A central challenge in immunology is determining why two hosts exposed to identical infections and in the same environmental conditions exhibit different outcomes. One might show mild symptoms and recover, while the other faces severe illness or death. Cat fleas *(Ctenocephalides felis)* are an

important vector for bacterial transmission, as they carry chronic infections that they transfer to their host via bite or defecation. In this study, we examined the capacity of females to overcome a systemic bacterial infection in their hemocoel. Specifically, fleas were injected with an ampicillin-resistant, GFP-expressing strain of *Escherichia coli* using a Nanoject III Automatic Nanoliter Injector. After two hours, we recorded survival at 2-, 4-, 6-, 8-, 10-, and 24-hours post-injection. At each time point, dead fleas were removed, homogenized, plated on selective media, and the resultant colony-forming units were used to determine the bacterial load upon death. After 24 hours, the bacterial load in living fleas was quantified. Data were collected as survival rates and colony counts to measure bacterial load. Our data showed there is no correlation between time of death and infection load, but that dead fleas have much higher infection loads than live ones. This suggests that infection outcome is determined by how long it takes the individual flea to mount an effective bacterial response and that hosts die if a certain threshold is reached.

83 WSIT: Supporting Workers in an Age of Workplace Monitoring Proliferation

Morgan McErlean

The Workplace Surveillance Incident Tracker, our project, is a tool aimed at promoting worker empowerment in the face of a proliferation of workplace monitoring. Workplace monitoring is any way in which an employer intrusively surveils their employee. Workplace surveillance technologies (WSTs) are becoming increasingly prevalent in the workplace, with over two-thirds of workers reporting being electronically monitored, according to Hertel-Fernandez. Further, WSTs are often pervasive, opaque, and harmful to workers in a myriad of ways; this can look like discriminating against workers, negatively impacting their well-being, invading their privacy, or diminishing the quality of their work. Exacerbating this problem, worker accounts are hard to collect.

The WSIT attempts to remedy these challenges faced by workers by providing insight into ways companies surveil their workers through providing an incident tracker; creating a form for workers to report surveillance; and supplying workers with ways to resist (through legal avenues, organizing, and "tech hacks") surveillance practices in their workplace. Through our data collection and content analysis, we collected and analyzed 256 cases–all taken from journalistic sources–of workplace surveillance across 200 companies in the United States from 2010 onwards. This data collection revealed several interesting findings; privacy was the most prevalent harm, AI/algorithmic systems the most used device/mode, and employee activity the most collected data.

To improve upon our tool, we conducted pilot study interviews with seven individuals, focused on whether or not they felt workers would trust this tool. We found through these studies that we needed to center workers more prominently, increase the accessibility of our tone, and neutralize any political language. In the future, we are focused on continuing development of the tool, centering workers in our approach. Upon finishing our development, this project will culminate in a co-design session with workers and advocacy groups, supported by our partners at Coworker.org and the Center for Democracy and Technology.

84 Bayesian Wind Farm Layout Optimization

Michael Melnikov, Taylore Keesler, Allen Zhou, Sophia Xiao

Maximizing the annual energy production (AEP) of large-scale wind farms is a challenging blackbox optimization problem. Each candidate layout requires an expensive wind-farm simulation, gradient information is unavailable, and strict geometric constraints on turbine spacing and site boundaries must be satisfied. In collaboration with Lawrence Livermore National Laboratory'sCenter for Applied Scientific Computing, we investigate constrained Bayesian optimization (BO) algorithms for efficiently exploring the design space of the wind farm layout optimization (WFLO) problem.

We first evaluate standard BO with Expected Improvement and Lower Confidence Bound acquisition functions on benchmark problems. For the WFLO task, we compare four constrained BO strategies: (1) a vanilla BO baseline using IPOPT (an interior-point method) for constraint handling, (2) the Hybrid BO–IPOPT algorithm for constrained optimization, (3) SCBO (Scalable

Constrained Bayesian Optimization), and (4) FuRBO (Feasibility-Driven Trust Region Bayesian

Optimization), a trust-region approach that adapts to the feasible set. We also experimented with custom covariance kernels designed to exploit the geometry of turbine layouts. Empirical results show that FuRBO and the Hybrid BO–IPOPT method consistently outperformboth SCBO and the vanilla BO baseline, identifying feasible layouts with substantially higher AEP.

85 RNA-Seq Analysis of HSATII Knockdown in Cancer Cells Reveals Downregulation of Genes Implicated in Oncogenic Pathways

Lisa Messier, Benjamin Lipchin, Christina Rabeler, Dawn Carone • Swarthmore College
lmessie1@swarthmore.edu

Human satellite II (HSATII) is a tandemly repeated DNA sequence that is normally silenced in healthy cells but aberrantly transcribed in many cancers. The resulting HSATII RNA accumulates in the nuclei of cells and contributes to genomic instability, making it a potential therapeutic target. This study investigates the effects of HSATII knockdown using Gapmers, antisense oligonucleotides designed to target and degrade HSATII RNA, with a focus on RNA-seq analysis, downstream changes in the transcriptome, and pathway enrichment analysis.

RNA-sequencing data from U2OS cells transfected with a 16-base pair HSATII Gapmer, a MALAT1 Gapmer, or no Gapmer control were analyzed to assess the efficiency of HSATII knockdown and genome-wide changes. A computational pipeline was developed in RStudio incorporating Kallisto for pseudoalignment, tximport for mapping transcripts to genes, DESeq2 for differential expression, and g:Profiler for pathway enrichment analysis.

Computational analysis confirmed that Gapmer treatment effectively reduced HSATII RNA, with knockdown observed across nearly all HSATII sequences. Differential expression analysis revealed broad changes in gene expression, including downregulation of oncogenic signaling pathways such as EGFR and MAPK signaling. These findings suggest that HSATII may influence cancer cell survival and proliferation through its impact on oncogenic signaling networks, highlighting its potential as a therapeutic target.

86 Additively Manufactured Quick-Acting Watertight Door Dog Analysis

Olivia Montini

This research project was conducted as part of the Naval Research Enterprise Internship Program (NREIP) under NAVSEA and the Naval Surface Warfare Center Philadelphia Division (NSWCPD). It was part of a multi-phase test plan evaluating the potential use of an Additive Manufacturing (AM) Quick-Acting Watertight Door (QAWTD) Dog on U.S. Navy Surface Ships and Carriers. The function of a QAWTD Dog is to ensure a watertight seal on doors located throughout various classes of Ships and Carriers. This study focused specifically on Dogs that are part of a linkage assembly, which allows all Dogs on a QAWTD to be operated simultaneously by using the door handle.

The AM Dog is manufactured using Laser Powder Bed Fusion (LPBF), a 3D printing form of metal manufacturing. My fellow intern and I conducted dimensional analysis checks, 3D modeling, and Finite Element Analysis (FEA) using SolidWorks software to compare the AM Dog to the Navy Standard Dog currently in use. Our results showed that all dimensions of the AM Dog fell within the required tolerances, and FEA indicated stress concentrations in expected areas—particularly around the relief cut—with minimal displacement under applied forces, consistent with the Navy Standard Dog.

This research provides proof of concept that the AM Dog can serve as a valid substitute for the Navy Standard Dog when deployed at sea and can now advance through Naval Testing such as Hydrostatic and Shock Testing. If future testing is successful, the long-term goal is to implement LPBF machinery aboard ships and carriers to enable in-situ replacement of damaged or broken Dogs while deployed.

87 Who's Logging On? School Staff Engagement With Online Mental Health & Equity Courses

Allison Morales, Beatriz Cabello MPH, Dr. David W. Johnson • Northwestern University Lurie Children's Hospital of Chicago, Center for Childhood Resilience

amorale1@swarthmore.edu

Unmet youth mental health needs represent a critical U.S. public health concern, compounded by declining well-being and care access barriers. Schools are pivotal in addressing these challenges, serving 58% of treated youth. Professional development (PD) is essential for preparing school staff; however, empirical research on wellness and equity-focused PD remains sparse, often overlooking personalized or socio-ecological approaches. This perpetuates a research-practice gap, exacerbated by financial and time constraints for staff. Online PD, like that from the Learning & Resource Hub (LRH), offers promise for overcoming these barriers, but understanding who is engaging with these courses and why is essential for addressing gaps in research, tailoring learning content, and fostering motivation.

This mixed-methods study (N=5,416) investigated school staff engagement with three LRH wellness/equity courses, delineating demographic patterns in course completion and motivations. Thematic analysis, guided by Self-Determination Theory, informed motivation analysis. Logistic linear regression results indicate certain topics resonated more with specific demographics, and uncovered general low course-taking among certain groups. While mandates drove participation, many crucial subjects were overlooked. These insights underscore the need for targeted, effective PD interventions responsive to diverse staff and student needs. Ultimately, these findings can inform policy, enhance online PD effectiveness, and cultivate more supportive school environments for youth mental health.

88 Modeling the Transmission Dynamics of the Monkeypox Virus Infection with Intervention Measures

Emiliano Morales-Lopez and Nyvisalsnuk Rith; Advisors: Nsoki Mavinga and Tendai Mugwagwa Swarthmore College

emorale2@swarthmore.edu

Mpox is an infectious disease caused by the monkeypox virus that can be spread between humans and animals, and is endemic to western and central Africa particularly in the Democratic Republic of the Congo (DRC). We develop a deterministic model to analyze the effectiveness of vaccination and other intervention measures for Mpox, while also demonstrating the transmission dynamics including the potential transmission event from a human to an animal. Through mathematical analysis, we show the positivity and boundedness properties of the solutions within the model. Furthermore, we derive the basic reproduction number R0 using the next generation method, and provide the necessary conditions for disease-free equilibrium to be locally stable through a combination of the linearization method and the Routh-Hurwitz criterion. Additionally, we give sufficient conditions for global stability of the disease-free equilibrium. The model is fitted using the nonlinear least square method to describe the dynamics of the disease based on reported cases of Mpox from DRC between 2023 and May 2025. Sensitivity analysis is performed to show the responsiveness of R0 with respect to the model parameters.

89 Multistep Generative Backmapping of Coarse-Grained Structures

John Nicholson, Yuefan Deng, Ph.D. • Stony Brook University

jnichol2@swarthmore.edu

Backmapping matters because it recovers atomistic detail after coarse-grained simulations that accelerate protein modeling. To gain speed, proteins are simplified; once runs finish, researchers must reconstruct the true structure – the backmapping task. These simulations illuminate folding and interactions, informing drug design and protein engineering. Yet data-driven backmapping from coarse-grained (CG) to fine-grained (FG) often suffers from limited accuracy, unstable training, and poor physical realism—challenges that are especially acute for complex protein systems.

The purpose of our study was to introduce a novel iterative framework by using conditional

Variational Autoencoders and graph-based neural networks, specifically designed to tackle the challenges associated with such large-scale biomolecules.

Our method enables stepwise refinement from CG beads to full atomistic details. We outline the theory of iterative generative backmapping and demonstrate via numerical experiments the advantages of multi-step schemes by applying them to proteins of vastly different structures with very coarse representations. This multistep approach not only improves the accuracy of reconstructions but also makes the training process more computationally efficient for proteins with ultra-CG representations.

We found for the protein eIF4E, the 2-step scheme significantly reduces the RMSD, especially at the highest CG bead size (10 beads, $\rho = 18.10$), where the RMSD drops from 7.56 Å (1-step) to 1.50 Å (2-step). Improvements are also consistent at finer resolutions ($\rho = 9.53$ and 3.62), with RMSD values falling below 1.00 Å for the finest CG. For another protein, PED00151, the more flexible IDP, results show a clear but more moderate improvement with the 2-step scheme. The RMSD decreases from 7.49 Å (1-step) to 5.37 Å (2-step) at $\rho = 9.60$ and from 5.71 Å to 4.12 Å at $\rho = 6.00$. These gains are 18% less dramatic than in eIF4E, highlighting the inherent challenges in backmapping disordered proteins. In terms of steric clashes, PED00151 shows extremely high scores with the 1-step baseline (nearly 100%), indicating severe structural artifacts. The 2-step scheme dramatically reduces these values to 25.61% and 13.63%, respectively, showing that iterative refinement significantly enhances physical realism.

Beyond raw performance, our multistep scheme brings practical engineering benefits. First, it reduces and smooths the optimization search space for each subtask, leading to better convergence and less susceptibility to local minima. Second, by isolating different levels of resolution, the approach allows greater architectural flexibility; different layers or loss functions can be used at each step to better capture the geometric or chemical constraints relevant to that scale. Third, it facilitates error detection: training and validating each step independently helps identify specific failure points in the reconstruction process. Collectively, these advantages yield a framework that is not only more accurate but also more interpretable and maintainable during development.

90 Exploration of Peptoid Nanosheets as a Novel Water Filtration Membrane Material

Lucas Oberdiek and Professor Anna Yang • Swarthmore College Department of Chemistry and Biochemistry

loberdi1@swarthmore.edu

Within the past 20 years water filtration membranes have emerged as an energy efficient and robust method of purifying water for waste management, drinking, and industrial purposes. However, there still exist problems with current membrane materials such as the trade-off between permeate flux and contaminant selectivity, as well as the issue of membrane fouling. While extensive research into improving water filtration membrane materials to address these problems has been conducted, there exists a gap in easily tunable membrane materials to answer fundamental research questions and streamline the design and fabrication process of membranes with specific needs for large-scale usage. Peptoids are a biomimetic polymer invented by Zuckermann et al. which are synthesized via the sub-monomer method and differ from peptides only in position of attachment of side-chains to the amide nitrogen rather than the alpha carbon. Various peptoid motifs have been shown to self-assemble into a variety of supramolecular architecture including nanosheets, consisting of a hydrophobic core and hydrophilic outer layers. Peptoid nanosheets' high tunability, smoothness, and hydrophilicity make them an ideal candidate to fill the gap in high-performance tunable membrane materials.
In this work we optimize the self-assembly process of peptoid nanosheets to increase output while maintaining their characteristic structure and morphology and characterize the formed nanosheets with confocal fluorescence microscopy. Peptoid nanosheets were then shipped to collaborators at Argonne National Laboratory to test whether nanosheet size, quantity, or morphology was layered by the shipping process. A photochemical reaction to create biphenyl crosslinks in the nanosheet cores was explored to improve nanosheet stability during testing. Lastly, experiments on characterization of a polyethersulfone membrane support by confocal microscopy and deposition of peptoid nanosheets onto the membrane support were conducted and set the basis for future work on the project.

91 Investigating the complex mechanisms modulating the dissolution of silver nanoparticles: pH, size & the presence of biomolecules

Mojisoluwa Oludare, Kathryn Riley • Department of Chemistry and Biochemistry, Swarthmore College
moludar1@swarthmore.edu

Silver nanoparticles (AgNPs) are widely used in commercial and medical products, yet their fate and reactivity in biological systems is poorly understood. Here, we describe the kinetics of AgNP dissolution, which is important to AgNP toxicity mechanisms. Specifically, we studied the impact of environmental pH, nanoparticle diameter, and the presence of biomolecules on the dissolution of citrate-stabilized AgNPs. Our experimental studies will contribute to our understanding of AgNP reactivity. Linear sweep stripping voltammetry (LSSV), an electrochemistry technique, was used to measure the amount of silver ions released into solution from dissolved AgNPs at five-minute intervals over two-hour periods. The dissolution rate constants of AgNPs were then calculated. It was found that dissolution rate constants increased at low pH and decreased at high pH, suggesting that multiple mechanisms contribute to the pH-dependent dissolution of AgNPs. Furthermore, dissolution rate constants decreased as nanoparticle size increased. Dissolution rate constants of AgNPs increased in the presence of low concentrations of glutathione (GSH), a biomolecule of environmental and biological importance, and decreased at higher concentrations of GSH. Together, these studies show the complex nature of AgNP dissolution and the need for continued investigation of these systems.

92 Multivariate classification of visual image categories from scalp EEG data

Elle Pedaci, Youssef Ezzyat • Department of Psychology, Swarthmore College, PA, 19081
epedaci1@swarthmore.edu

The human brain rapidly categorizes encodes visual information for later retrievalso that it can be later remembered, yet the neural dynamics underlying this process remain an active area of investigation. Advances in machine learning now allow researchers to decode category-specific neural patterns in scalp EEG data when people view images from different visual categories. This suggests that scalp EEG could also be used to measure memory encoding and retrieval of specific categories of visual information., providing new insight into how the brain distinguishes between visual categories. Here, we report our initial investigations into using multivariate statistical methods to decode visual category representations from scalp EEG data. In the present study, we employed Support Vector Machines (SVMs) across two experiments to assess the discriminability of visual stimuli. In the first experiment, we examined the N170 event-related potential, a well-established marker of early face-selective processing, by comparing neural responses of famous faces and everyday objects. The second experiment extended this approach by including famous faces, well-known scenes, and everyday objects, serving as a localizer for subsequentce memory-related research. The goal of these experiments was to determine if these image categories could be reliably decoded upon during visual perception. To ensure attention and engagement, participants indicated when images repeated throughout the experiment. Behavioral results showed that participants were highly accurate in detecting repeated images, as reflected in high revealed strong d' values, confirming high discriminative accuracy across categories in both experiments. We then applied support vector machine (SVM) classifiers to participants' EEG data to determine whether neural activity recorded at the scalp contained information about the visual category being viewed. We found that Further, the SVM classifier predicted image categories significantly above chance in all participants, with stable performance observed between 200-800 ms after image onset, validated through leave-one-block-out cross-validation in both experiments. Building on these findings, our next step will be to investigate whether these category-specific neural patterns can be decoded during extend to memory processes. In a forthcoming memory paradigm, participants will encode images in short category trains, complete a distractor task, and perform a retrieval task involving both studied and novel lure images. By utilizing the neural signatures identified in the localizer as training data, we will test the ability of SVMs to decode visual category from EEG data during encoding and retrieval.

93 Implementation of a culturally-grounded ENDS intervention program for Hawai'i's youth

Natalie Pham, Scott K. Okamoto, Ph.D.; Secondary mentors: Tessa Palafu, Kelsie H. Okamura, Ph.D.
University of Hawai'i Cancer Center, Honolulu, HI

npham1@swarthmore.edu

Hawai'i currently leads the nation in the use of Electronic Nicotine Delivery Systems (ENDS), with 18% of middle school students reporting usage—one-third of whom identify as Native Hawaiian or Pacific Islander (NHPI). NHPI populations have the highest incidence and mortality rate of lung cancer, compounded by limited access to care and lack of public health education. As emerging research continues to link ENDS use to elevated lung cancer risk, there is an urgent need for targeted, culturally responsive interventions across the islands.

Ho'ouna Pono ("to send with righteousness") is a nine-lesson, video-based, culturally-grounded drug prevention curriculum originally developed on Hawai'i island. The curriculum draws from real drug encounters highlighted by Hawai'i's youth through focus groups. To promote research engagement, Hawai'i's youth were invited to participate in the development of the short films used in the curriculum. While the original curriculum demonstrated effectiveness, it requires adaptation to address the rising prevalence of ENDS use among youth. To meet this need, three ENDS-specific lessons are currently in development and are slated for pilot implementation in Fall 2025. In collaboration with youth participatory action research project *Mohala Na Pua Ui I Ka Wai O Na Kuahiwi* ("the youth thrive, being nourished by the waters of the mountain range"), an ENDS-focused lesson was piloted at a Windward O'ahu middle school to gather real-time feedback from students and educators. Students were asked to evaluate two Ho'ouna Pono lessons and were assessed on resistance strategies to determine efficacy of ENDS curriculum.

Students are receptive to the new ENDS curriculum and find ENDS-use more relevant than other substances. Since Hawai'i is ethnically diverse and isolated from the mainland United States, a culturally-grounded curriculum proves to be successful in teaching drug resistance behaviors compared to a universal curriculum approach. Using student feedback, evaluation data, and culturally-grounded lesson planning, the three new ENDS lessons will be finalized for submission to the Department of Education for piloting in Fall 2025. After approval, the curriculum will be tested for efficacy at rural schools on Hawai'i island.

ENDS is a public health threat, especially in rural and NHPI communities. Imparting resistance strategies through culturally responsive psychoeducation is the first-line defense for lung cancer prevention in rural NHPI populations. With continued development and community engagement, *Ho'ouna Pono* and *Mohala Na Pua* aim to more effectively meet the needs of local youth, and ultimately reduce cancer risk within NHPI communities.

94 Backward Scrunching: Planarian Escape from Predation

Hannah Poon, Liesel Blau, Dr. Eva-Maria Collins • Swarthmore, Pennsylvania

Hpoon2@swarthmore.edu

To survive, animals have evolved a number of behaviors to escape dangerous conditions. In the Collins lab, we study escape behaviors of the freshwater planarian *Dugesia japonica.* This planarian reproduces solely by tearing itself into a head and a tail piece, which then regenerate within about a week into two complete worms. Regenerating pieces are especially vulnerable to assault by predators, including conspecifics in this cannibalistic worm species. Our previous work has shown that *D. japonica* produce escape behavior in response to various adverse stimuli, including amputation, low pH, heat, and certain chemicals. Both intact animals and head pieces respond with a stereotypical gait called scrunching, in which the planarian or anterior piece moves forward via periodic body contractions, away from the stimulus.

We studied a variant of this escape behavior that is shown by tail pieces following amputation and in response to stimuli applied to their anterior wound site. We named this escape behavior "backward scrunching" because it, too, is a periodic elongation-contraction behavior except that it moves a

posterior piece backward. To test if backward scrunching is the reverse analog of forward scrunching, we measured quantitative parameters of backward scrunching through computational image analysis, and compared them to forward scrunching parameters. We found that they were quantitatively different, likely due to anatomical differences of heads and tails. Using electrical stimulation, we found that backward scrunching requires moderate levels of stimulation to their anterior end and stronger stimuli than forward scrunching. Amputation and predation exceed that threshold. Determining the biological relevance of this behavior required testing whether backward scrunching was a laboratory behavior or had significance in natural conditions. We knew from previous literature that asexual planarians reproduce through fission - ripping themselves into a head and tail piece that then heal and regenerate the wounds from the process within about a week. By recording the behavior of a group of planarians over days, we found that intact planarians attacked tail pieces from fissioned worms and induced backward scrunching in these tail pieces, demonstrating that natural conditions could trigger the escape behavior. Through other experiments, we showed that backward scrunching could be induced by other stimuli but required a stimulus of medium intensity and that worms would turn instead of scrunch if the stimulus threshold was not reached. This suggests that planarians, like humans, can sense and respond differentially to different stimuli.

95 Biophysical Characterization of Intramolecular Left-Handed G-Quadruplexes

Katleo Pule*, Erin Coyle*, Andrew Hendrickson, Eric Xing, and Liliya A. Yatsunyk
Department of Chemistry and Biochemistry, Swarthmore College
presenting authors

ecoyle1@swarthmore.edu and kpule1@swarthmore.edu

Left-handed G-quadruplexes (LHG4) are a subset of the non-canonical DNA structure known as the G-quadruplex (G4). LHG4 differ from the more typical right-handed G-quadruplexes (RHG4) in their opposite helical twist. While their formation of LHG4 is highly sequence dependent, the exact nature of this sensitivity is still poorly understood. The biological relevance of LHG4 and their ability to interact with traditional G4 ligands are also underexplored. We studied four sequences, M1M1, M2M2, M1M2, and M2M1, designed to form intramolecular LHG4s. We determined whether these sequences maintained their LH fold with additions of single nucleotides to either the 5' or 3' end. We also characterized their interactions with N-methylmesoporphyrin IX (NMM), a known G4 binder. We tackled these questions using biophysical studies that include Circular Dichroism scans and thermal melts, thermal difference spectra, PAGE, and UV-vis titrations. We found that all four sequences were sensitive to any additions of G, while only M2M1 was able to tolerate both 5' and 3' additions of A, T, or C. The other sequences displayed sensitivity to either 5' (M1M1/M1M2) or 3' (M2M2) addition of A, T, or C. The sequences also display differing interactions with NMM, with biophysical data indicating that M2M2 refolds into an RH conformation while the other sequences refold into LH/RH hybrid. All sequences display weak binding constants of 0.9-2.2 μM-1 with NMM. Overall, our work further elucidates the sequence dependence of LHG4s and their mode of interaction with G4 ligands.

96 Fluorescence lifetime imaging to assess amyloid polymorphism

Jai Rapaka

In this research, we utilize Fluorescence lifetime imaging microscopy (FLIM) in order to investigate amyloid protein polymorphism. This project focused on evaluating Rhodamine 110 (Rho110) as a potential alternative to Thioflavin T (ThT) for imaging amyloid proteins, using hen egg white lysozyme (HEWL) as a model system. Initial experiments optimized dye concentration, revealing that 10 μM Rho110 produced oversaturation and poor FLIM image quality, whereas 2 μM enabled clearer images. Kinetics assays indicated that prolonged incubation at 40 °C caused aggregation and gel-like behavior of Rho110, suggesting sensitivity to heat exposure. In order to establish baseline fluorescence lifetime characteristics, Rho110 was imaged in aqueous environments including ddH_2O, PBS, and increasing concentrations of glycerol and ethanol. Initial phasor analysis of these samples yielded inconclusive results with points lying outside the universal circle, traced to incorrect microscope gain and frequency divider settings. Adjusting these parameters corrected the measurements and produced

the expected 4 ns lifetime for Rho110. Furthermore, FLIM data processing using GS Labs software demonstrated that Gaussian Mixture Model–based clustering could differentiate species with distinct lifetimes, though additional image editing was required to remove background clusters. Experiments comparing HEWL fibrils incubated under acidic or neutral pH and with or without Rho110 provided insights into dye–protein interactions and environmental effects on fluorescence behavior, but further data is needed to obtain concrete results.

97 Stability and Bifurcation Analysis on Fishery Models with Strong Allee Effect and Holling's Type III Functional response

Nyvisalsnuk Rith, Advisor: Nsoki Mavinga • Dept. of Mathematics and Statistics, Swarthmore College

nrith1@swarthmore.edu

Fish harvesting is an important economic sector worldwide. They also play an important role in the aquatic ecosystem and over-exploitation could have a devastating consequence in the environment. Therefore, harvesting models has gathered much interest in mathematical bio-economics. In this research, we present differential equation models that describe the dynamics of the fish population under harvesting activity. We assume that the growth of the fish population follows the logistic growth and the strong Allee effect which is the correlation between the population size to its individual fitness. The harvesting rate is given by the Holling's type III (Sigmoid) functional response where the maximum effort exerted by the predator-human is constant. We provide the conditions for the existence of nonnegative equilibrium solutions and prove the stability of each equilibrium solution. Through bifurcation analysis, we formulate a family of parameter values that guarantees the occurrence of a saddle-node bifurcation within the model. Our results show that the strong Allee effect has a significant impact on the dynamics of the fish population, especially in the extinction and the population threshold within the fishery. Numerical simulations are performed to further comprehend the theoretical result.

98 Exploring the evolution of chordate innate immunity through the study of tunicate blood cells.

Gabriela Rodriguez, Bradley Davidson • Swarthmore College

grodrig5@swarthmore.edu

The innate immune system acts as the first line of defense against pathogens in a wide range of organisms. Thus, understanding the development, deployment, and function of blood cell types within the innate immune system is a question of great interest across species. Our lab exploits the low cell numbers and simple chordate body of the tunicate *Ciona robusta,* one of our closest invertebrate relatives, to begin exploring these blood cell types. Recently, to begin investigating the evolution of innate immunity, our collaborators utilized single-cell RNA sequencing (scRNA-seq) and morphological analysis to characterize blood cells in *Ciona robusta.* Their scRNA-seq analysis identified 33 transcriptionally distinct *Ciona* blood cell states. Twenty-four cell state morphologies were annotated in fixed samples using marker gene expression. Our lab characterized seven states by in vivo morphology and behavior using fluorescent reporters. While *Ciona* blood cells express orthologs to vertebrate innate immune genes, most do not appear to be specified using conserved regulatory pathways. Recently, the lab also discovered a giant multi-nucleated blood cell morphotype that was not observed in the scRNA-seq analysis or in any previous *Ciona* studies. Preliminary results suggest these giant cells arise in response to severe inflammation or necrosis through macrophage fusion, a process observed under pathological conditions in human macrophages. Future studies will focus on the diversification of blood cells among Cionid species and will allow us to productively evaluate hypotheses of cell type and immune gene evolution. Studies of *Ciona* blood cells like these will reveal shared ancestral traits among chordate innate immune cells and how they have diversified.

99 Investigating the Role of Intron Retention in the Heat Shock Response in Arabidopsis

Brenda Maria Yañez Romero, Professor Nick Kaplinsky • Swarthmore College Biology Department
byanezr1@swarthmore.edu

Environmental stressors and disease can cause protein misfolding, a universal threat to cellular function that can lead to the formation of cytotoxic aggregates. Stressors like elevated temperatures trigger what is called the heat shock response (HSR) which results in the production of heat shock proteins (HSPs) that counter protein denaturation by preventing protein aggregation and reversing protein misfolding. The HSR and HSPs also underpin a characteristic shared by nearly all organisms – the ability to survive normally-lethal temperatures after exposure to an initial non-lethal heat shock (HS). This phenomenon is known as acquired thermotolerance (AT). In Arabidopsis, survival after an otherwise lethal 45°C HS peaks at an acclimation temperature of 37°C. Notably acclimation at 40°C – a non-lethal temperature – does not confer AT and is insufficient to protect Arabidopsis from a subsequent 45°C HS. This observation suggests that the HSR differs in some crucial way at 37oC and 40°C.

Previous work has highlighted the potential role of alternatively spliced HSP mRNA transcripts, which specifically retain intronic sequences, in modulating the HSR. Therefore, we decided to investigate the functional role of intron retention in Arabidopsis plants transformed with recombinant HSP101 or HSA32 constructs. For each gene, two transgenes will be built – one containing intronic sequences, the other without. Within these transgenes, HSP101 or HSA32 will also be fused to a gene coding green fluorescent protein (GFP) which will allow us to visualize the kinetics of HSP production in the roots of live plants subjected to a HS. In addition to this, we will test the hypothesis that intron retaining (IR) HSP mRNA transcripts prevent the acquisition of AT at 40°C. To do this, we will assess the survival of homozygous seedlings following a 45°C HS after acclimation at either 37°C or 40°C.

This summer, I successfully constructed the HSP101 genomic, HSA32 genomic and HSA32 no introns constructs. I also transformed Arabidopsis with the HSP101 genomic and HSA32 no introns transgenes and collected T1 heterozygous seeds. With these T1 seedlings we were able to verify HSP:GFP production in response to a HS. The next steps will consist of growing T1 seeds to generate homozygous T2 seeds. We will then be able to perform our AT and HSP:GFP experiments to elucidate the molecular basis behind the differing effects of acclimation at 37°C and 40°C. Understanding how the HSR is modulated could inform future strategies for engineering productive crops that are resistant to high temperatures.

100 From food waste to worm food: Quantifying greenhouse gas emissions from vermicomposting

Jesus Saucedo Bucio, Sintana E. Vergara • Department of Engineering, Swarthmore College
jsauced1@swarthmore.edu

Vermicomposting—the use of earthworms to decompose organic waste and create compost— has been used for years in varying capacities. Using compost on land provides many benefits, including enhanced crop growth, increased water retention rates, and better soil aeration. Improved aeration decreases the likelihood of methanogenesis. Composting methods have also supported more sustainable and eco-friendly alternatives for waste management. However, vermicomposting likely reduces CH4 emissions relative to other composting methods, while its N2O emissions remain uncertain [Raza et al., 2024]. This project analyzes vermicomposting's benefits by measuring greenhouse gas (GHG) emissions (CO2, CH4, N2O). The goal is to better quantify the environmental or climatic impacts of vermicomposting relative to other waste management methods, especially anaerobic ones, via a decentralized, low-technology, low-investment process.

The project uses a 10-bin (113 L) replicated system. Each bin started with 1,000 worms *(Eisenia fetida),* egg cartons, and unbleached paper towels as bedding. They are fed about 2 kg of uncooked fruit and vegetable waste, cut and homogenized, weekly. GHG concentrations were measured using laser spectrometers with a smart chamber (LI-7810, LI-7820, 8200) three times per week in triplicate. Moisture and temperature were monitored continuously (HOBO MX 2307). Gas measurements were

taken using a closed system with a custom lid fitted to the smart chamber collar. Preliminary results show that, across all bins, daily mean concentrations are significantly above ambient (661 ± 28.3 to 1084 ppm) for CO2, slightly elevated and show low variability (1683 ± 41 to 2079 ppb) for CH4, and N2O concentrations are modestly elevated with higher variability (398 ± 0.410 to 616 ppb). Emissions, especially N2O, are higher on feeding days, likely due to increased worm respiration and activity. By comparing our emissions factors with those from traditional waste management strategies, including other composting methods, we can determine the impact of vermicomposting on climate change and its benefits.

101 Diffraction Analysis of Chalcogenide Glass Structure

Grady Savage, Hillary Smith • Swarthmore College

gsavage1@swarthmore.edu

This summer I researched Chalcogenide and Metallic glasses in Hillary Smith's Materials research lab, with a focus on a few chalcogenide glass systems. The goal of my research is to understand glass formation and structures through investigating the local short range ordering of amorphous and crystalline structures of several Selenium and Arsenic based Chalcogenide glasses. I have been investigating the structure of these glasses using neutron diffraction data obtained at Oak Ridge National Laboratory (ORNL), however information about disordered and amorphous structures can't be obtained from diffraction data directly, unlike with crystalline materials, so I have been analysing the neutron diffraction data using a technique called the Pair Distribution Functions (PDF). PDFs are a real space representation of material structures obtained through the Fourier transform of diffraction data. This summer I worked in the ORNL analysis cluster to produce PDFs of our glasses at various temperatures and after crystallization. I first produced diffraction patterns through python scripts, then I performed empty can subtractions so only the glass structure would be observed and not the crystalline aluminum can's structure. By scaling and Fourier transforming these diffraction patterns I produced three versions of PDFs for all the glasses being investigated: the PDF, the reduced PDF, and the Radial Distribution Function (RDF). Using the PDFs of the crystallized structures I fit lattice parameters and crystal structure to existing phase data using PDFGui. In order to learn about the local structure of the glasses from the PDFs I analyzed the Nearest neighbor and second nearest neighbor peaks in the glasses. I analyzed these first two peaks, associated with the first two coordination shells in the local structure, by fitting them to a gaussian and recording the peak center position and the Full Width at Half Max (FWHM). With the peak position and width for each glass at each temperature I can then analyze how the structure differs between different chemical compositions in the glasses as well as how the local structure changes with temperature. By unifying this work with computer modeling/simulations as well as prior work on structural relaxation and dynamics we hope to gain a more clear and complete understanding of the structure of these amorphous materials as well as the processes that lead to the formation and alteration of these structures. By understanding these aspects of the physics underlying glasses we hope to learn more about how these materials can be produced and used in industry.

102 Electrical Energy Harvesting From Vortex Induced Vibrations Abstract

Charlie Schuetz

Vortex induced vibrations are a phenomenon that occurs when a non-rigidly mounted bluff body, like a cylinder, is placed in flow. These vibrations happen when vortices are shed from the bluff body at a frequency close to the natural frequency of the structure. When this occurs, the vortex shedding frequency "locks in" to the natural frequency and drives the system. Whether these vibrations will happen and their magnitude can be predicted based on the parameters of each individual situation. The goal of the research done this summer was to analyze the behavior of these vibrations and determine if and how these vibrations could be utilized for energy harvesting applications. This was done by systematically testing the behavior of a cylinder in the wind tunnel and the wake behind it within a variety of different parameter situations for a progression of different wind speeds. To do this, a preexisting VIV testing setup was modified to decrease mass and damping, and to maximize its modularity for a number of different parameters, including mass, cylinder diameter, and spring

constant. Testing was accomplished for a total of eight parameter situations with constant mass but variable spring constant and cylinder diameter. Testing was intended for seven more combinations of cylinder diameters and spring constants but due to setbacks in testing resources, the data collection was cut short. Despite this, data collected provided consistent data that mirrored the data achieved by prior studies in very different parameter spaces. Future testing and analysis still needs to be done to determine how energy can be harvested from these vibrations with optimal efficiency.

103 Exploring Independent Sets of Trees

Akiva Sherin, Pat Devlin • Swarthmore College

asherin1@swarthmore.edu

Graphs are a mathematical structure that consist of vertices connected by edges. Some sets of these vertices are called independent sets if they exhibit certain properties. Usually these independent sets (when ordered by size) exhibit a unimodal distribution, but this is not guaranteed. If a graph has no loops, it is a special type of graph called a tree. Trees come up all the time in real-world applications. It has been conjectured that the independent set sequences of trees will always be unimodal. My advisor, Prof. Pat Devlin, and I, set out to disprove this conjecture (i.e. find a tree where the independent set sequence is not unimodal). To do this we used a programming environment called Sage to randomly generate many trees and check whether or no their independent set sequence is not unimodal. There are a vast number of trees, so we had to limit our search. We focused on trees similar to a unique one recently discovered by other researchers. This tree broke another expected property of trees: log-concavity. Log-concavity is a stronger form of unimodality, so the fact that a tree can break log-concavity provides hope that unimodality can also be broken. Although we did not discover any trees without unimodal independent set sequences, we did find vast amounts of trees that break log-concavity. In fact, we found some ”regions” in the space of trees where almost half break log-concavity. This is quite exciting given that it wasn't long ago we believed these trees didn't exist. Even though we did not find a tree that breaks unimodality, the abundance of non-log-concave trees is very promising.

104 “Nowcasting” Flu Hospitalizations using Google Search Data

Hanqi (Sunny) Shi ’27, Kaito Hikino ’26, advised by Professor Shaoyang Ning • Swarthmore College

khikino1@swarthmore.edu, hshi1@swarthmore.edu, sning1@swarthmore.edu

The 2024–2025 influenza season was one of the deadliest in recent history, with hospitalization rates matching or exceeding the highest totals from the past 15 years. Accurate real-time tracking of flu activity helps public health officials make timely decisions that could save lives. Our research builds on previous work tracking influenza-like illness (ILI) on the national, regional, and state levels using the ARGO (AutoRegression with GOogle data) methodology. We wish to extend this methodology to predict weekly flu hospitalization rates.

We focused on the national level over the summer. We use hostapilzation rate data from National Healthcare Safety Network (NHSN), which is limited to data after the COVID-19 pandemic. However, the original ARGO methodology require at least three year of training data for each prediction, which leaves a very short period for evaluation. Therefore, we tested models that would address this issue.

One attempt is to reduce the number of training data required for each year. Cross validation on lags of 26, 32, and 52 weeks, training lengths of 52 and 104 weeks, and different rate transformations selected three top-performing models. Another attempt is to impute earlier hospitalization data using ILI and FluSurv-NET, a separate network collecting hosptitalization data. This method is inspired by existing methodoly which imputes state-level data. We adapted this model to a two-part model which takes into account flu and off-season periods. We also incorporated ILI as an exogenous predictor both through directly including ILI from previous weeks and through using predicted ILI of the current week.

Overall, our results show that ARGO can be adapted effectively to predicting hospitalization rates. Our research is still ongoing, and in the future, we hope to combine these methods to select the best model on the national level and extend to state level.

105 Development of a Lightweight Hydrogen Fuel Cell Vehicle

Matthew Shiley, Nora Jiang, Carr Everbach • Swarthmore College Department of Engineering
mshiley1@swarthmore.edu

This project continues the development of a hydrogen-powered vehicle for competition in the Shell Eco-marathon, an international program challenging students to design and build fuel-efficient vehicles. Our vehicle utilizes a hydrogen fuel cell as a clean energy source. Unlike combustion engines, which emit greenhouse gases and other pollutants, hydrogen fuel cells generate electricity through an electrochemical process whose only byproducts are water and heat. Fuel cell vehicles offer several advantages over gasoline-powered and electric vehicles, offering longer ranges than battery-powered vehicles while requiring only minutes to refuel. The primary barriers to the adoption of hydrogen fuel cell vehicles are the lack of infrastructure and the high cost of producing hydrogen.

The original vehicle, built by Swarthmore engineering students in 2013, utilized a welded aluminum chassis. The iteration of the vehicle currently in development features a primarily carbon fiber chassis, greatly reducing the vehicle's weight while maintaining strength. It is our hope that the reduced weight of the chassis will improve the vehicle's speed and fuel efficiency. The modular system of carbon fiber tubes and aluminum linkages used in the chassis also allows for the design to be modified more easily. At the time of writing, the carbon fiber chassis has been assembled, and the front and rear suspension systems are in the process of being attached. To meet competition requirements, near-term goals include completing the front and rear suspension; integrating steering and braking; installing the floor of the vehicle; mounting the power system; and building a low-drag exterior enclosure. We aim to enter the vehicle into the Shell Eco Marathon competition in the Spring. The original vehicle, built by Swarthmore engineering students in 2013, utilized a welded aluminum chassis. The iteration of the vehicle currently in development features a primarily carbon fiber chassis, greatly reducing the vehicle's weight while maintaining strength. It is our hope that the reduced weight of the chassis will improve the vehicle's speed and fuel efficiency. The modular system of carbon fiber tubes and aluminum linkages used in the chassis also allows for the design to be modified more easily. At the time of writing, the carbon fiber chassis has been assembled, and the front and rear suspension systems are in the process of being attached. To meet competition requirements, near-term goals include completing the front and rear suspension; integrating steering and braking; installing the floor of the vehicle; mounting the power system; and building a low-drag exterior enclosure. We aim to enter the vehicle into the Shell Eco Marathon competition in the Spring.

106 Investigating the Relationship between Lpp Activity and Trauma Exposure in Undergraduate Students

Sakura Shimozono, Dora Cai, Brian A. Metzger • Swarthmore College
sshimoz1@swarthmore.edu

PTSD prevalence in undergraduates has recently doubled (3.4% to 7.5%); with one study reporting ~70% of participants to have experienced at least one traumatic event (Zhai & Du, 2024; Cusack et al., 2018). Progress is hindered by an inadequate understanding of the neural underpinnings of the disorder. We use the late positive potential (LPP) to understand the relationship between motivated attention and PTSD-related hypervigilance to threat. Specifically, we aim to clarify the influence of trauma on emotional perception. Prior research has shown weak associations between trauma exposure, as measured by the PTSD checklist for civilians (PCL-C), and LPP amplitude (Fedorenko et al. 2023). However, it remains unknown whether PTSD symptomology or trauma history are associated with LPP activity. Forty undergraduate participants will provide EEG data while viewing pleasant, unpleasant, and neutral images. LPP amplitude (mean window) will be correlated with PTSD symptomology, as measured through the PCL-C subscores for re-experiencing, avoidance, and hyperarousal (PCL-C subscales B, C, and D, respectively). As expected, pilot data show greater LPP amplitude for unpleasant versus neutral and pleasant images. Additional analyses include predicting LPP amplitude from valence and PCL-C subscores. We expect greater LPP amplitude in trauma-exposed individuals and correlations between LPP amplitude and the three subscales. This research deepens our understanding of the LPP and trauma's impact on perception, potentially guiding interventions targeting altered affective processing in PTSD.

107 B+ Index Tree for Swarthmore Database (SwatDB)

Yara Shobut, Dr. Tia Newhall • Swarthmore College

yarashobut2@gmail.com

The B+ index tree is a foundational data structure in database systems, providing efficient insertion, deletion, and range-based query operations. Its design maintains keys in sorted order, achieves logarithmic-time complexity for updates and lookups, and links leaf nodes to enable fast sequential access. Because of these properties, B+ trees remain central to the performance of large-scale data management.

During the summer of 2025, with Dr. Newhall's guidance, I designed and implemented a B+ index that supports navigation, storage, and retrieval across multiple node levels for the Swarthmore Database (SwatDB) system. Core functionality for insertion, deletion, and search has been implemented, with preliminary testing confirming correctness in entry placement, node splitting, and leaf-level traversal.

Planned extensions include expanding test coverage, and refining exception handling/ documentation. With these capabilities in place, the implementation enables the development of a new course lab through which students can directly explore indexing, query execution, and storage management in a practical setting.

108 Exploring How Proteins Regulate Cell Signaling

Presley Simelus, Jibin Sadasivan, Lindsay Case • Department of Biology, MIT, Cambridge, MA

Cell migration plays a critical role in regulating various biological processes, such as embryonic development and wound healing. Defective cell migration is a hallmark of cancer metastasis. Central to cell migration are multimeric protein complexes called focal adhesions (FAs). FAs serves as the primary mechanical link between the cytoskeleton and the extracellular matrix. We recently showed that the phase separation of several focal adhesion adapter proteins including focal adhesion kinase (FAK) promotes focal adhesion formation and signaling. FAK, a non-receptor protein tyrosine kinase, is essential for initiating FA signaling through its autophosphorylation. However, FAK signaling is inhibited by its endogenous inhibitor FAK related non-kinase (FRNK), a protein domain derived from FAK gene but lacking the N-terminus kinase domain. Using in vitro reconstitution, we found that FRNK also inhibits the phase separation of FAK. FRNK with single FAT domain (1X FAT) inhibits FAK phase separation, whereas adding a second FAT domain (2X FAT) rescues FAK phase separation. Based on these observations, we hypothesized that FRNK inhibits FAK signaling by modulating FAK phase separation. To test this, we expressed 1X FAT, 2X FAT, and additional FRNK variants in mouse embryonic fibroblasts and measured phosphorylated FAK (pFAK) levels to assess changes in FAK signaling. Preliminary results show that the expression of 1X FRNK inhibits FAK signaling whereas 2X FAK enhances FAK signaling. Thus, FRNK may interfere with FAK signaling by regulating FAK phase separation. Understanding how FRNK modulates FAK could provide insights into potential cancer therapies targeting this regulatory mechanism.

109 Multi-Scale Testing of Novel Cross-Laminated Timber (CLT) Buildings for Century-Scale Carbon Sequestration

Zoe Sperduto, Kenneth Relovsky, Fiona O'Donnell • Swarthmore College, Northeastern University

krelovs1@swarthmore.edu, zsperdu1@swarthmore.edu

Utilizing Design for Deconstruction and Reuse (DfDR) principles and constructing with Cross-Laminated Timber (CLT) enables long-term storage of biogenic carbon in timber, contributing to the decarbonization of the built environment (which is currently responsible for 40% of global carbon emissions). The greater research project aims to develop a new structural system consisting of deconstructable steel frames with CLT floor diaphragms to allow for carbon-negative infrastructure on a century-scale. Strategies to achieve carbon negativity include the development of a deconstructable steel-CLT connector, the usage of local and underutilized wood species in the CLT, and the integration of bio-based non-structural materials.

This research focuses specifically on assessing the use of local and underutilized wood species,

Eastern Hemlock and Eastern White Pine, in the structural system to decrease emissions associated with material transportation and promote the development of local markets for mass timber in the Northeastern United States. Knowledge of the material properties of these species is essential for understanding design constraints and for developing accurate computational models of the larger building system. Material characterization tests beginning at the clear wood scale and continuing to CLT characterization tests are in the process of being conducted on the underutilized and traditional Spruce/Pine/Fir lumber used in CLT to identify differences material properties; future testing will continue to the beam and diaphragm scale of the hybrid structure. Ongoing Finite Element Modeling (FEM) takes advantage of these results to model the behavior of the low value species. Initial data comparing material properties is presented at the clear wood and CLT-scale which shows promising results for the usage of underutilized species in the larger hybrid system.

110 Traits of immediate male social partners do not alter female behavior in a social beetle *(Bolitotherus cornutus)*

Sophia Springer, Vince Formica • Mountain Lake Biological Station, Swarthmore College

sspring1@swarthmore.edu

Male-male aggression is common across the animal kingdom and is an important component of sexual selection, yet its effects on female behavior are often overlooked. The Forked Fungus Beetle *(Bolitotherus cornutus)* is a long-lived species where males vary in aggression levels, with older males generally displaying higher aggression levels. However, the effects of male aggressiveness on the behavior of female *B. cornutus* are unknown. We examined how female behavior differs in populations with older or younger males, and whether male aggression at the population or local partner level influenced female behavior. We quantified female time spent on fungus (their primary habitat and resource), acceptance of male courtship, and the number of males with which females interacted over a four week-long study in a semi-wild environment. Our results indicate that female fungus use, and courtship acceptance were not influenced by the average aggression or age of their male social partners. The number of males a female interacted with was also not affected by average aggression levels of those males but was affected by the age of males in her population: females in the old-male treatment interacted with approximately 1.5 more males than those in the young-male treatment. Therefore, our results suggest that age-related male traits, other than aggression, may influence the likelihood of female-male interactions. Population level age structure may play a larger role in the social environment females experience rather than the traits of her immediate social partners.

111 Looking at Density and Number in Depth

Nichole Suero Gonzalez, Frank Durgin • Singer 351

nsuerog1@swarthmore.edu

Density is a visual property that might be relevant to the estimation of visual number, such as estimating the number of M&Ms scattered on a surface. There is some dispute in the literature about the extent to which number might be estimated more directly, with some arguing that density and number are entangled, and others suggesting that number is primary. Evidence for entanglement include the observation that perceived density is strongly biased by patch size (larger patches appear denser), and number perception is weakly affected. One reason patch size may affect density is that density itself is a distance cue, as is size, so a larger patch might be a nearer patch that is, in fact, higher in density.

To study effects of patch size on density and number in a more naturalistic situation in which depth matters, we used virtual environments, rendered in a high-resolution head-mounted display (HMD). The basic task consisted of a brief presentation of a circular dot texture (of about 30 dots) at 1 m viewing distance, followed by a second dot texture at another viewing distance (0.5 – 2m). The second texture was varied in size, number, and density. Participants either made number comparisons (was the second patch more or fewer dots than the first?) or density comparisons (was the second patch denser or less dense than the first?) in separate sessions.

A primary manipulation pitted retinal matches against simulated size matches. That is, in the baseline

condition, the dots and patches were properly simulated, such that they grew retinally smaller at far distances, and retinally bigger at near distance, just as would happen in the real world. In the retinal match condition, the simulated dots and patches of dots were enlarged when presented at a farther distance so as to project the same retinal sizes (and shrunk when presented at a near distance.)

Across both conditions, we consistently found that both number and density judgments were strongly and equally affected by the relative sizes of the two patches. This shows that, in a simulated real-world context, participants' judgments of relative number and of relative density are closely linked together.

Theoretically, number is a property that is invariant with distance, but density is a variant property that must take distance "into account". The fact that judgments of density and of number are both responsive to variations in patch size supports the idea that even invariant numbers are indeed entangled with variant density.

112 Biophysical Characterization of BRAF-Derived DNA Sequences that Hold the Potential to Form Five-Tetrad G-Quadruplex Structures

Emily Sun, Liliya Yatsunyk • Swarthmore College

esun2@swarthmore.edu

G-quadruplexes (G4s) are non-canonical secondary structures of DNA formed by the stacking of planar guanine tetrads (G-tetrads). These structures are biologically relevant and commonly occur in cancer-associated genomic regions, where they regulate gene expression, replication, and genome stability. Due to their roles in oncogene promoters and telomeres, G4s are considered promising therapeutic targets for cancer and neurodegenerative diseases. Most G4s consist of three or four stacked G-tetrads, and in this study, we investigate the biophysical properties of a series of DNA sequences derived from the BRAF gene that have the potential to form a five-tetrad G4 structure. Sixteen variants, BR1-BR16, were characterized in 1K buffer. Thermal difference spectra (TDS) confirmed G4 formation across all variants. Using circular dichroism (CD) spectra, we identified hybrid topologies with prevalence for both parallel and antiparallel topologies. CD melting experiments indicated high stability, with melting temperatures ranging from 68.0°C to 73.4°C. Thermal analysis displayed the successful unfolding and refolding of the DNA when heated and cooled, revealing a nearly reversible two state system and monomolecular structure. Native PAGE displayed singular, intense bands, indicating a high degree of structural homogeneity. We set crystal screening trays for sequences BR1-BR6 using Helix and Natrix well conditions. Overall, this study provides understanding of the biophysical characteristics of different BRAF variants, which all have the potential to form stable, homogeneous likely five-tetrad G4 structures.

113 Modifying R-group electron-modifying substitutions on the TriNOx ligand system

Kyler Sy, Christopher R Graves • Graves Lab

ksy1@swarthmore.edu

(HHTriNOx^{3-})Al is a novel aluminum complex that features TriNOx, a non-innocent tripodal nitroxide-based ligand. Aluminum is particularly interesting due to its availability, low cost and nontoxicity. However, it has previously struggled with being used as a viable redox-based reagent due to favoring its lack of multi-electron redox properties, favoring only the Al3+ oxidation state.

The purpose of the research is to find the optimal ligand system capable of extending its redox properties to the aluminum complex allowing it to perform reversible, multi-electron chemical processes. This was achieved by modifying the ligand system, functionalizing R groups attached meta to the nitrogen arm of the complex. Namely, the R groups added are the electron-withdrawing trifluoro group (–CF3) and the electron-donating methoxy group (–OMe) compared with the default (HHTriNOx^{3-})Al complex. The intuition behind adding these electronically tuning R groups is that they can raise the HOMO and lower the LUMO of the ligand, making oxidation and reduction favorable respectively while aluminum can retain its single oxidation state. Chilled single-layered crystallization was used to obtain pure (HHTriNOx^{3-})Al and (HHTriNOx^{3-}OMe)Al crystals. This was inspired by finding a mixed product distribution present in the methoxy variation, occurring at room temperature upon stirring. ;pFurthermore, heating (HHTriNOx^{3-}OMe)Al resulted in product

distribution shifting to an unstable radical byproduct undetectable by NMR due to peak broadening. This is demonstrated through a stacked NMR plot where in the Al-Me and the methoxy group disappear as temperatures rise.

114 Distinguishing Stochastic Fluctuations from Deterministic Population Dynamics

Zoe Tang, James Flagg, Paris Lewis; advised by Dr. Mason Manning & Dr. John Nagy
Arizona State University
ztang1@swarthmore.edu

Long-term prediction and conservation planning of ecological systems is challenging as a result of chaos, in which small differences in initial conditions can lead to drastically different outcomes over time. Traditional methods for detecting chaos, such as those based on Lyapunov exponents (LEs), seem unreliable when high levels of noise are present in field data. In this study, we address a critical gap in the literature: quantifying the extent to which prediction error is due to deterministic variance versus stochastic noise. In our work, the reliability of the LE is assessed by quantifying the proportion of forecast error due to noise. We introduce an ensemble-based framework that perturbs observed initial conditions and propagates forecasts through a local surrogate model to estimate the contribution of deterministic divergence, intrinsic stochasticity, and measurement error to total forecast variance. Additionally, we explore applications of this framework within ecological data. Preliminary results suggest that increasing levels of noise require greater measurement uncertainty to account for the observed dynamics through deterministic models. Our approach potentially enables the more accurate detection of chaos and yields insight into the forecasting of complex ecological systems.

115 Modeling Interferometric Pressure Sensors Using COMSOL

Bella Thoen, Professor Lynne Molter • Swarthmore College
ithoen1@swarthmore.edu

This research focuses on how the rate of pressure change affects the output of interferometric pressure sensors. Our sensor utilizes interferometry, a commonly used method wherein the light from a laser is split into two beams, and a stimulus is applied to one of the beams. When the two beams are recombined, they interfere with each other, creating a distinctive interference pattern. Varying the stimulus – in this case the air pressure – changes the distance that the light travels in the affected path, which changes the interference pattern at the end. By examining the interference pattern over time, we can understand how different rates of pressure change appear as sensor output. It is difficult to vary the rate of pressure gain in a controlled manner with our experimental setup, so we use COMSOL – a modeling software that uses numerical methods to compute theoretical solutions for systems with complex physics – to study the impact of the rate of pressure gain on sensor output.

The main goal that we have accomplished thus far is creating a model of our pressure sensor in COMSOL that is dependent on both pressure and time. In addition, inputting linear, quadratic, and quintic rates of pressure change revealed that faster gains in pressure result in higher frequency interference oscillations. The next steps in our research are to align the parameters of our COMSOL model to our physical model, and input more complex rates of pressure change on experimentally realistic time scales. Once this has been achieved, we will be able to compare our theoretical results with our experimental data, allowing us to determine the rate of pressure loss from our pressure cell.

116 On the reactivity of ($TriNOx^{3-}$) metal complexes with CH_2X_2 (X = Cl, Br, I)

Elizabeth Ting and Christopher R. Graves • Swarthmore College
eting1@swarthmore.edu

Developing metal coordination complexes capable of metal-ligand cooperative (MLC), activation of small molecules is a compelling area of research. We are currently investigating the coordination chemistry of group 13 metal complexes supported by non-innocent ligand frameworks, with a focus on the tripodal, tris(nitroxide) ligand system, $TriNOx^{3-}$. In this contribution, we present our investigation into the reactivity of the ($TriNOx^{3-}$)M (M = Al, Ga) complexes with CH_2X_2 (X = Cl, Br, I) and examine the influence of halogen identity on this reactivity.

117 Privatizing Queries over a Large Corpus of Real-World Network Data

Jaron Tinsley, Julian Krauze, Vasanta Chaganti (Advisor) • Swarthmore College
jtinsle1@swarthmore.edu, jkrauze1@swarthmore.edu, vchagan1@swarthmore.edu

As digital networks continue to pervade every aspect of corporate and personal lives, information about the performance of these networks becomes increasingly important to network administrators and legislators, allowing them to ensure these networks continue to meet our needs. Unfortunately, groups that collect network data have become increasingly unwilling to release this data due to the threat of both public outcry and legal action in the event that their release inadvertently reveals individuals' private information.

In our poster, we discuss how queries under Differential Privacy, a technique that guarantees the inclusion of any one individual in a dataset will not have a significant impact on a query's result, thus protecting their privacy, can be optimized to have the greatest utility while minimizing privacy loss. While this may seem like a simple solution, there are many challenges presented by the privatization of network data. In our research, we work around the issues that come with high sensitivity and time series present in network data. By reviewing past research methods successfully proven to ensure the privacy of network data, we report a taxonomy of private queries. This compilation of queries reveals many generalizable methods to apply differential privacy to protect individuals' network information, while maintaining the queries' utility. Some of the most useful methods were: synthetic data generation under DP, how the discrete Fourier transform can be used to privatize time-series data, and how packet-level queries can be privatized while maintaining utility.

In addition to the research required in the construction of the taxonomy, we demonstrate how several common queries can be implemented on our dataset while satisfying the differential privacy guarantee. The data, provided by Akamai Technologies, consists of ASNs worldwide and their aggregated hitcounts for each hour of the day over the course of a month. With regards to non-time-correlated queries, we utilize the Laplace Mechanism with each ASN being the individual protected via the differential privacy guarantee. Moreover, we produce a multitude of private sum, count, and joint dp query responses that showcase useful statistics for the network dataset, such as the most popular hour and total hitcounts in a country. We gauge the utility of the query responses using Absolute Error and Mean Squared Error, measuring the tradeoff between the privacy budget and utility.

We find that with a taxonomy of queries to draw from, Differential Privacy presents itself as a viable, although by no means perfect, solution for protecting sensitive network data. This is due to the difficulty of implementation and the strict requirements of large datasets to maintain utility. Despite its issues, DP effectively mitigates the risk that comes with releasing a dataset to the public, allowing more network data to be shared without the possibility of the accidental release of sensitive information.

118 Gravitational Delensing Analysis of a Dusty-Star Forming Galaxy

Angelo Phillipe Valencia, Abigail Reed, Jesus Rivera • Swarthmore College
avalenc1@swarthmore.edu, areed3@swarthmore.edu

Dusty-Star-Forming Galaxies (DSFGs) represent an optically obscured population of ultra-luminous galaxies that exhibit star formation rates of up to three thousand solar masses per year. Using carbon monoxide data from the Northern Extended Millimeter Array (NOEMA), we present a preliminary gravitational lensing analysis performed with the specialized software *pixsrc* (Tagore & Keeton 2014) and *lensmodel* (Keeton 2011) on a per-channel basis to investigate the intrinsic properties and kinematics of a strong-lensed DSFG. We initially found the best-fit parameters of the reconstruction using an integrated moment map of the NOEMA CO(4-3) data. We then used the best-fit model from the moment map as the seed to run Markov Chain Monte Carlo (MCMC) simulations, aiming to find the best-fit model for a representative subset of all the channels. Future endeavors will involve using the best-fit model from the MCMC simulation to find the de-lensed properties, such as luminosity and star-formation rate, of the DSFG.

119 Swimming behaviors of veliger in response to vorticity

Luciana Valencia, Professor Karen Chan • Swarthmore College

lvalenc1@swarthmore.edu

The ocean is an extremely dynamic environment and all species caught in its constant water movement are affected. Early stages of marine invertebrates are planktonic larvae that cannot actively swim against these currents. And yet, these larvae must navigate moving waters to avoid predators, search for food, and find spots to settle. Because of this, turbulence potentially serves as a mechanical cue for larvae to change their swimming behavior. Here we investigated the larval responses to vorticity, a single component of turbulence, for its relevance to larval size. Using the veliger of the Atlantic slipper limpet, *Crepidula fornicata,* we quantified larval behaviors in varying intensities of vertical and horizontal vorticity through ontogeny. Across 2, 6, and 18 days post-release, veligers swam opposite of the vorticity vector until a certain intensity. As expected, the older, larger larvae had a higher vorticity threshold. However, when the vorticity vector and gravity were anti-aligned and larvae were spun counterclockwise, the change in swimming behavior was weakened. Swimming in the opposite direction ceased at a lower intensity. Our work showcases that larvae can sense and react to mechanical cues and use them to navigate moving waters. These responses highlight the importance of understanding larval behaviors to predict dispersal and population dynamics in a changing ocean.

120 Identifying heterogeneity at the neural plate border in *Xenopus laevis*

Lily von Behren, Dr. Lara Busby • Megan Martik Lab, UC Berkeley

lvonbeh1@swarthmore.edu

The neural crest (NC) is a migratory, multipotent embryonic stem cell population that arises at the neural plate border (NPB) during neurulation. The cranial neural crest cell (CNCC) subpopulation is unique in defying traditional germ layer theory: though they originate in the ectoderm, CNCCs produce both traditional ectodermal derivatives (neurons, glia, pigment) as well as mesoderm-like derivatives known as ectomesenchyme(chondrocytes, osteocytes, and odontoblasts).1, 2 In the field of NC research, a central question remains regarding whether the developmental fate of NC cells is determined before or after migration, i.e., when do cells decide to adopt ectomesenchymal identity? Previous research has identified a role for extrinsic factors (FGF) in the induction of ectomesenchymal fate in migrating CNCCs, while another study discovered an intrinsic gene regulatory network that confers potency to produce ectomesenchyme.3 My supervisor's single cell transcriptomics data has revealed conserved ectomesenchymal genes across evolutionarily diverse vertebrates. The expression of one such conserved gene, *Twist1*, has been observed during early, pre-migratory stages in frog (*Xenopus*) embryos.4 However, my supervisor has noted a much later *Twist1* expression pattern in sea lamprey, zebrafish, and chicken, suggesting potential heterochronic ectomesenchyme gene expression across vertebrates, with frogs as the outlier.

To identify potential further heterogeneity at the NPB in *Xenopus* (indicating early fate determination), we aimed to use double chromogenic in situ hybridization (CISH) to characterize the spatiotemporal expression patterns of putative ectomesenchymal markers (*Alx1, Alx4, Fli1, Inka1, Pdgfra, Prrx2*). My project focused on the cloning and synthesis of antisense RNA in situ probes, optimizing the CISH protocol in neurula stage (NF 14-21) frog embryos, and performing an initial characterization of the markers' expression profiles.

By testing published CISH protocols, I found that treatment of neurula frog embryos with proteinase K severely damaged the embryonic ectoderm, and consequently removed this step from the protocol to achieve a procedure that preserved embryo integrity. In addition, chromogenic development using the FastRed AP substrate resulted in low sensitivity and low contrast staining, motivating further troubleshooting that is ongoing in the lab. My single CISH experiments revealed that Pdgfra has a cranial-specific expression pattern, bearing strong resemblance to that of *Twist1*. Alx1 and Alx4 also exhibited cranial-specific expression, though only in the first stream of migrating NC. On the other hand, Inka1 was not restricted to the cranial region, with expression also observed in the trunk, and Fli1 and Prrx2 began expression during post-migratory stages.

These initial single CISHs not only validated probe efficacy, but also provided valuable preliminary insights into spatiotemporal expression patterns: an ectomesenchymal transcriptional profile during early neurulation suggests that ectomesenchyme fate is induced earlier on in frogs than other vertebrates. Altogether, my results will contribute to ongoing research in the NC field that is uncovering when and how cell fate determination occurs in CNCCs.

121 Developing a Digital Dictionary for Endangered Languages

Alina Vykliuk, Jonathan Washington • Swarthmore College
avykliu1@swarthmore.edu

We present an online dictionary with a built-in paradigm generator to support endangered languages, with initial implementation for Urum, a Turkic language spoken by ethnic Greeks in southeastern Ukraine. The system was designed to go beyond standard bilingual dictionaries by integrating morphological analysis, fuzzy semantic search, and paradigm generation.

Paradigm generation automatically produces full sets of Urum word forms, filling integrated paradigm tables, giving learners insight into the inflectional system of a morphologically rich language. Morphological analysis identifies the lemma of an inflected input and shows its relationship to the base word. Semantic fuzzy search, powered by pre-trained English and Ukrainian embeddings, suggests semantically related terms even when the user's query does not exactly match a dictionary entry. These combined features allow learners to find inflected forms in the dictionary even without being able to find the stem, and help learners move beyond memorization of wordlists to a deeper understanding of grammatical structure.

The dictionary was implemented within the Apertium ecosystem, extending two key tools: Apertium HTML-Tools, which provides a localized React-based web interface, and Apertium APy, a Python backend service using Tornado that handles linguistic processing requests. A new dictionary mode was added to Apertium HTML-Tools, giving users an interactive interface for searching words, viewing generated paradigms, and exploring related vocabulary. On the backend, Apertium APy was expanded with three new helper modes dedicated to dictionary functionality, enabling new query features and more sophisticated querying logic.

We have implemented support for the Urum-English, Urum-Ukrainian, Urum-Russian, and Russian-Ukrainian language pairs, with full paradigm integration for Urum. Because the tool is built on the Apertium framework, the system can be easily extended to any language with Apertium-compatible tools, making it broadly applicable for endangered language maintenance and revitalization, offering a sustainable pathway for community members and learners to strengthen, preserve, and pass on their linguistic heritage.

122 A Spatiotemporal Model of T-Cell Population Dynamics in the Lymph Node

Howard Wang

Traditional non-spatial models of immunology treat the lymph node (LN) as a homogeneous "wellmixed" system, ignoring the impact of its complex architecture on the immune response. To investigate the role of spatial organization, we developed a three-dimensional spatiotemporal model of T-cell dynamics within a realistic, swelling murine LN geometry. The model is governed by a system of reaction–advection–diffusion partial differential equations (PDEs) that simulate the proliferation, differentiation, apoptosis, and transport of activated (A) and memory (M) T-cells. Our simulations reveal that seeding the initial response within a localized T-cell zone (paracortex) creates vast, multi–order-of-magnitude concentration gradients between this proliferative "hot zone" and the quiescent periphery. This local heterogeneity is critical for reconciling the small initial precursor pool with the large systemic cell counts observed experimentally. Strikingly, we found that the total systemic T-cell population over time is remarkably robust and insensitive to the initial location of the seed region. This suggests that while local cell dynamics are highly dependent on spatial positioning, the integrated systemic response is governed by global kinetic parameters. This work underscores the necessity of spatially explicit models to uncover the mechanistic link between LN microanatomy and immune function, revealing local phenomena masked by systemic measurements.

123 Lump Sum Investing vs. Dollar Cost Averaging: Evidence from Historical Data and Bootstrapped Simulations

Jeffrey Wang, Qinghai Wang

This project compares lump sum investing and dollar cost averaging strategies using historical monthly returns of stocks and Treasury bills. The baseline analysis assumes a 10 year holding period with $1 million invested at the outset. Under LS, the entire amount is invested immediately in stocks. Under DC, funds are split according to prespecified rules: in the simple case, $1 million is invested equally over the first 100 months, with unallocated funds temporarily placed in Treasury bills. Alternative DC strategies respond to market conditions, shifting between stocks and T-bills after large market drops or run-ups. To evaluate robustness, both direct historical simulations and block bootstrapping are employed. In the bootstrap procedure, 10-year holding periods are constructed from randomly drawn 4-year blocks of stock and T-bill returns, preserving time series features while generating many artificial samples. Across both historical and bootstrap analyses, results show that lump sum investing tends to outperform dollar cost averaging in terms of average cumulative returns and in the frequency with which LS exceeds DC. These findings suggest that while DC may reduce perceived timing risk, it typically comes at the cost of lower long term performance.

124 Behavioral Data for different levels of prediction error in event boundaries

Aviva Weiser, Youssef Ezzya • Swarthmore College

aweiser1@swarthmore.edu

Event boundaries are points at which people tend to parse continuous experiences into separate events and are key for understanding and processing information. Event boundaries can be formed by sudden increases in prediction error or based on the statistical structure of the events experienced, which indicates how predictable they are. For example, leaving a dorm and heading to class could cause an event boundary because the experience of the dorm and the class is more predictable, while walking to class tends to be a lot more variable, so the unpredictability causes a boundary to form. Segmentation due to increases in prediction error tends to use reactive processing, while segmenting using knowledge about changes in contextual stability uses proactive processing, according to the information-optimization account of event segmentation. However, it remains unclear exactly how uncertainty in boundaries affects parsing of those boundaries. Therefore, we wanted to see how varying levels of uncertainty affected the participant's conception of event boundaries. This experiment implements four levels of novel boundaries to determine the effect of different types of uncertainty (for instance the starting boundary node being unpredictable as opposed to the ending boundary node being unpredictable). The specific procedure builds on Ezzyat and Clements 2024, exposing participants to a stream of stimuli generated using a random walk through a specific community structure, with boundaries that they learn throughout this phase (learned boundaries). Participants were then asked to parse event boundaries, both novel and learned. From preliminary pilot data, participants segmented the sequence both at learned boundaries and novel boundary events at higher rates than nonboundaries. This indicates that participants did learn the "structure of the events" of the data and were able to segment events based on the learned structure.

125 GapmeR Mediated Knockdown of HSATII RNA

Lester Wessels, Christina Rabeler, Dawn Carone • Swarthmore College

lwessel1@swarthmore.edu

HSATII RNA is aberrantly expressed in many cancers, where it accumulates in nuclear foci and sequesters regulatory proteins such as MeCP2 and TDP-43 into cancer-associated satellite transcript (CAST) bodies. These CAST bodies, unique to cancer cells, disrupt chromatin regulation and protein distribution.. The goal of this study was to determine whether antisense oligonucleotides known as GapmeRs could target HSATII RNA, disrupt CAST bodies, and restore protein localization.

Using nuclear RNA sequencing data from the U2OS osteosarcoma cell line, differential gene expression analysis identified tandem repeat regions of HSATII on chromosomes 7, 9, and 17 as potential knockdown targets. Custom GapmeRs were designed and validated for specificity using

BLAST. GapmeRs were then transfected into U2OS osteosarcoma cells, a line with high HSATII RNA expression. Knockdown efficiency was evaluated using RNA FISH and visualized with Imaris 3D microscopy.

Preliminary results showed that GapmeRs effectively reduced HSATII RNA levels by RNA FISH. GapmeRs targeting chromosome 17 sequences were particularly effective, achieving higher knockdown efficiencies compared to those targeting chromosomes 7 and 9. Reverse complement GapmeRs also demonstrated knockdown activity, with a potential emphasis on the importance of GapmeR sequence orientation in successful knockdown. Standardization of RNA FISH quantification methods is underway to ensure reproducibility and accuracy across experiments.

These findings highlight the potential of GapmeR-mediated HSATII knockdown as a promising approach to restore regulatory protein availability and nuclear integrity in cancer cells. Future studies will expand the analysis to additional HSATII regions and further refine imaging pipelines, with the broader goal of establishing GapmeR-based strategies as viable interventions for HSATII RNA dysregulation.

126 Saline Irrigation Effect On Total Phenolic Content in Pistachio Seed Coats

Ania Wong, Monika Sommerhalter • Hayward, California

awong7@swarthmore.edu

Pistachio trees in semi-arid regions face increasing amounts of soil salinity stress due to reduced availability of irrigation water. Global warming reduces rainfall and increases evaporation, decreasing freshwater availability and forcing farmers to rely on brackish water sources. These plants may develop salt tolerance through enhanced antioxidant production, including polyphenolic compounds concentrated in the pistachio seedcoats. This study investigated whether salinity stress increases polyphenolic content in pistachio seedcoats as a tolerance mechanism.

UCB1 and PG1 rootstocks grafted with Kerman variety pistachios were subjected to four salinity treatments (0.3, 4.0, 8.0, and 12.0 dS/m). Individual pistachio seedcoat samples were analyzed using the Folin-Ciocalteu assay to quantify total polyphenolic content. Due to non-normal data distribution, non-parametric Kruskal-Wallis tests were used to compare treatments within each rootstock. No significant differences in polyphenolic content were found between salinity treatments for either PG1 or UCB1 rootstocks. High sample variation was observed across individual plants.

Results suggest both rootstock varieties possess adequate salt tolerance mechanisms that do not rely on increased polyphenolic antioxidant production within the tested salinity range. These rootstocks may utilize alternative physiological strategies for salt adaptation, such as ion exclusion or osmotic adjustment. The tested salinity levels (0.3-12.0 dS/m) may be insufficient to trigger polyphenolic stress responses for the Kerman varieties. Future research should examine higher salinity thresholds or investigate alternative stress response mechanisms in pistachio salt tolerance.

127 Exploring factors associated with Pediatric Post-Heart Transplant Pulmonary Vein Stenosis: A single-center retrospective chart review

Katherine Wu, Deepa Mokshagundam, M.D. • Washington University School of Medicine

kwu3@swarthmore.edu

Pulmonary Vein Stenosis (PVS) is a disease with high morbidity and mortality. It has been observed in post-heart transplant patients. There are limited treatment options for PVS. Existing treatment, angioplasty and stent placement, are considered palliative at best due to recurrent stenosis of the reactive tissue found in the pulmonary veins. In post-transplant patients, it is crucial to understand the factors associated with the development of PVS and its impact on graft and patient outcomes. We performed a retrospective chart review of patients who underwent heart transplantation at St Louis Children's Hospital from January 2016 through October 2023. We recorded demographic data, surgical and catheterization history, imaging data (echocardiogram, angiography, cardiac CT), transplant details, and patient outcome. RedCap was used to enter and extract data. Descriptive statistics were carried out and reported. We identified n = 140 patients who underwent heart

transplantation within the study period. Five patients were identified who had post-transplant PVS, representing 3.6% of the total cohort. All five patients with post-transplant PVS had single ventricle congenital heart disease pre-transplant

(Hypoplastic Left Heart Syndrome n = 4, Hypoplastic Right Heart Syndrome, n = 1). Four of the five had no pre-transplant PVS. One patient had a remote history of PVS that was treated with intra-operative balloon angioplasty. Three of five patients were found to have restrictive atrial septum. Of the two who did not, one patient's septum was aneurysmal, while one did not show abnormalities. All cases of post-transplant PVS were discovered within a year of their transplant date. Four of the five underwent transplant before the age of one year and were diagnosed with PVS before the age of two years. Three of the patients received interventions on their pulmonary veins post-transplant: stent placement in 2 and angioplasty-only in 1. Three of the five patients were still alive at the time of data collection (60%) compared to 110/135 (82%) of the remaining patients. PVS can occur in patients post-heart transplant and has significant morbidity and mortality. Factors that may be associated include single ventricle heart disease, atrial septal abnormalities, and prior pulmonary vein abnormalities. These factors should be taken into consideration when determining both transplant candidacy and post-transplant surveillance.

128 Interaction of a Hybrid LH/RH G-Quadruplex with a G4 Ligand

Eric Xing, Liliya Yatsunyk • Swarthmore College

exing1@swarthmore.edu

Left-handed G-quadruplexes (G4) are a non-canonical DNA structure discovered in 2015, distinguished from their right-handed counterparts in their helical twist, from which they derive their names. Formation of left-handed (LH) G4s has been found to be highly sequence dependent, with only variations of two minimal sequences, Motif1 (G(TGG)3TG) and Motif2 ((GGT)3GTG), forming this secondary structure. All reported LHG4s form a distinct structure, with 2 subunits, at least one of which is left-handed, containing 2 G-tetrads each and display a thymine capping, where T-loops fold over the outer G-tetrad. A prior study suggests that the presence of these thymine caps prevents traditional G4 ligands from directly binding LHG4s, but research on the subject is still sparse. We used biophysical methods (UV-vis spectroscopy, circular dichroism, native polyacrylamide gel electrophoresis) and X-ray crystallography to characterize the interaction of a sequence M1M2-5T designed from the LH minimal motifs with the G4-binding ligand N-methylmesoporphyrin IX (NMM), known to select for parallel G4s. CD data indicate that the sequence forms an LH/RH hybrid G4 and suggest that NMM preferentially binds the RH subunit. On the other hand, crystallization of the M1M2-5T complex reveals a 1:2 DNA:NMM binding stoichiometry, with one NMM molecule binding each subunit. Notably, binding to the LH subunit involves displacement of the T17 cap, indicating that traditional G4 ligands can remodel thymine caps to bind LHG4s. Finally, job plot and UV-vis. titrations reveal a 1:1 DNA:NMM binding stoichiometry in solution with a weak-to-moderate binding constant of 1.1 μM-1.

129 Advancing Quantitative Analysis Tools to Evaluate the Environmental Reactivity of Nanoplastics

Yuki Yamada, Kathryn R. Riley • Swarthmore College

yyamada1@swarthmore.edu

Plastic is a useful material due to its flexibility, transparency, and lightweight property. Despite the usability, a sufficient waste management system is underdeveloped. As of 8300 million metric tons (Mt) of plastic that had been produced by 2017, 79% was accumulated in landfills or the natural environment. If current trends continue, the amount of plastic waste that will be in landfills or in the natural environment is estimated to reach 12,000 Mt. Once plastic products are exposed to the environment, they undergo biotic and abiotic degradation (e.g. mechanical wear, heat, UV degradation, or biological factors), producing nano-scale plastics spread broadly in the soil, air, and oceans. Nanoplastic particles (NPs) behave uniquely compared to macro or microscale plastics due to their high surface-to-volume ratio. In particular, their aggregation behavior, transportation fate, and

influence of the eco-corona are unique. The eco-corona is a biofilm on the surface of NPs as a result of attachment of biomolecules, such as proteins. It has been reported that the eco-corona changes NPs' aggregation, distribution, and toxicity.

In response to the increasing need to understand the unique behaviors of NPs, the project aims to evaluate their environmental reactivity through quantitative analysis. Using polystyrene particles (PSPs) as the model of NPs, the project investigates three characteristic behaviors; homoaggregation, heteroaggregation, and metal sorption. In the homoaggregation project, homoaggregation of PSPs with different surface functionality (amino or carboxyl-coated PSPs, PS-NH2 or PS-COOH, respectively). The tool used is dynamic light scattering (DLS), which enables to track the particles' size changes based on their Brownian motion. Coagulation concentrations (CCC) is a useful parameter to characterize the aggregation behavior, and the poster presents the CCC values of PS-NH2 and PS-COOH that were determined in different media (seawater, sea urchin spent-media seawater, and individual salt solution). The calculation was conducted based on the colloidal aggregation theory (i.e. DLVO theory).

In the heteroaggregation project, the heteroaggregation between PSP and clay minerals was investigated. Capillary electrophoresis (CE) is a technique that enables us to separate substances based on their size and charge. Among a family of the CE, the primary technique used was affinity capillary electrophoresis (ACE), which examines the interaction between substances and ligands. Lastly, Linear sweep stripping voltammetry (LSSV) is used in the metal adsorption project to quantify the adsorption of Ag(l) or Cu(ll) to PSPs. LSSV uses redox reactions to quantify the concentration of metals present in the solution. For the heteroaggregation and metal sorption protects, the poster presents the preliminary optimization study and future directions.

130 Developing Interactive Exercises for Dive Into Syst

Bohou Zhang, Jay Iyer, supervised by Tia Newhall and Kevin We rtin Hall, Swarthmore College

jiyer1@swarthmore.edu and bzhang2@swarthmore.edu

We developed new exercises for Dive Into Systems, creating interactive exercise components covering topics like binary, assembly, computer architecture, and multithreading. Our components procedurally generate "good" practice problems that test the students on edge-cases and important details. We also worked on data collection tools to gather anonymous usage data from students and measure how the exercises are being used.

131 The Relationship Between PFAS Exposure in Artificial Turf and Cancer

Hannah Zhang, Andy Xin, Anna Hansson, Grace Chen, Ryleigh Vallejo, Gerry Huang, Steve Wang Swarthmore College

hzhang4@swarthmore.edu, axin1@swarthmore.edu, ahansso1@swarthmore.edu, gchen3@swarthmore.edu, kvallej1@swarthmore.edu, shuang5@swarthmore.edu

The idea for this project started with the news that six Phillies players have died of a rare type of brain cancer — a Philadelphia Inquirer article claimed that baseball players had three times the rate of brain cancer as compared with U.S. adult males. Additionally, many reports have speculated that artificial turf may be a contributing factor, due to the presence of Per- and Polyfluoroalkyl Substances (PFAS). PFAS are a group of toxic, man-made chemicals and are often referred to as "forever chemicals" and have been studied by the U.S. Environmental Protection Agency and linked to cancer, liver disease, and asthma disorders. Additionally, PFAS have been used in consumer products and sporting facilities for many years. They do not break down easily and are believed to release volatile organic compounds when exposed to intense heat, which are then inhaled by players, resulting in serious health consequences. However, there have not been any studies confirming this suspicion.

This study looked at the turf exposure of Major League Baseball (MLB) players and accounted for variables such as heat and compared health outcomes between MLB players rather than with the general population, which differs significantly in terms of demographics and lifestyle. The time period of the players was also an important factor of this study. Because turf became widely popular in 1970, and slowly got phased out beginning in 2003, the subject list was restricted to players who

played enough turf games within this time period. Baseball players are ideal subjects because their chemical exposure can be determined by examining their game-by-game data. Studying carcinogens, particularly the role of PFAS exposure in causing cancer, is a very relevant topic of research. The results of this study could lead to more information about the factors that are linked with the higher rate of brain cancer in baseball players.

132 Preparation of Membrane Mimics for Structural Characterization of Influenza A M2 Protein

Winston Zhang, Kathleen Howard • Department of Chemistry & Biochemistry, Swarthmore College, Swarthmore, PA, 19081

wzhang5@swarthmore.edu

Matrix protein 2 (M2) is a membrane protein found in the viral coat of influenza and on the surface of cells that have been infected by the virus. The M2 protein plays an integral role in the viral life cycle, exhibits high sequence conservation across influenza strains and is considered a valuable target for a universal flu vaccine to protect humans from a wide range of circulating influenza strains. The binding of a range of antibodies to the N-terminal domain of M2 is an active area of vaccine research. Currently, the conformation of the N-terminal domain of M2 is unknown, which makes an atomic-level understanding of M2-antibody complexes very challenging. As a small oligomeric membrane-bound protein, M2 is difficult to study using standard modern techniques. To make structural studies tractable, our lab binds a monoclonal antibody to make a protein antibody complex large enough to study. We currently study the biophysical properties of M2 bound to 14C2, which is a tight-binding antibody characterized in previous literature. However, unlike many studies that use solubilized truncated forms of M2, we use a more physiologically relevant full-length M2 sample embedded in a membrane mimic called nanodiscs. When we create M2-nanodiscs, the result is three subpopulations: empty nanodiscs, single M2-containing nanodiscs, and clustered nanodiscs (with multiple M2 proteins). It is important to remove the empty nanodiscs to perform electron microscopy on our

M2-nanodisc samples. This summer, I performed a range of experiments to optimize the assembly of M2 in nanodiscs. These experiments included metal affinity chromatography, fast protein liquid chromatography, and SDS-PAGE gel electrophoresis for characterization. Finally, after characterization of binding via biolayer interferometry, our lab prepared several samples to continue negative stain electron microscopy. Specifically, we prepared empty nanodiscs,

M2-nanodiscs, and M2-nanodiscs with 14C2. The results of this experiment will inform us if we can proceed to cryogenic electron microscopy, which is a promising technique to characterize the structure and binding of M2.

133 Ab initio Molecular Dynamics study of Ab Initio Molecular Dynamics Simulation of $Pt_{60}Cu_{20}P_{20}$ Bulk Metallic Glass

Wuqian Zhang

This study investigates the structural properties of the bulk metallic glass Pt60Cu20P20 using Ab Initio Molecular Dynamics (AIMD) simulations implemented in VASP. This work aims to provide an model to complement previous experimental thermodynamic measurements. An amorphous structure was prepared via a simulated melt-quench procedure, starting from a random configuration. The system was subsequently equilibrated at several key temperatures: in the liquid phase, at and above the glass transition temperature (Tg), and at room temperature. The local atomic structure and its temperature-dependent evolution were then characterized using total and partial pair radial functions and Voronoi analysis.

134 Covering Radius of Translation Surfaces

Xiuming Zhang, Finnegan McKibbin, Gaocheng Liu, Milan Tenn; Advised by Professor Nate Fisher
Swarthmore College

Xzhang3@swarthmore.edu

This project is an exploration of the expected covering radii of 2n-gon translation surfaces in the orbit of $SL_2(\mathbf{R})$. A translation surface is a surface formed by identifying, or gluing, parallel sides of Euclidean polygons. The covering radius of a translation surface is the maximum distance from a point on the surface to the nearest singularity (a point where Euclidean/normal Geometry breaks). The field has seen major contributions from Mathematicians such as the late Fields medalist Mirzakhani, as well as Masur, Rafi, Randecker, Uyanik, Work, and others, whose results form the foundation of this project.

Our project aims to find the expected covering radius of a translation surface formed from a 2n-gon on its moduli space. We examine the regular 2n-gon with unit area, which undergoes linear transformations from the group $SL_2(\mathbf{R})$, or some combination of shear and dilation. Relying on the invariance of the surface under cut-and-paste, we discover methods of calculating the covering radius of specific 2n-gon translation surfaces, develop an algorithm for this method,, provide numerical results for the expected covering radius of 2n-gons, and use these results to propose a concrete, closed-form formula of the expected covering radius of all 2n-gon translation surfaces, as a function of n.

We give our sincere thanks to the College, the Math/Stats Department, Professor Nate Fisher, the Joel Dean Summer Research Fellowship, the Robin M. Shapiro'78 Summer Research Fellowship, the Swarthmore College Honors Fellowship, the Eugene M. Lang Summer Research Fellowship, and everyone who has offered valuable encouragement and inspiration for making this project possible.

135 DNA Sequences with Potential to Form Five-Tetrad G-quadruplexes

Jennifer Zhao, Liliya Yatsunyk • Swarthmore College

jzhao3@swarthmore.edu

G-quadruplexes (G4s) are a type of non-canonical DNA structure composed of four guanines in a square planar geometry held together by Hoogsteen hydrogen bonds and are often stabilized by metal cations. π-π stacking occurs when multiple tetrads stack on top of each other, resulting in further stability. Folded g-quadruplexes can be characterized by three distinct topologies: parallel, antiparallel, and hybrid. Sequences in the genome with potential to form these structures are typically found in telomeric regions and gene promoters. Due to their presence in oncogene promoter regions and telomeres, G4s have potential to be targets for cancer treatment. The formation of G4s in DNA blocks polymerases from reading the sequences, potentially being able to block the transcription of genes and other processes in cancerous cells. Understanding these structures could help further development of cancer treatments. As of recent, most resolved structures of G4s had been of three-tetrads and a few of four-tetrads.5 Very few studies have been conducted on five-tetrad G4s, and it is unclear whether or not these structures can exist in vitro or in vivo. If these five-stacked structures do form, they have the potential to be better targets for potential gene targeting in cancer therapeutics due to their rarity in the genome. In this study, we aimed to characterize 33 artificially created sequences with five guanine stretches with varying thymine loop lengths. The variance of loop length in these sequences potentially affects their stability. Characterization of these sequences could help us better understand what is needed to make the formation of five-tetrad g-quadruplexes possible.

136 Generation of SDHA and SDHD Knockout Cell Lines to Investigate Metabolic Consequences of Rare pheochromocytomas and paragangliomas (PPGLs) Mutations

Anzel Zhen, Qianjin Guo • Justin Annes Lab, Stanford School of Medicine, Stanford, CA

azhen1@swarthmore.edu

Succinate dehydrogenase (SDH), also known as complex II of the electron transport chain (ETC), catalyzes the oxidation of succinate to fumarate in the tricarboxylic acid (TCA) cycle while

transferring electrons to the ETC. The four SDH subunits (A, B, C, and D) function as tumor suppressors, and loss-of-function mutations impair both the TCA cycle and ETC. This disruption leads to intracellular succinate accumulation, inhibition of α-ketoglutarate–dependent enzymes, and histone hypermethylation, ultimately contributing to tumorigenesis.

Mutations in SDH subunits are strongly associated with pheochromocytomas and paragangliomas (PPGLs), and distinct subunit mutations are linked to different clinical phenotypes. *SDHB* mutations confer the highest risk of metastatic disease and are extensively studied, whereas *SDHA* and *SDHD* mutations, often associated with head and neck paragangliomas, remain rare and less well characterized. To address this gap, cellular models were generated to investigate the metabolic and biological consequences of *SDHA* and *SDHD* loss.

Eight knockout lines were designed in UOK269 cells, a human renal cell carcinoma model. Four variants retained *SDHB* expression while four lacked SD*HB.* Within these, CRISPR/Cas9 editing targeted early exons of *SDHA* (exons 2 and 3) and S*DHD* (exons 1 and 2), maximizing the likelihood of complete loss of function. Guide RNAs were delivered using GFP-expressing vectors, allowing the edited populations to be sorted by fluorescence-activated cell sorting (FACS), after which single-cell clones were established for downstream analyses. Mixed-population western blots were performed to assess the efficacy of guide RNAs, with knockdowns present in all four exons, particularly exon 3 of *SDHA* and both exons of *SDHD.*

The next phase of work involves validation of knockouts via western blotting of the single clones, followed by functional assays to define metabolic alterations. Assays that may be utilized include mass spectrometry to quantify succinate accumulation and Seahorse extracellular flux analysis to measure oxygen consumption rate as a proxy for mitochondrial function.

These models provide an experimental framework to study the underexplored roles of S*DHA* and S*DHD* mutations in PPGLs. Establishing these knockouts may enable future identification of metabolic vulnerabilities and inform therapeutic strategies for SDH-deficient cancers.

137 Brainstem and Central Autonomic Connectivity Alterations in Neonates with Congenital Heart Disease

Nicholas Zuk, Josepheen De Asis-Cruz M.D., Ph.D • Developing Brain Institute, Children's National Hospital, Washington D.C. 20010

nzuk1@swarthmore.edu, jocruz@childrensnational.org

There is limited research examining how connectivity in the brainstem and central autonomic nervous (CAN) region neonatal brains differ. Prior research has examined how demographic information is indicative of congenital heart disease (CHD) or how connectivity in regions of the brain differ in neonates with CHD. We sought to analyze how connectivity in the CAN region of the brain is affected by demographic data, and how predictive statistical models can be at predicting CHD in neonates. To analyze differences in the functional connectivity between the brainstem and other regions of interest (ROI) of the central autonomic network (CAN) of neonates born with CHD and without and determine how effectively statistical models can predict case versus control. We analyzed T2-weighted MRI images of 58 neonates (Table 1). MRI images were preprocessed using pipelines refined for newborns. Fisher-z tables were generated for CAN ROIs and statistically analyzed to determine interconnectivity of CAN regions in CHD and control patients. Both time-series (for logistic) and voxel based (for linear) MRI data for CAN regions were statistically analyzed using patient demographics to determine linear and logistic relationships. The UNC neonatal atlas (93 label), based on adult brain structures, was used to classify regions of the neonatal brain. In elastic net models, variable importance was determined by nonzero coefficients. Head circumference was the most consistent linear predictor (significant in 15/21 regions ($p<0.05$), with larger hc associated with increased brain region connectivity. Logistic elastic net regression showed high connectivity between the brainstem and other CAN regions using time-series data. Demographically, in the brainstem, lower APGAR scores 5 minutes after birth and head circumferences were predictive of CHD. Further, brainstem connectivity to the left (L) and right (R) Superior, Middle, and Medial Orbitofrontal Cortex, R Rectus Gyrus, R Hippocampus, and L and R Thalamus. ROC and AUC values were calculated

for the logistic model and indicated high model effectiveness and discriminatory power (Graph 1; AUC=0.9308, 95% CI: 0.8669 - 0.9946). Clusterized pearson correlations (p=0.001, q=0.05, V=32) between voxel based data for CHD and control patients showed increased connectivity between the brainstem and the R superior frontal gyrus (24), L cuneus (45), R thalamus (78), and R Cerebellum (92). Our findings demonstrate that neonates with CHD exhibit altered functional brainstem connectivity in both central autonomic ROIs as well as distal cortical and subcortical regions. Further, head circumference and APGAR scores 5 minutes after birth were consistent clinical predictors of connectivity differences. Voxelwise analyses revealed increased brainstem connectivity to the superior frontal gyrus, cuneus, thalamus, and cerebellum in CHD patients. These results indicate that CHD-related connectivity disruptions affect CAN regions of the brain as well as non-central areas. Further studies with larger sample sizes are needed to determine the neurodevelopmental significance of these connectivity alterations.

NOTES

SIGMA XI

THE SCIENTIFIC RESEARCH HONOR SOCIETY

www.sigmaxi.org

SWARTHMORE

www.swarthmore.edu